75

# ALABAMA HIGHWAY RESEARCH

## HPR REPORT NO. 7

# INSTANTANEOUS AND TIME-DEPENDENT DEFLECTIONS OF SIMPLE AND CONTINUOUS REINFORCED CONCRETE BEAMS


PART - I

BY DAN E. BRANSON

PART - II

BY GENE A. METZ

DEPARTMENT OF CIVIL ENGINEERING

AUBURN UNIVERSITY


JUNE 1965


SPONSORED BY

ALABAMA HIGHWAY DEPARTMENT

IN COOPERATION WITH

U S DEPARTMENT OF COMMERCE

BUREAU OF PUBLIC ROADS

# INSTANTANEOUS AND TIME-DEPENDENT DEFLECTIONS OF SIMPLE AND CONTINUOUS REINFORCED CONCRETE BEAMS

**PART I**

by

Dan E. Branson
Associate Professor of Civil Engineering
Auburn University

DEPARTMENT OF CIVIL ENGINEERING
AND
AUBURN RESEARCH FOUNDATION
AUBURN UNIVERSITY
1963

# FOREWORD

This is a report of research performed under Project No. 5026C-1, Auburn Research Foundation and sponsored by the State of Alabama Highway Department in cooperation with the U. S. Department of Commerce, Bureau of Public Roads. The project was conducted by personnel of the Department of Civil Engineering, Auburn University.

Grateful acknowledgment is made to Mr. J. F. Tribble, Chief, Bureau of Research and Development and Mr. F. L. Holman, Assistant Research Engineer, State of Alabama Highway Department for their cooperation, and to Mr. D. R. Luger, Graduate Assistant, for conducting the laboratory tests of the investigation. Appreciation is also expressed to the American Cast Iron Pipe Company, Birmingham, Alabama for donating the iron bricks used as loads in the study.

## ABSTRACT

Presented in this report is a study of instantaneous and time-dependent deflections of simple and continuous reinforced concrete beams with particular emphasis on effects of cracking, continuity, shrinkage warping and steel percentage. A study of the pertinent factors affecting both initial and time-dependent deflections of reinforced concrete flexural members is made, and a summary of existing methods, guides and rules of thumb for predicting these effects presented.

A new and practical method is presented for computing shrinkage warping which agrees more closely with test data than previous methods advanced. A number of observations are made with regard to the experimental curvatures and deflections obtained which refer to the effects of steel percentage, cracking and the phenomenon of the shifting neutral axis with time on deflections.

A detailed analysis is made of the effects of cracking on deflections and recommended design procedures presented for predicting these effects. A method is demonstrated for including the effect of moment redistribution due to cracking in computing deflections of statically indeterminate beams. Deflections computed by these procedures compared reasonably well with the experimental data obtained in this investigation and other data on deflections of simple and continuous reinforced concrete beams.

TABLE OF CONTENTS

# LIST OF TABLES

# LIST OF FIGURES

# I. INTRODUCTION

## 1.1 Object and Scope of the Study

With the present-day tendency toward the use of higher strength concrete and reinforcing steel, and shallower sections, the problem of deflections is assuming greater and greater importance. The purpose of this investigation is to consolidate information on deflections as much as possible and to study the complex deformational behavior of reinforced concrete beams as influenced by the interrelated effects of cracking, shrinkage warping, creep, tensile and compressive steel percentage, continuity, moment redistribution in statically indeterminate beams, etc.

The experimental phase of the program was designed to elucidate certain aspects of the deflection problem not heretofore clearly defined, such as the relative effects of high quality concrete, effects of sustained loads sufficient to cause moderate cracking, and the effects of special combinations of singly-reinforced steel percentages in companion simple and continuous beams.

Particular emphasis is placed on a study of the effects of random cracking on deflections; especially with regard to moment redistribution in continuous beams resulting from cracking. Shrinkage warping and creep deflection are also analyzed from both theoretical and empirical points of view. Analytical procedures for predicting the various aspects of the deflection problem are discussed and, in certain cases, new procedures advanced. Comparisons are made with test data to show the nature of the agreement that can be expected.

## 1.2 Notation

| | | |
|---|---|---|
| Avg. $I_{eff}$ | -- | average effective moment of inertia for simple spans (Eq. 24) |
| $A_s$ | -- | area of tensile steel |
| $A'_s$ | -- | area of compressive steel |
| a | -- | incremental length of beam |
| b | -- | width of beam at the compression side |
| b' | -- | width of beam at the tension side |
| C | -- | constant, also used to denote compressive force |
| $C_t$ | -- | creep coefficient defined as ratio of creep strain to initial strain |
| D | -- | total depth of beam |
| d | -- | effective depth of concrete section |
| d' | -- | distance from centroid of compressive steel to extreme compressive fiber |
| EI | -- | flexural rigidity |

| | |
|---|---|
| $E_c$ | --modulus of elasticity of concrete, short duration of loading |
| $E_{ct}$ | --reduced or sustained modulus of elasticity of concrete, long duration of loading |
| $E_s$ | --modulus of elasticity of steel |
| $\overline{E}_s$ | --average effective modulus of elasticity of steel when participation of tensile concrete is taken into account (see Eq. (9)) |
| e | --distance between the centroids of the uncracked transformed section (using $n_{ct}$) and the steel area |
| $e_g$ | --distance between the centroids of the gross concrete section and the steel area |
| $f_c$ | --compressive stress in concrete |
| $f'_c$ | --concrete compressive strength at age 28 days, or other age if specified |
| $f'_{cb}$ | --modulus of rupture of concrete |
| $f_s$ | --steel stress |
| $f_y$ | --yield point of steel |
| H | --relative humidity (H = 70 for 70% herein) |
| $I_{av}$ | --average effective moment of inertia for continuous beams (Eqs. 25 and 26) |
| $I^t_{cr}$ | --moment of inertia of the cracked transformed section |
| $I_{ct}$ | --moment of inertia of the uncracked transformed section using $n_{ct}$ |
| $I_{eff}$ | --effective moment of inertia at an individual section (Eqs. 21, 22, 23) |
| $I_g$ | --moment of inertia of the gross concrete section (neglecting all steel) |
| $I^t_{ucr}$ | --moment of inertia of the uncracked transformed section |
| kd | --distance from extreme compression fiber to neutral axis for cracked transformed section |
| L | --span length |
| M | --bending moment of beam |
| Mcr | --moment corresponding to flexural cracking |
| m | --a constant power |
| max | --subscript denoting maximum value |
| n | --modular ratio defined as $E_s/E_c$ |
| $n_{ct}$ | --increased modular ratio defined as $E_s/E_{ct}$ |
| p | --tensile steel percentage defined herein as $(A_s/bd)(100)$ % |
| p' | --compressive steel percentage defined herein as $(A'_s/bd)(100)$ % |
| $p_w$ | --steel percentage in T-beams defined as $(A_s/b'd)$ |
| $p_f$ | --steel percentage in T-beams defined as $(A_{sf}/b'd)$, where $A_{sf} = (0.85)(f'_c)(b - b')(t)/f_y$ |
| Q | --equivalent concentrated load |
| T | --tensile force |
| $T_s$ | --total compressive force induced in steel by shrinkage |
| t | --flange thickness for T-beams |

| | |
|---|---|
| $t$ | --denotes time interval, also used as subscript denoting time-dependent |
| $u$ | --subscript denoting ultimate value |
| $V$ | --beam shear |
| $w$ | --uniformly distributed load, also unit weight of concrete in Eq. (1) |
| $w_{DL}$ | --uniform dead-load |
| $w_{SL}$ | --uniform superimposed-load |
| $y$ | --beam deflection |
| $y_t$ | --distance from neutral axis to the extreme fiber in tension |
| $\Delta$ | --maximum deflection |
| $\Delta^t_{cr}$ | --computed maximum deflection using the cracked transformed section moment of inertia |
| $\delta_t$ | --specific creep or unit creep strain defined as creep strain per unit stress |
| $\epsilon$ | --unit strain |
| $\epsilon_s$ | --steel strain |
| $\epsilon_{sh}$ | --free shrinkage strain |
| $\theta$ | --beam slope |
| $\sigma$ | --unit stress |
| $\phi$ | --curvature or angle change per unit length of beam |
| $\phi_{sh}$ | --curvature due to shrinkage warping |
| $\bar{\Phi}$ | --equivalent concentrated angle change |
| $\psi$ | --coefficient taking into account the participation of concrete in tension (see Eq. 9) |

# II. NATURE OF THE DEFLECTION PROBLEM FOR REINFORCED CONCRETE FLEXURAL MEMBERS

## 2.1 Primary Factors Involved in Deflection Prediction and Control of Reinforced Concrete Flexural Members

The problem of predicting and controlling deflections of reinforced concrete flexural members under working loads is extremely complex as a result of the large number of significant yet uncertain factors involved. A partial list and brief discussion of the more important factors follows:

1. Lack of accurate knowledge, in advance, of pertinent concrete properties; such as modulus of rupture and compressive strength, modulus of elasticity, and shrinkage and creep characteristics. Knowing minimum specified strengths is not enough since this does not provide sufficient information of, for example, shrinkage and creep behavior. Higher strength concretes may or may not shrink and creep less than lower strength concretes. It can obviously be said, however, that when minimum strength and modulus values and maximum shrinkage and creep values are used, computed deflections will tend toward the high side.

2. Ambient temperatures and humidities, which affect the items in 1. The primary influence here is usually the effect of humidity on shrinkage and creep.

3. Concrete age when sustained loads are applied, which primarily affects creep behavior.

4. The effective section properties under instantaneous load along the beam, including primarily the effect of "extent of cracking". The cracked and uncracked transformed section properties are the two theoretical extremes and then only for linear-elastic materials. Differences in the gross and uncracked transformed section properties are seldom worth considering, and the gross section is much more convenient to use for design purposes. Involved in the determination of the effective flexural rigidity is the contribution of concrete in tension between cracks. Also involved is the effect of steel percentage, varying depths and the flanges of T-beams (especially for continuous beams) on the effective section properties along the beam.

5. Difficulty in determining shrinkage warping and creep deflections, including the effects of a given crack pattern as well as the phenomenon of progressive cracking under sustained loads. Involved is a movement of the neutral axis with time as a result of the time-dependent deformations in the nonhomogeneous composite concrete-steel structural member. Also of

importance is the effect of compression steel in reducing shrinkage and creep deflections. This is especially important with regard to ultimate strength designs where it is usually more economical, from a strength standpoint, to place additional steel in tension rather than use compression steel.

6. The determination of what constitutes critical deflections; that is, the difficult question of serviceability.

7. Other factors include the increase (above the 28-day values used in design) in concrete strength and modulus of elasticity with time, the effects of bond creep, member size, slab action, etc.

The difficulties involved in rationally analyzing the above effects are virtually insurmountable in the average design office if not in the research office. The problem appears to be primarily one of a statistical nature involving statistically optimum designs and confidence intervals for computed deflections. The large number of variables involved, the variability of these parameters and the interdependence of most of the variables strongly supports this point of view. Nevertheless, a deterministic formula or formulas, however approximate, which incorporates all of the factors that may be pertinent in a given design situation would be of benefit to both the designer and the researcher. It is to this task that the report herein addresses itself, particularly with regard to the effects of cracking, warping, continuity and steel percentage.

## 2.2 Review and Discussion of Existing Methods, Guides and Rules of Thumb for Predicting Deflections

Presented in the following paragraphs is a brief discussion of existing methods, guides and rules of thumb for determining deflection parameters and deflections themselves of reinforced concrete flexural members. Items 1 through 6 of Section 2.1 are considered in that order:

### 1., 2. and 3. Concrete Properties:

Values of modulus of rupture and modulus of elasticity of concrete are not accurate functions of compressive strength alone. Nevertheless, for most practical applications, the following approximate formulas are usually satisfactory:

[1,2] $$E_c = 33\sqrt{w^3 f'_c} \qquad (1)$$

or $$E_c = 57{,}700\sqrt{f'_c} \quad \text{for concrete weighing 145 pcf} \qquad (2)$$

[3] $$f'_{cb} = 7.5\sqrt{f'_c} \qquad (3)$$

where $E_c$ is the instantaneous modulus of elasticity, w is the unit weight of concrete, $f'_c$ is the compressive strength and $f'_{cb}$ is the modulus of rupture.

Concrete strength, modulus of elasticity, shrinkage and creep continue to increase for very long periods of time. In the case of shrinkage and creep properties it is only possible to generalize within rather broad limits, and accurate test data which incorporates the effects of local conditions should be used when available. In the absence of test data, the following shrinkage and creep information is often useful:

Schorer's[4] formula is probably adequate for calculating shrinkage strains for most design purposes:

$$\epsilon_{sh} = 12.5 \times 10^{-6} (90 - H) \tag{4}$$

where $\epsilon_{sh}$ is the free shrinkage strain in inches per inch and H is relative humidity (H = 70 for 70% rel. hum.). This formula gives an ultimate or design total shrinkage strain as a function of relative humidity, but other variables account for rather wide variations under certain conditions. However, most shrinkage data agree with Eq. (4) within 25%.

In considering the effects of creep on the deflection of concrete members, the use of a unit creep strain $\delta_t$ (creep per unit stress) or a creep coefficient $C_t$ (ratio of creep strain to initial strain) amounts to the same thing, since the concrete modulus $E_c$ must be brought in in either case and

$$C_t = \delta_t E_c \tag{5}$$

This is seen from the relation

$$\text{Creep Strain} = (\sigma_{constant})\ \delta_t = (\epsilon_{initial})\ C_t \tag{6}$$

where $$E_c = (\sigma_{constant}) / (\epsilon_{initial}) \tag{7}$$

Which to use is a matter of convenience depending on whether it is desired to apply the creep factor to applied stress or strain when computing creep strain in Eq. (6).

Approximate ultimate values for the creep coefficient for normal weight concrete under average design conditions are shown in Table 1, where, in each case, the larger of the values corresponds to an earlier loading age.

Table 1. Creep Coefficients

| Ultimate $C_t = C_u$, (Ratio of Ultimate Creep Strain to Initial Strain) | | | |
|---|---|---|---|
| Concrete Strength | Average Relative Humidity | | |
| | 100% | 70% | 50% |
| Ordinary | 1 - 2 | 1.5 - 3 | 2 - 4 |
| High | 0.7 - 1.5 | 1 - 2.5 | 1.5 - 3.5 |

## 4. Effective Section Properties Under Short-Term Loading

The stress distribution and effective moment of inertia of reinforced concrete beams vary considerably along the length of the beam. In regions of small moment the concrete works in tension, and the uncracked transformed section properties are effective in determining stresses and deflections under short-term loads. In regions where the bending moment is greater than the moment corresponding to flexural cracking, $M_{cr}$, the concrete cracks, although tensile concrete between cracks still contributes significantly to the flexural rigidity of the beam.

The cracked transformed section properties (neglecting all concrete on the tension side of the neutral axis) are not unreasonable for use in calculating stresses in cracked regions under working loads, because the governing stresses usually refer primarily to maximum moment sections. Also, any discrepancies encountered in computing stresses using the cracked section properties are on the high or safe side, and are reflected, at least in part, in well tested safety factors. The question with regard to deflections is serviceability, not safety; and here it is not generally possible to provide limits of serviceability for all types of structures. In other words, there is more of a premium on being able to predict deflections accurately, than to compute fictitous numbers called stresses. Also, deflections are seen and felt.

The effective flexural rigidity can vary greatly along a reinforced concrete beam in regions of cracking. The ratio of uncracked to cracked transformed moment of inertia for "low" steel-percentage beams is often of the order of five and larger. The effective moment of inertia at any section that is cracked has some value between the uncracked and cracked moments of inertia, which depends primarily on the magnitude of the moment for a given beam and materials.

An acceptable method in many cases is to simply use an average of the uncracked and cracked transformed moments of inertia for the entire length of beam. An European Concrete Committee[5] recommends that the gross-section flexural rigidity be used for that part of the load that produces first cracking and a modified cracked-transformed-section flexural rigidity for the remainder of the load, with the computed deflection not to exceed the "cracked transformed section" deflection. This provides a consideration of loading stages but does not account for variations in flexural rigidity along the beam. With the question of loading stages, however, arises the thought that the portion of the beam that cracks under maximum load no longer is uncracked (even under the first increments of reload) upon reloading.

Since the sections being discussed are gross and transformed concrete sections, the concrete modulus of elasticity is, of course, used in any flexural rigidity (EI) expression.

Yu and Winter[6] developed an expression for an average effective moment of inertia to take into account the participation of tensile concrete in resisting deflections. Their results were stated in the following form: Multiply (and thus reduce) deflections, computed using the cracked transformed section properties, by the factor

$$\left(1 - b'\frac{M_1}{M}\right) \tag{8}$$

where $M_1 = 0.1\ (f_c')^{2/3}\ (D)\ (D - kd)$

$M$ = moment under working loads

$b'$ = width of beam at the tension side

$D$ = total depth of the beam

The derivation of this expression followed an elastic-theory approach with the factor 0.1 having been determined empirically from beam tests.

The moment M was a pure bending moment in the derivation, and the factor 0.1 was determined on the basis that M is the maximum moment in the span for the beams tested. It does suffice to suggest that the effective moment of inertia at a given section might be obtained by dividing the cracked transformed moment of inertia by some factor similar to Eq. (8), where M is the moment at the given section.

The modification factor given by Eq. (8) has a similar effect on computed deflections as the method of Murashev[7] for taking into account the participation of tensile concrete in resisting deflections. This method uses the cracked transformed moment of inertia and an increased effective steel modulus of elasticity, $\overline{E}$, given by Eq. (9).

$$\overline{E} = E/\psi\ , \qquad \psi \leq 1.0 \tag{9}$$

where $\psi = 1 - C\ (M_{cr}/M)^2$ and C is a constant. This method is based on the consideration that between cracks the steel stress and hence deformation is less than right at the cracks; therefore, the average effective steel modulus of elasticity, $\overline{E}$, should be greater than the actual steel modulus, E, at the cracks. A value for the constant, C, of 2/3 was recommended.

Specific locations of sections of first cracking can be determined by Eq. (10),

$$M_{cr} = \frac{f'_{cb}\ I^{t}_{ucr}}{y_t} \tag{10}$$

where $M_{cr}$ is the moment corresponding to flexural cracking, $f'_{cb}$ is the modulus of rupture, $I^{t}_{ucr}$ is the moment of inertia of the uncracked transformed section and $y_t$ is the distance from the neutral axis of the uncracked transformed section to the extreme fiber in tension. For most purposes and most cases, Eq. (10) can be replaced by the simpler Eq. (11),

$$M_{cr} = \frac{f'_{cb}\ I_g}{y_t} \tag{11}$$

where $I_g$ is the moment of inertia of the gross concrete section alone (neglecting all steel) and $y_t$ refers to the same gross concrete section.

There would be 2 of these $M_{cr}$-sections in a typical reinforced concrete simple beam under service loads. Where cracking occurs in both positive and negative moment regions, 4 such $M_{cr}$-sections would exist in fully continuous beams and 3 in beams with only one end continuous. Consideration of the effects of continuous T-beam flanges and beams of varing depths would affect the above only in details. Also, the effect of varying tensile and compressive steel percentages along the beam would usually be a minor factor in locating a given $M_{cr}$-section and would not be involved at all when Eq. (11) is used.

At a time when low working stresses were used, it was deemed satisfactory to use the cracked transformed section properties in computing deflections. An American Concrete Institute Deflection Committee Report[8] in 1931 recommended this for general use. However, in the last twenty-five years or so it has become common practice to use the gross section properties in computing deflections under working loads. The Portland Cement

Association has recommended this practice for many years.

The new ACI Code[2] contains the same gross-section provision but modifies it slightly to provide for the use of the cracked transformed section properties when $pf_y$ is greater than 500. This is an attempt to guard against underestimating deflections (using the gross moment of inertia) when high steel stresses exist, such as where high working steel stresses are used, or when high yield-point steel is used in ultimate strength design.

In ultimate strength designs by Whitney's method[9], a balanced steel percentage is given by Eq. (12).

$$T_u = C_u$$

$$A_s\, f_y = 0.85\, f_c'\, b\, (0.537d)$$

$$p_{bal} = 0.46\, \frac{f_c'}{f_y} \tag{12}$$

Investigators [10, 11] have felt that a deflection warning should be sounded when the ratio p for singly-reinforced beams, $(p - p')$ for doubly-reinforced beams and $(p_w - p_f)$ for T-beams exceeds $0.18\, f_c'/f_y$. This ratio is close to the balanced steel ratio by elastic theory and less than one-half the balanced design ratio by ultimate strength theory.

For singly-reinforced beams the marginal steel percentage is

$$p = 0.18\, f_c'/f_y \tag{13}$$

and $\quad pf_y = 0.18\, f_c' = 540$ when $f_c' = 3000$ psi.

Hence the ACI value of $pf_y = 500$ is selected for ordinary strength concrete.

For the cases where $pf_y$ is less than $0.18\, f_c'$, the previous reasoning calls for the use of the gross section properties. However, the PCA[12] showed that the use of gross-section properties could be dangerous when steel percentages are low and where working stresses are relatively high. It follows from the previous observation that the effect of steel percentage alone on effective flexural rigidity tends to be contradictory.

The AASHO[13] and others have for a long time advocated the use of the gross-section properties to determine the flexural rigidity of continuous beams for purposes of indeterminate analysis as well as for computing deflections. This, admittedly, has been a rather vague compromise, but one that was dictated by the nature of the problem. In the case of continuous T-beams (flange usually cracked in negative moment regions) and beams of varying depth, an average of the positive and negative moment section properties is often used in estimating deflections using conventional formulas for prismatic members.

Since the use of the cracked transformed moment of inertia tends to overestimate deflections, a reduced modular ratio (such as n = 8 for all strength concretes recommended by the AASHO[13] for computing deflections under short-term loads) is often used in an attempt to offset the high computed deflections. This reduced modular ratio has the same effect as that provided by an increased effective concrete modulus of elasticity. Another technique that has been suggested[14] is to reduce the deflections, computed using the cracked transformed moment of inertia, by the following empirical factors:

$$
\begin{aligned}
\text{Deflection, } \Delta &= 0.9 \ \Delta^{t}_{cr} \text{ for simple beams} \\
&= 0.8 \ \Delta^{t}_{cr} \text{ for one end continuous} \qquad (14) \\
&= 0.7 \ \Delta^{t}_{cr} \text{ for both ends continuous}
\end{aligned}
$$

where $\Delta^{t}_{cr}$ is the computed deflection using the cracked transformed moment of inertia. For continuous beams, the section properties corresponding to the points of maximum positive and negative moments are usually used in this method as constant I's throughout the regions of positive and negative moment, respectively.

The misuse of the cracked transformed section properties tends to be more pronounced in continuous beams than in simple beams, as indicated by the factors in Eqs. (14). A greater length of beam will normally be uncracked in continuous beams as compared to simple beams (moment gradients are greater in continuous beams and hence maximum moments drop off faster). For example, consider the following extreme case: if a uniformly-loaded, continuous, prismatic reinforced concrete beam with the same positive and negative moment reinforcement has a cracking moment capacity of $wL^2/24$, 0.82L or 82% of the span will be uncracked. For the same simple beam, but with the load multiplied by 2/3 to account for the smaller allowable load on the simple beam (the ratio of the maximum moments for the two cases), only 0.29L or 29% (18% if the load were not reduced) of the span will be uncracked. However, certain factors such as distribution of loads, varying section depth, steel percentage, etc., can cause the use of these factors to lead to erroneous results.

## 5. Shrinkage Warping and Creep Deflection

Concrete shrinkage induces stresses in both statically determinate and indeterminate reinforced concrete structures. In determinate members the shortening of the beam resulting from shrinkage is resisted by the reinforcing steel, inducing compressive stresses in the steel and tensile stresses in the concrete. The tensile concrete stresses are maximum in the vicinity of the reinforcement and thus combine with tensile stresses resulting from transverse loads to cause additional cracking. Shrinkage of the girders in redundant frames also induces additional bending moments which are subject to direct analysis.

When reinforcement is unsymmetrical, shrinkage causes a nonuniform strain distribution which results in warping of the cross-section. Although shrinkage and creep are undoubtedly interdependent, the coefficients defining the magnitude of these effects are usually expressed separately for practical purposes. There are exceptions to this that are discussed later in this section. Even though the effects of shrinkage might be considered (in an approximate manner) apart from those of transverse load, shrinkage warping is obviously affected by cracking and therefore by transverse load.

Shrinkage warping formulas have been developed for both uncracked and cracked sections[12, 15, 16, 17], in which an equivalent elastic analysis is employed. In considering cracked sections, however, the effect of load and shrinkage must be considered simultaneously, since the extent of cracking is a direct function of the transverse load. Since shrinkage warping frequently has only a secondary effect and seldom a predominant effect on total deflections, the simpler uncracked section method is probably just as adequate as the other method and can be used without regard to effects of transverse load.

Considering an uncracked transformed section (either singly or doubly-reinforced beams, with or without flanges), the warping curvature at any cross-section due to shrinkage is given by

$$\phi_{sh} = \frac{M}{EI} = \frac{T_s e}{E_{ct}\, I_{ct}} \; * \qquad (15)$$

where $\phi_{sh}$ = warping curvature resulting from shrinkage

* Note that Ferguson[16] did not include the effects of creep in the expression for EI as does Eq. (15).

e = distance between the centroids of the uncracked transformed section (using $n_{ct} = E_s/E_{ct}$) and the steel area

$E_{ct}$ = sustained modulus of elasticity as defined by Eq. (19)

$I_{ct}$ = moment of inertia (using $n_{ct} = E_s/E_{ct}$) of the uncracked transformed section

and $$T_s = (A_s + A_s')\ \epsilon_{sh}\ E_s \tag{16}$$

where $T_s$ = total compressive force induced in the steel

$A_s$ = tensile steel area

$A_s'$ = compressive steel area

$\epsilon_{sh}$ = free shrinkage strain

$E_s$ = modulus of elasticity of steel

For singly-reinforced beams, $A_s' = 0$. When $A_s$, $A_s'$ and e are essentially constant along the span, the maximum shrinkage deflection for a simple beam becomes,

$$\Delta = \phi_{sh}\ \frac{L^2}{8} = \frac{T_s\ e\ L^2}{8\ E_{ct}\ I_{ct}} \tag{17}$$

where $\Delta$ is the midspan deflection and L is the span length.

In considering the distribution of shrinkage strains and corresponding shrinkage warping, creep effects should be included, because shrinkage stresses are sustained stresses. However, the use of the usual creep factors, for concrete under constant compressive stress, are rather nebulous, since shrinkage stresses are variable (increasing at a decreasing rate with time), and are tensile in nature. Also, the effective concrete modulus of elasticity of interest here should refer to concrete in tension. It is obvious from this discussion that the solutions of shrinkage warping using quasi-elastic concepts leave much to be desired. They, nevertheless, do provide rough estimates of shrinkage deflections that can be compared with experimental data with partial success.

Miller[18] has presented an interesting and different approach to the shrinkage warping problem for singly-reinforced beams only. His basic assumption is that the extreme fiber of the beam on the side away from the reinforcing steel shrinks the same amount as the plain concrete (Ferguson[16] disagrees with this).

Following this assumption, the beam curvature is given by

$$\phi_{sh} = \frac{\epsilon_{sh} - \epsilon_s}{d} = \frac{\epsilon_{sh}}{d}\left(1 - \frac{\epsilon_s}{\epsilon_{sh}}\right) \qquad (18)$$

where $\epsilon_s$ is the steel strain and d is the usual effective depth measured from the center of gravity of the steel to the opposite extreme fiber. Miller suggests empirical values of $\epsilon_s/\epsilon_{sh} = 0.1$ for heavily reinforced members and 0.3 for moderately reinforced members. This type of simplified empirical approach seems to have merit, and is discussed further in Section 5.1.

Time-dependent deflections of reinforced concrete flexural members, resulting solely from effects of sustained load (creep deflections), are usually greater than, and often two to three times as great as, deflections resulting from all other effects combined during the life of a structure subjected predominantly to sustained loads. Thus, creep deflections are of primary interest and should always be considered in addition to those resulting from instantaneous loads and shrinkage.

In addition to the difficulty of computing the creep-time history of a particular concrete under constant, uniformly-distributed sustained stress, a reinforced concrete flexural member is subject to a nonuniform stress distribution and very often a variable-load history. An accurate analysis of the effects of a variable stress history even for uniformly loaded specimens, requires creep-time curves and a knowledge of the loading history. The rate-of-creep method[19] or the superposition method[20] can then be used when detailed creep and loading information are available.

The rate-of-creep method, illustrated in Fig. 1, is straight forward. Consider an extreme case in which a concrete specimen is subjected to a compressive stress $\sigma$ for a time interval $t_1$. At the end of this interval, the stress is removed completely.

According to the rate-of-creep method, the creep strain at time $t_1$ is $\sigma \delta t_1$, the product of the sustained stress and the unit creep strain for the time considered. Once the stress is removed, there is no further change in creep strain and at a time, say $2t_1$, the creep strain is still $\sigma \delta_{t_1}$.

The superposition method, illustrated in Fig. 2, predicts the same creep strain at time $t_1$ of $\sigma \delta_{t_1}$. However, rather than assuming directly that the compressive stress is removed at time $t_1$, it is assumed that the specimen is subjected to an additional stress of $\sigma$ in tension and creeps under two opposing fictitious stresses. For example, assuming that the creep characteristics of the concrete are the same in tension and compression and are independent of the concrete age when loaded, the compressive creep

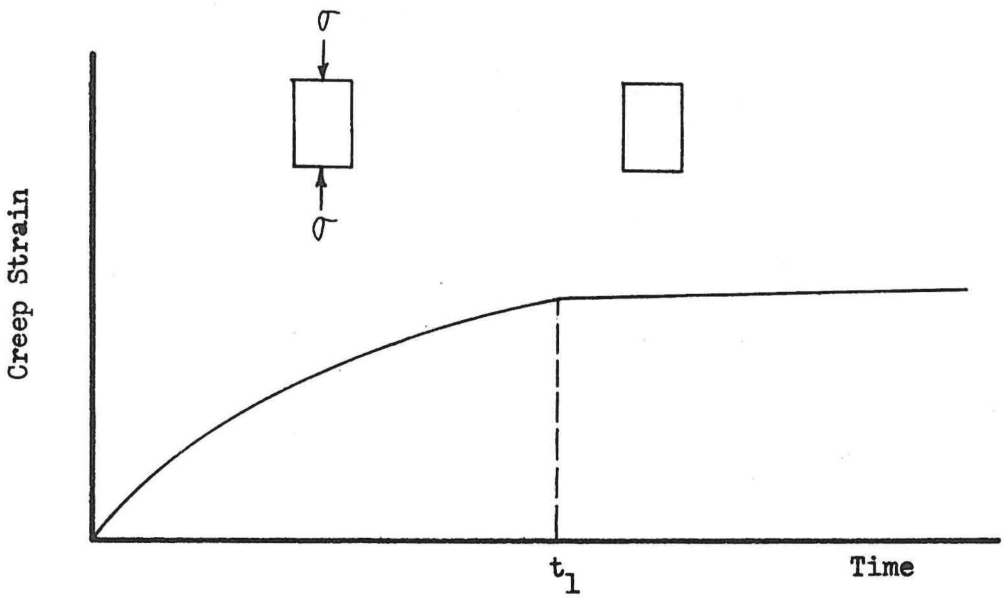


Fig. 1--Creep strains by the rate of creep method

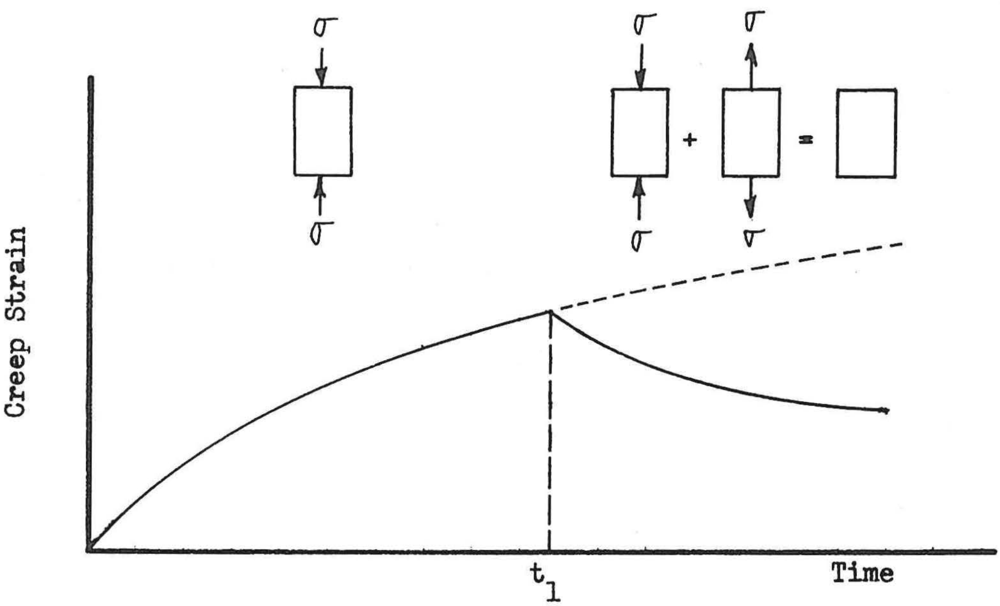


Fig. 2--Creep strains by the superposition method

strain at time $2t_1$ is $\sigma\delta_{2t_1}$ while the tensile creep strain is $\sigma\delta_{t_1}$, since the tensile stress is a new stress applied for a time interval $t_1$. The total compressive creep strain at time $2t_1$ is thus $\sigma(\delta_{2t_1} - \delta_{t_1})$ and represents a reduction with respect to the creep strain at time $t_1$, since $(\delta_{2t_1} - \delta_{t_1})$ is less than $\delta_{t_1}$ (primary creep curve increases at a decreasing rate with time).

Usually such a detailed analysis is not feasible, and a shorter, more approximate method is used. One such method is the sustained-modulus method which refers to concrete under a constant sustained stress. In this case a reduced or effective modulus called the sustained modulus of elasticity is used for computing initial-plus-creep deflections.

$$E_{ct} = \frac{\sigma_{constant}}{\epsilon_{initial} + \epsilon_{creep}} = \frac{\sigma_{constant}}{\epsilon_{initial}\,(1 + C_t)} = \frac{E_c}{1 + C_t} \qquad (19)$$

where $E_{ct}$ = sustained concrete modulus of elasticity

$E_c$ = ordinary concrete modulus of elasticity under instantaneous load

$C_t$ = creep coefficient defined as the ratio of creep strain to initial strain

When the sustained modulus of elasticity is used with, say the gross section properties in computing deflections, the resulting creep deflections are simply equal to the initial deflections multiplied by the creep coefficient. It seems inappropriate however, to use the term flexural rigidity (EI) or beam stiffness in connection with the sustained modulus of elasticity, since the effect of creep is to increase deflections but not to decrease the bending stiffness of the beam (such as for additional short-term loads, etc.).

Most recommended methods for computing creep deflections follow some ramification of this approach. Usually the deflections computed using the gross-section properties are obtained and creep factors (or deflection factors), which include compressive steel effects, specified. Both shrinkage and creep deflections tend to be drastically reduced when compressive steel is used. Only the quasi-elastic method (Eq. 17), and not the method of Miller (Eq. 18), refer to shrinkage warping for doubly-reinforced beams.

The CRSI[21] suggests the following method for computing combined shrinkage and creep deflections: Use the gross concrete section properties and a shrinkage-plus-creep factor of 3; that is, the total deflection is 4 times the initial deflection or $E_{ct} = E_c/4$. For a compression steel area equal to the tension steel area, use one-half the usual shrinkage-plus-creep factor or 1.5 for simple beams and one-third the usual factor or 1.0 for continuous beams.

Yu and Winter[6] presented an empirical table of such shrinkage-plus-creep factors for different durations of loading up to five years. The new ACI Code[2] adopted their 5-year or "ultimate" values as follows: "The additional long-time deflections may be obtained by multiplying the immediate deflections caused by the sustained part of the load by 2.0 when $A_s' = 0$; 1.2 when $A_s' = 0.5\ A_s$; and 0.8 when $A_s' = A_s$." Typical differences are seen for such recommended factors by comparing the CRSI and ACI values of 3 with 2 and 1.5 or 1.0 with 0.8. The reason for such variation is that other factors, such as concrete quality, age when loaded, loading duration, relative humidity, etc., significantly influence time-dependent concrete deformations.

Total time-dependent (combined shrinkage and creep) deflections might be computed simultaneously, with the use of some combined shrinkage-plus-creep factor, using any method advocated for computing creep deflections alone. The combination of these two effects is probably satisfactory for broad-approximate design procedures, but leaves much to be desired in analytical work where reasonably precise results are desired in unusual as well as typical structures.

In addition to the fact that the strain distribution is nonuniform in any flexural member, even though linear, creep of the reinforced concrete beam seems to have the effect of moving the neutral axis toward the tension zone. This effect can be obtained by the use of a cracked transformed section method where an increased modular ratio (resulting in an increased effective steel area), is defined by

$$n_{ct} = \frac{E_s}{E_{ct}} = n(1 + C_t) \qquad (20)$$

where $n = E_s/E_c$. However, in regions where cracking is limited or nonexistent, this method tends to lead to computed deflections that are too large, as does the use of the cracked transformed section for short-term loads with the usual modular ratio n.

## 6. Serviceability

Deflections of reinforced concrete flexural members should be controlled so as not to affect adversely the appearance and serviceability of a structure. This statement is completely general but is of primary concern to the design engineer.

Should the matter of serviceability be subject to "specification or code laws" as in the case of safety? Can general limits of serviceability be provided for all types of structures? And of what value are prescribed minimum depth-span ratios? The answers to these questions are not within the scope of this report but are mentioned in an effort to present a more complete picture of the deflection problem. A detailed review of European span-depth limitations (which tend to be more liberal than those of the new ACI Code[2]) is presented in the CEB Report[5].

The question of serviceability is radically different in bridge and building structures, primarily because of the problem of damage to plastered ceilings, partitions, window sashes, etc., in the case of buildings. Also, cambering is more efficiently used in the case of reinforced concrete bridge structures to offset excessive deflections. However, in both cases adequate deflection-control still depends on the ability of the designer to predict instantaneous and time-dependent deflections with reasonable accuracy.

## 7. Summary

It seems worth mentioning that most, if not all, of the suggested methods, guides and rules of thumb in this section will provide rough estimates of reinforced concrete beam deflections in most cases involving "typical designs" and "ordinary" conditions. However, the fundamental behavior of a reinforced concrete flexural member is so complex that a great deal of judgement is needed when any significant aspect of a design is somewhat unusual or marginal. Answers to particular questions regarding deflections very often depend largely on the case at hand.

# III. DESCRIPTION OF EXPERIMENTAL INVESTIGATION

## 3.1 Specimens and Instrumentation

The experimental phase of this investigation included primarily the measurement of instantaneous deflections; time-dependent deflections; and concrete strains resulting from elastic shortening, shrinkage and creep. Two simple-span beams and two continuous beams (each continuous over two spans) were the principal test specimens. One simple (SB-1) and one continuous beam (LB-1) were reinforced with one #3 bar and the other simple (SB-3) and continuous beam (LB-3) were reinforced with three #3 bars. All spans were 9 feet (continuous beams, 18 feet long). Duplicate shrinkage specimens containing one #3 bar, three #3 bars, and also containing no steel were used. These were placed on their sides on a smooth surface in order to minimize frictional effects.

The geometry and details of the test beams are shown in Fig. 3. No stirrups were required in the beams of this investigation. The shrinkage specimens were the same size as the simple beams. The design details of the test beams are shown in Table A.1.

The slump of the concrete was 1.5 in., and the 28-day concrete cylinder strength and modulus of elasticity were 5130 p.s.i. and $4.4 \times 10^6$ p.s.i., respectively. The concrete mix design, per cubic yard of concrete, was as follows:

| | |
|---|---|
| Cement (Type I) | 423 lb |
| Sand | 1335 lb |
| Stone | 1930 lb |
| Water | 20 gal |

The tensile yield point of the hard grade billet steel reinforcement averaged 52,000 p.s.i.

A Whittemore mechanical strain gage, shown in Fig. 5, (ten-inch gage length providing direct readings to $10 \times 10^{-6}$ inches per inch) was used to measure the concrete strains. The gage points were stainless steel inserts imbedded in the concrete. Each beam had one gage near the top and one near the bottom on both sides and at three different locations along the beam, as shown in Fig. 3. The strain gage points on the shrinkage specimens were placed in the same locations as those of the simple beams except on one side only, since these shrinkage specimens were placed on their sides. A total of 12 strain gages (24 gage points) were used on each simple and continuous beam and 6 strain gages (12 gage points) used on each shrinkage specimen. Strains resulting from temperature changes were

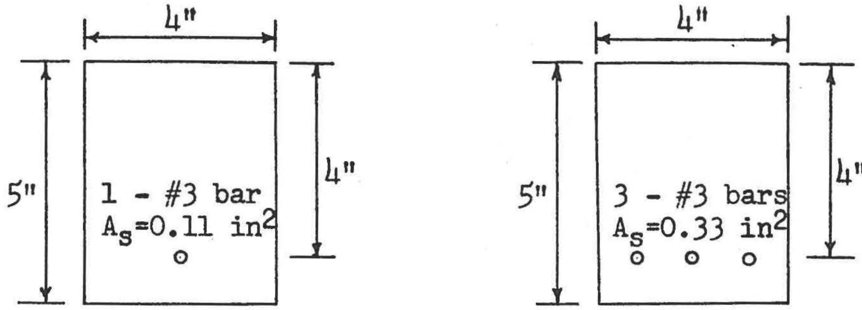


Notes: 1. These sections inverted (same section) in negative moment regions.
2. No web reinforcement was used.
3. All main reinforcement in continuous beams was cut off one foot beyond the elastic inflection points (quarter-points). No bent-up bars were used.

(a) One-bar and three-bar cross-sections

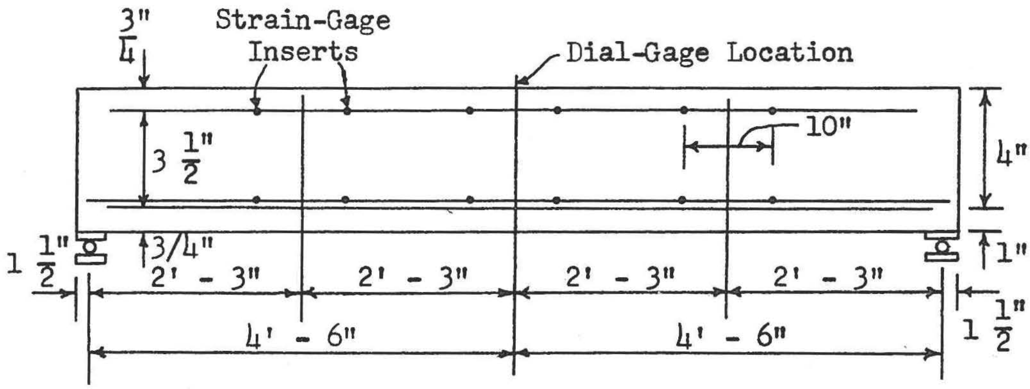


(b) Simple beam

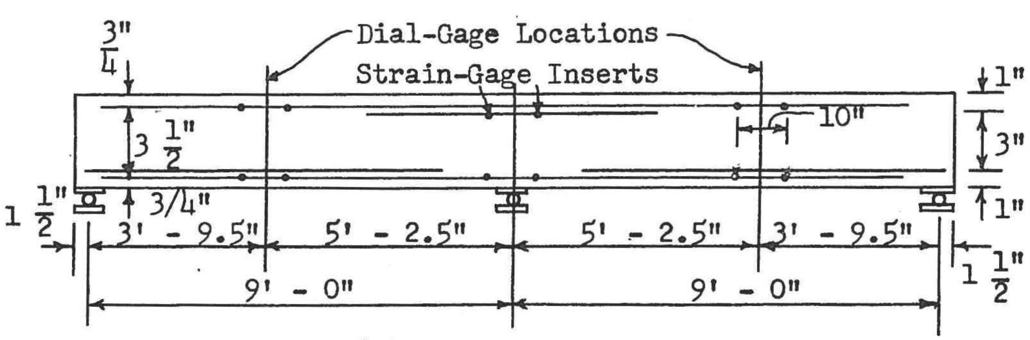


(c) Continuous beam

Fig. 3--Geometry and details of test beams

Fig. 4--View of test beams, shrinkage specimens and instrumentation

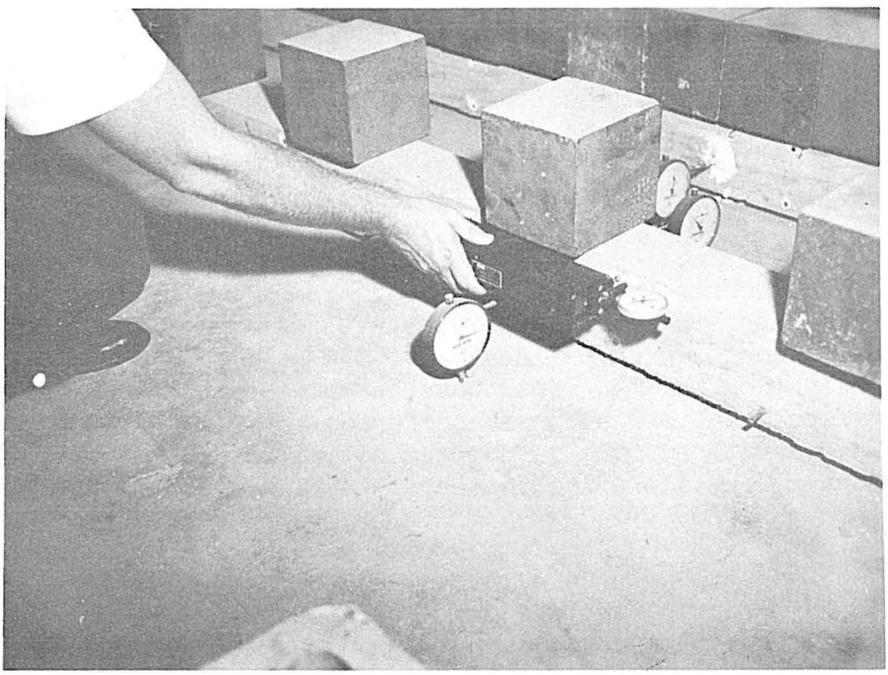

Fig. 5--View showing close-up of Whittemore gage and dial gage

eliminated from all shrinkage and creep data by means of a control gage having the same thermal coefficient as the concrete. The inner bar of the Whittemore gage is made of invar metal.

Dial gages were used on both sides of each simple beam at midspan and at the point of maximum elastic deflection for the continuous beams. The accuracy of the dial gages (0.0001 in.) for measuring deflections provided excellent data for this part of the study.

## 3.2 Experimental Results

All beams were loaded at age 28 days with the beam dead-load plus a uniformly distributed superimposed-load. Iron bricks were used for the additional loading. The bricks were placed continuously along the 3-bar beams and spaced uniformly along the 1-bar beams (in the latter case the difference between the deflections computed for the intermittent-load and the equivalent continuous-load was of the order of 1% and was ignored in the study). A superimposed-load to dead-load ratio of 2.0 was used for the 1-bar beams and 5.5 for the 3-bar beams. The total loads resulted in computed maximum concrete compressive stresses that were the same for the corresponding simple and continuous beams (the 1-bar beams--also the 3-bar beams); also resulted in computed maximum concrete compressive stresses that were the same at all points along the 1-bar and 3-bar simple beams--also the same at all points along the 1-bar and 3-bar continuous beams.

A comprehensive schedule of deflection and strain measurements was maintained throughout the test period of 60 days. Each deflection and strain value reported is an average of the readings on both sides of the beam in the same position. Thus, any small effects resulting from warping or accidental eccentricities of loading were compensated for. Also, only the average of the corresponding strain readings on the duplicate shrinkage specimens, the quarter-point strain gages for the simple beams and the strain gages located at the points of maximum elastic deflection for the continuous beams were reported. This provided a statistical approach for determining experimental values. The variations were random and not significant. The basic strain, curvature and deflection data are shown in Figs. A.1 through A.10.

Additional data obtained include temperature and relative humidity data. The average ambient temperature was 84 degrees F. with extremes recorded of 79 and 91 degrees F. The average ambient relative humidity was 59% with extremes recorded of 32 and 72%. Pictures of the test specimens and instrumentation are shown in Figs. 4 and 5.

## IV. EFFECTS OF CRACKING ON INSTANTANEOUS DEFLECTIONS OF SIMPLE AND CONTINUOUS REINFORCED CONCRETE BEAMS

As discussed in Section II, a relatively large number of methods, guides and rules of thumb have been recommended from time to time for computing instantaneous and time-dependent deflections of reinforced concrete flexural members with varying degrees of success. Conflicting aspects of the existence of a complex problem and the need for quick, practical design methods have resulted in an over-emphasis on the latter. It now seems evident that it is probably not possible to describe an acceptable method for predicting deflections that is as brief as desirable and still includes provisions for all eventualities.

Irrespective of the difficulties of not knowing, in advance, the material properties and time-dependent characteristics of the particular concrete to be used, it is, nevertheless, of utmost desirability to prescribe design methods that incorporate all of the pertinent aspects of the problem. The business of getting concrete that meets specified conditions is largely one of quality control; an area that is subject to improvement in keeping with the demand for such improvement.

Instantaneous deflections are of primary importance in considering deformational behavior of reinforced concrete beams under transient live-loads as well as in determining initial deflections under sustained loads. Most practical methods for computing creep deflections are based on the initial computed deflections.

Considered in this section are the effects of cracking on deflections of réinforced concrete beams under short-term loads. This requires an evaluation of the effective section properties along the beam as influenced by effects of cracking and participation of tensile concrete between cracks. Since behavior under repeated loading (not necessarily in the sense of fatigue loading) should generally be considered, the effective sections along the beam under all increments of loading should be taken as those under the maximum load, or neglecting the effect of loading stages. That is; the portions of the beam that have cracked under maximum load, can no longer be uncracked under smaller loads, if healing effects are neglected. Overloads would affect this consideration but would tend to be offset by the continued increase in concrete strength with time. A distinction might be made between short-term live-load deflections, where reloading occurs, and initial sustained-load deflections such as under dead-load, which may be applied only once. However, this distinction is probably not justified in most cases and is considered of secondary importance in the analyses to be discussed. Also of interest is a practical method for integrating the effects of cracking along the length of the beam in the case of both simple and continuous beams.

## 4.1 Development of an Analytical Method for Including the Effects of Cracking in the Prediction of Instantaneous Deflections

In regions of cracking the effective moment of inertia, $I_{eff}$, under instantaneous load is less than the uncracked transformed moment of inertia, $I^t_{ucr}$, but greater than the cracked transformed moment of inertia, $I^t_{cr}$, due to the participation of tensile concrete between cracks. The actual value of $I_{eff}$ at a given section depends primarily on the extent of cracking or the magnitude of the bending moment, M, in addition to the section details and concrete strength.

One logical form of an expression for $I_{eff}$, at a given section, that satisfies the boundary conditions (when $M = M_{cr}$, $I_{eff} = I^t_{ucr}$; and when $M \gg M_{cr}$, $I_{eff} \rightarrow I^t_{cr}$), is given by Eq. (21).

When $M \geqq M_{cr}$,

$$I_{eff} = I^t_{ucr} - \left[ I^t_{ucr} - I^t_{cr} \right] \left[ 1 - \left( \frac{M_{cr}}{M} \right)^m \right] \quad (21)$$

where m is an unknown power. A precedent for a power function relation relative to the distribution of cracking effects was established by Murashev's Eq. (9) in a totally different form. However, a considerably different value for the power is determined herein, although initially it was thought that a second degree function was reasonable, as in the case of Eq. (9).

Since the uncracked transformed moment of inertia is usually only slightly larger than the gross section moment of inertia, the latter is used in the remainder of the discussion. In cases involving heavily reinforced members, it might be desirable to use the uncracked transformed section value.

Rewriting Eq. (21) and replacing $I^t_{ucr}$ with $I_g$,

$$I_{eff} = \left[ \left( \frac{M_{cr}}{M} \right)^m \right] I_g + \left[ 1 - \left( \frac{M_{cr}}{M} \right)^m \right] I^t_{cr} \quad (22)$$

It is seen that the sum of the two bracketed terms is always equal to unity, and, hence, $I_{eff}$ in Eq. (22) always has some value between $I_g$ and $I^t_{cr}$ when $M > M_{cr}$.

If an acceptable evaluation can be made of the appropriate value for m, Eq. (22) should provide an effective means for determining the severity of cracking at a given section under applied moment in a form directly applicable to the computation of deflections. A study of Eq. (22) reveals the following weighted values for the two section properties corresponding to different magnitudes of moment greater than $M_{cr}$:

$$I_{eff} = C_1 I_g + C_2 I_{cr}^t$$

| | $M = 1.2\ M_{cr}$ | | $M = 2.0\ M_{cr}$ | | $M = 4.0\ M_{cr}$ | |
|---|---|---|---|---|---|---|
| | $C_1$ | $C_2$ | $C_1$ | $C_2$ | $C_1$ | $C_2$ |
| m = 1 | 0.83 | 0.17 | 0.50 | 0.50 | 0.25 | 0.75 |
| m = 2 | 0.69 | 0.31 | 0.25 | 0.75 | 0.06 | 0.94 |
| m = 3 | 0.58 | 0.42 | 0.13 | 0.87 | 0.02 | 0.98 |
| m = 4 | 0.48 | 0.52 | 0.06 | 0.94 | 0.00 | 1.00 |
| m = 5 | 0.40 | 0.60 | 0.03 | 0.97 | 0.00 | 1.00 |

An exhaustive study was made of the current and other experimental data involving statically determinate rectangular and T-beams to determine the appropriate value or values for m, corresponding to the effective moment of inertia at the individual sections. The Newmark[22] numerical procedure (illustrated in Fig. 6) was used for this purpose. Results using m = 4 for both rectangular beams and T-beams are seen in Table 2, Col. F to agree with test data in all cases within ± 25% and in 65% of the cases within ± 10%. Twenty-three test results were used in the comparison.

In addition, test data for eleven continuous rectangular beams were compared with the calculated results using m = 4. The Newmark procedure, as used in these solutions (illustrated in Fig. 7), provides a method for incorporating the effects of moment redistribution due to cracking in statically indeterminate beams. As shown in Table 2, Col. F, the computed results agree with the test data in all cases within ± 17% and in 70% of the cases within ± 10%.

All of the test beams, concrete properties and computation details referred to are summarized in Tables 3 and 4.

Thus, for determining the effective moments of inertia at individual sections, Eq. (23) is suggested:

For Rectangular Beams and T-Beams

$$I_{eff} = \left[\left(\frac{M_{cr}}{M}\right)^4\right] I_g + \left[1 - \left(\frac{M_{cr}}{M}\right)^4\right] I_{cr}^t \qquad (23)$$

Following the above evaluation, it was deemed desirable to attempt to obtain appropriate values for the power m in an expression that could be used as an average effective moment of inertia for the entire length of a beam. The general expression provided by Eq. (22) is of a form that should accommodate such an evaluation, since it includes both extremes of moment-of-inertia values along the beam as well as appropriate moment variables. Since all of the test data involved uniformly distributed loads, other distributions of moment might be expected to result in a different evaluation of m. In cases involving heavy concentrated loads, for example, the more general solution such as that provided in the Newmark numerical solution with the use of Eq. (23), should be employed.

In effect, the use of Yu and Winter's Eq. (8) along with the cracked transformed moment of inertia provides an average effective moment of inertia for an entire length of beam. However, the empirical constant of 0.1 was based on test beams that were all rather severely cracked. The results in Table 3, Col. X for beam LB-3 suggest that Eq. (8) may not apply generally in cases where beams are only moderately cracked; a condition that was included in the evaluations herein.

For determining an average effective moment of inertia over the entire length of a simple reinforced concrete beam, Eq. (24) was found to be appropriate (see Table 2).

For Rectangular Beams and T-Beams

$$\text{Avg. } I_{eff} = \left[\left(\frac{M_{cr}}{M_{max}}\right)^3\right] I_g + \left[1 - \left(\frac{M_{cr}}{M_{max}}\right)^3\right] I_{cr}^t \qquad (24)$$

Because of the way in which these equations are bounded by reasonably well-established limits ($I_g$ and $I^t_{cr}$) in addition to the experimental verifications herein, the use of Eq.(24) should be acceptable for general use with a considerable degree of confidence. The results of the experimental evaluation of the powers in Eq. (24) is shown in Table 2, Col. H. These solutions using Eq. (24) differed from those using the more involved numerical solutions and Eq.(23) by a maximum of 3%. This comparison is shown in Table 2, Col. I.

This short-cut approach for obtaining average effective moments of inertia for simple beams was found to be applicable to beams continuous at one end using the following weighted average for the positive and negative moment regions (see Table 2):

$$I_{av} = \frac{2}{3}\left[\text{Pos. Mom.Avg.}I_{eff}\right] + \frac{1}{3}\left[\text{Neg.Mom.Avg.}I_{eff}\right] \quad (25)$$

Although, the experimental data did not include beams continuous at both ends, it is believed that an acceptable solution for obtaining an average effective moment of inertia for beams continuous at both ends is as follows:

$$I_{av} = \frac{2}{3}\left[\text{Pos.Mom.Avg.}I_{eff}\right] + \frac{1}{6}\left[\text{Meg.Mom.Avg.}I_{eff}\right] \text{ Left End}$$

$$+ \frac{1}{6}\left[\text{Neg.Mom.Avg.}I_{eff}\right] \text{ Right End} \quad (26)$$

In either case (involving Eqs.(25) or (26) the positive moment section properties have the dominant influence on deflections. Results using Eqs.(24) and (25) are shown in Table 2, Col. H to agree with test data in all cases within $\pm$ 15%. Eleven test results were used in the comparison. The redundant moments were determined on the basis of elastic analysis for prismatic members in these solutions.

## 4.2 Outline of Computational Procedures

The following procedures are outlined for computing instantaneous deflections using the previous equations and Eq.(11);

### Simple Beam (Constant Concrete Dimensions)

1. Computed the cracking moment, $M_{cr}$, using Eq.(11).

2. If the maximum bending moment under service loads is less than $M_{cr}$, use E $I_g$ for the flexural rigidity at all points along the beam in computing the beam deflections.

3. If the maximum moment (including overloads if desired), $M_{max}$, is greater than $M_{cr}$, compute values for $I_{eff}$ using Eq.(23) at a sufficient number of sections in the cracked regions and compute the service-load deflections using the moments of inertia thus determined. The conjugate beam method or, preferably, the Newmark numerical procedure (illustrated in Fig. 6) are well suited for this purpose.

3(a). Sufficient accuracy can usually be obtained with the use of a constant moment of inertia value determined by Eq. (24).

Continuous Beam (Constant Concrete Dimensions, Including T-Beams)

1. Compute the cracking moment, $M_{cr}$, for both positive and negative moment regions (same value for both except for T-beams, in which case the flange overhangs should be neglected in computing the negative-moment value) using Eq. (11).

2. If the maximum bending moment (determined from a prismatic beam analysis) under service loads is less than $M_{cr}$ in both positive and negative moment regions, use E $I_g$ for the flexural rigidity at all points along the beam in computing the beam deflections.

3. If the maximum negative moment using prismatic beam analysis (including overloads if desired), $M_{max}$, is greater than $M_{cr}$, computed values for $I_{eff}$ using Eq. (23) at a sufficent number of sections in the negative moment region or regions. Do the same thing for the positive moment region. If the maximum moment is less than $M_{cr}$ in only one of the regions, use $I_g$ in that region. Compute the service-load deflections using the moments of inertia thus determined and the Newmark numerical procedure (illustrated in Fig. 7 for a beam continuous at one end only) which includes the effect of moment redistribution due to cracking.

3(a). Sufficient accuracy can usually be obtained with the use of a constant moment of inertia value determined by Eq. (24) and Eqs. (25) or (26).

Continuous Beam (With Variable Depths)

1. Determine values for M, $M_{cr}$, $I_g$, $I^t_{cr}$, and $I_{eff}$ in the Newmark solution (also using Eqs. (11) and (23)) and compute the deflections at the same time. A unique solution can be found which incorporates the effects of moment redistribution resulting from cracking, although a number of trials will usually be required. A shorter method in this case can easily lead to erroneous results. However, a very rough short-cut estimate could be obtained by following the procedure outlined for constant-dimensioned beams using Eqs. (24) and Eqs. (25) or (26).

In many cases computed deflections using the ordinary gross-section method will not be greatly different from deflections using the numerical procedure. However, the more extensive method is needed to take into account unusual conditions of proportioning, loading, etc.

The following is a summary of the boundary conditions, associated with different cases of statically indeterminate beams, required in the numerical solution to incorporate the effects of moment redistribution resulting from cracking in computing deflections of continuous reinforced concrete beams:

1. Single Span Beam, One End Fixed, One End Pinned

The solution of this problem is illustrated in Fig. 7. The procedure applies equally well to uniform and nonuniform beams (symmetrical or unsymmetrical), with variations in I properly taken into account for nonuniform beams. The trial shear distribution is required since no boundary condition is known for shear.

Boundary Conditions:
$V = ?$
$M = 0$ at pinned end
$\theta = 0$ at fixed end
$y = 0$ at both ends

2. Single Span Beam, Both Ends Fixed

A. Symmetrical Beam (uniform or nonuniform)
Consideration of half of the beam would be convenient in the numerical procedure. A trial moment distribution is required since no boundary condition is known for moment, in general. The procedure would be similar to that of Fig. 7 for Case 1 above, except that the distribution check would be made for slope instead of for deflection.

Boundary Conditions:
$V = 0$ at midspan
$M = ?$
$\theta = 0$ at end and midspan
$y = 0$ at end

B. Unsymmetrical Beam (uniform or nonuniform)
Consideration of the entire length of the beam would be required. Both trial shear and moment distributions are required. However, the unique solution would be found when all four boundary conditions (for slope and deflection) are satisfied.

Boundary Conditions:
$V = ?$
$M = ?$
$\theta = 0$ at both ends
$y = 0$ at both ends

## 3. Continuous Beam of Two Spans

A. Symmetrical Beam (uniform or nonuniform)
Same as Case 1 above.

B. Unsymmetrical Beam (uniform or nonuniform)
Consider the entire two spans in the numerical procedure. Trial shear distributions are required in both spans and would be temporarily established by the requirement that the moment for each beam end at the middle support is the same. Trial slopes are also required in both spans and would be adjusted until the slope for each beam at the middle support is the same. A final overall distribution requirement must be met for the boundary conditions on deflection, after which the unique solution would have been found.

Boundary Conditions:
$V = ?$
$M = 0$ at both outside ends; and the same for each beam end at the middle support.
$\theta =$ same for each beam end at the middle support.
$y = 0$ at all three supports.

## 4. Continuous Beam of Three or More Spans

A similar solution as for Case 3B would be possible for any number of spans.

Simple Beam

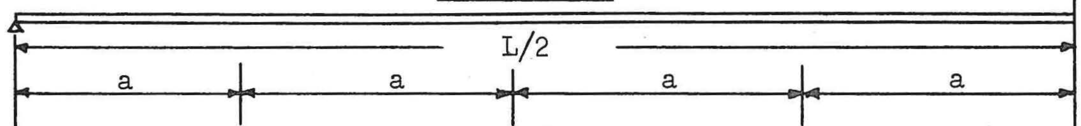


| Description | | | | | | | | | | | Multiplier |
|---|---|---|---|---|---|---|---|---|---|---|---|
| Moment, | $M$ | 0 | | 0.4375 | | 0.7500 | | 0.9375 | | 1.0000 | $wL^2/8$ |
| Curvature, | $\phi$ | 0 | | 0.4375 | | 0.7500 | | 0.9375 | | 1.0000 | $wL^2/8EI$ |
| [a]Equiv.Conc.Value, | $\bar{\phi}$ | | | 5.1250 | | 8.8750 | | 11.1250 | Start | 11.8750 | $wL^2a/96EI$ |
| Avg. Slope, | $\theta$ | | 31.0580 | | 25.9330 | | 17.0625 | | 5.9375 | (or 80) | " |
| Deflection, | $y$ | 0 | | 31.0580 | | 56.9910 | | 74.0535 | | 79.9910 | $wL^2a^2/96EI$ |

$$\Delta = 80\ \frac{wL^2(L/8)^2}{96\ EI} = \frac{5wL^4}{384\ EI}\text{, Exact Answer}$$

(a) Example of Ideal Solution for Constant EI Beam Under Uniform Load

| | | | | | | | | | | |
|---|---|---|---|---|---|---|---|---|---|---|
| $M$ | 0 | | 0.4375 | | 0.7500 | | 0.9375 | | 1.0000 | 16,400"# |
| [b]$M_{cr}/M$ | | | 1+ | | 0.732 | | 0.586 | | 0.549 | -- |
| [c]$I_{eff}$ | | | 41.7 | | 25.0 | | 21.0 | | 20.3 | $in^4$ |
| $\phi$ | | | 0.0105 | | 0.0300 | | 0.0446 | | 0.0493 | $16,400/E_c$ |
| [a]$\bar{\phi}$ | | | 0.135 | | 0.355 | | 0.525 | Start | 0.582 | $16,400a/12E_c$ |
| $\theta$ | | 1.306 | | 1.171 | | 0.816 | | 0.291 | | " |
| $y$ | 0 | | 1.306 | | 2.477 | | 3.293 | | 3.584 | $16,400a^2/12E_c$ |

$$\Delta = 3.584\ \frac{(16,400)(9/8)^2(12)^2}{(12)(4.4)(10)^6} = 0.203''$$ as compared to 0.206", computed by the approximate method recommended, and 0.153" determined experimentally. This example demonstrates the worst agreement between computed and measured deflections of thirty-four test results. The other extreme is illustrated in Fig. 7. The comparisons are shown in Table 2.

(b) Example of Solution in Which Cracking is Considered for Beam SB-3.

(Continued on next page)

a $\bar{\phi}_1 = \frac{a}{12} ( \phi_o + 10 \phi_1 + \phi_2)$, etc.

Example above: $\bar{\phi}_{5.125} = \frac{a}{12}\left[ 0 + (10)(.4375) + .7500 \right] = \frac{a}{12}(5.2150)$

b $M_{cr}$ computed using $M_{cr} = (f'_{cb} \; I_g)/(D/2)$

c Using $I_{eff} = \left[ \left( \frac{M_{cr}}{M} \right)^4 \right] I_g + \left[ 1 - \left( \frac{M_{cr}}{M} \right)^4 \right] I^t_{cr}$

Fig. 6--Example of Newmark[22] numerical solution for computing deflections of simple beams (Beam SB-3) using an effective moment of inertia at the individual sections.

Continuous Beam

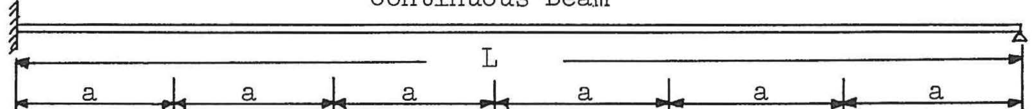


| Description | | | | | | | | | | | | | | | Multiplier |
|---|---|---|---|---|---|---|---|---|---|---|---|---|---|---|---|
| Distributed Load | | 1.00 | | 1.00 | | 1.00 | | 1.00 | | 1.00 | | 1.00 | | 1.00 | $135.2^{\#}/ft$ |
| [a]Equiv.Conc.Load, | Q | -- | | 1.00 | | 1.00 | | 1.00 | | 1.00 | | 1.00 | | -- | 135.2 a |
| [b]Assumed Avg.Shear, | V | | 3.25 | | 2.25 | | 1.25 | | Start 0.25 | | -0.75 | | -1.75 | | |
| | | | ← Follow Procedure Below → | | | | | | | | | | | | |
| Trial Deflection, | $y_t$ | 0 | | 0.878 | | 2.254 | | 3.366 | | 3.863 | | 3.757 | | [b]3.180 | $135.2a^4/12E_c$ |

[b]The shear distribution must be adjusted until the required linear deflection-corrections are zero (or small); in which case the deflection curve has been determined. Also, the effects of moment redistribution due to cracking in statically indeterminate beams are included in the solution.



| | | | | | | | | | | | | | | | |
|---|---|---|---|---|---|---|---|---|---|---|---|---|---|---|---|
| [a]Equiv.Conc.Load, | Q | -- | | 1.00 | | 1.00 | | 1.00 | | 1.00 | | 1.00 | | -- | 135.2a |
| [b]New V | | | 3.16 | | 2.16 | | 1.16 | | Start 0.16 | | -0.84 | | -1.84 | | " |
| Moment, M | | -3.96 | | -0.80 | | 1.36 | | 2.52 | | 2.68 | | 1.84 | | 0 | $135.2a^2$ |
| [c]$M_{cr}/M$ | | -0.623 | | -1+ | | 1+ | | 0.979 | | 0.920 | | 1+ | | - | -- |
| [d]$I_{eff}$ | | 21.7 | | 41.7 | | 41.7 | | 39.8 | | 35.0 | | 41.7 | | - | $in^4$ |
| Curvature, $\phi$ | | 0.1825 | | 0.0192 | | -0.0326 | | -0.0633 | | -0.0766 | | -0.0441 | | 0 | $135.2a^2/E_c$ |
| [e]Equiv.Conc.Value, $\bar{\phi}$ | | 0.713 | | 0.342 | | -0.370 | | -0.742 | | -0.873 | | -0.518 | | - | $135.2a^3/12E_c$ |
| Average Slope, $\theta$ | | 0 | -0.713 | | -1.055 | | -0.685 | | 0.057 | | 0.930 | | 1.448 | | " |
| | | | | | | | | | | | | | | (Small)[b] | |
| Trial Deflection, | $y_t$ | 0 | | 0.713 | | 1.768 | | 2.453 | | 2.396 | | 1.466 | | 0.018 | $135.2a^4/12E_c$ |
| Linear Correction | | 0 | | -0.003 | | -0.006 | | -0.009 | | -0.012 | | -0.015 | | 0.018 | " |
| Deflection, | y | 0 | | 0.710 | | 1.762 | | 2.444 | | 2.384 | | 1.451 | | 0 | " |

(Continued on next page)

$$\Delta = 2.444 \frac{(135.2)(9/6)^4(12)^3}{(12)(4.4)(10)^6} = 0.0548''$$ as compared to 0.0550", computed by the

approximate method recommended, and 0.056" determined experimentally. This example demonstrates one of the best agreements between computed and measured deflections of thirty-four test results. The comparisons are shown in Table 2.

---

[a] Values for Q can also be easily computed for other than uniform loads.

[c] $M_{cr}$ computed using: $M_{cr} = (f'_{cb}\ I_g)/\ (D/2)$

[d] Using $I_{eff} = \left[\left(\frac{M_{cr}}{M}\right)^4\right] I_g + \left[1 - \left(\frac{M_{cr}}{M}\right)^4\right] I^t_{cr}$

[e] $\bar{\phi}_0 = \frac{a}{12}\left(\frac{7}{2}\phi_0 + \frac{6}{2}\phi_1 - \frac{1}{2}\phi_2\right)$ Example above: $\bar{\phi}.713 = \frac{a}{12}\left[\frac{7}{2}\ (.1825) + \frac{6}{2}\ (.0192) - \frac{1}{2}\ (-.0326)\right] = \frac{a}{12}(0.713)$

$\bar{\phi}_3 = \frac{a}{12}(\phi_2 + 10\,\phi_3 + \phi_4)$, etc. Example above: $\bar{\phi}\ 0.742 = \frac{a}{12}\left[.0326 + (10)(.0633) + .0766\right] = \frac{a}{12}(0.742)$

---

Fig. 7--Example of Newmark[22] numerical solution for computing deflections of continuous beams (Beam LB-3) using an effective moment of inertia at the individual sections. Effects of moment redistribution due to cracking are incorporated in the numerical solution.

...BLE ... COI...ED ...ECT... CC...RED ...H T...DAT...

| Reference | Designation | Concrete Compressive Strength At Age-When-Loaded | [a]Measured Instantaneous Deflections | [b]Computed Deflections Using Newmark Procedure | Col. D / Col. E | [c]Computed Deflections Using Short-cut Procedure | Col. D / Col. G | Col. E / Col. G |
|---|---|---|---|---|---|---|---|---|
| | | psi | in. | in. | -- | in. | -- | -- |
| A | B | C | D | E | F | G | H | I |
| | | | | SIMPLE SPAN RECTANGULAR BEAMS | | | | |
| Current Investigation | SB-1 | 5130 | 0.041 | 0.050 | 0.82 | 0.050 | 0.82 | 1.00 |
| | SB-3 | 5130 | 0.153 | 0.203 | 0.75 | 0.206 | 0.74 | 0.99 |
| Washa and Fluck[23] | A1,A4 | 3630 | 0.53 | 0.61 | 0.87 | 0.62 | 0.85 | 0.98 |
| | B1,B4 | 3020 | 0.92 | 0.99 | 0.93 | 0.99 | 0.93 | 1.00 |
| | C1,C4 | 2940 | 1.58 | 1.75 | 0.90 | 1.75 | 0.90 | 1.00 |
| | D1,D4 | 2920 | 0.47 | 0.63 | 0.75 | 0.63 | 0.75 | 1.00 |
| | E1,E4 | 2990 | 2.34 | 2.07 | 1.13 | 2.06 | 1.14 | 0.99 |
| | A2,A5 | 3630 | 0.62 | 0.63 | 0.98 | 0.64 | 0.97 | 0.98 |
| | B2,B5 | 3020 | 0.98 | 1.02 | 0.96 | 1.02 | 0.96 | 1.00 |
| | C2,C5 | 2940 | 1.71 | 1.76 | 0.97 | 1.77 | 0.97 | 0.99 |
| | D2,D5 | 2920 | 0.56 | 0.64 | 0.88 | 0.65 | 0.86 | 0.98 |
| | E2,E5 | 2990 | 2.20 | 2.09 | 1.05 | 2.08 | 1.07 | 1.01 |
| | A3,A6 | 3630 | 0.67 | 0.66 | 1.02 | 0.66 | 1.02 | 1.00 |
| | B3,B6 | 3020 | 1.04 | 1.02 | 1.02 | 1.02 | 1.02 | 1.00 |
| | C3,C6 | 2940 | 1.88 | 1.83 | 1.03 | 1.82 | 1.03 | 1.01 |
| | D3,D6 | 2920 | 0.70 | 0.66 | 1.06 | 0.66 | 1.06 | 1.00 |
| | E3,E6 | 2990 | 2.48 | 2.10 | 1.18 | 2.09 | 1.19 | 1.01 |

TABLE 2. (Continued)

| A | B | C | D | E | F | G | H | I |
|---|---|---|---|---|---|---|---|---|
| | | | | SIMPLE SPAN T-BEAMS | | | | |
| Yu and Winter[6] | A-1 | 3680 | 1.34 | 1.25 | 1.07 | 1.24 | 1.08 | 1.00 |
| | B-1 | 3880 | 1.24 | 1.24 | 1.00 | 1.24 | 1.00 | 1.00 |
| | C-1 | 3530 | 1.19 | 1.24 | 0.96 | 1.23 | 0.97 | 1.00 |
| | D-1 | 3680 | 1.27 | 1.36 | 0.93 | 1.36 | 0.93 | 1.00 |
| | E-1 | 4260 | 0.51 | 0.61 | 0.84 | 0.60 | 0.85 | 1.02 |
| | F-1 | 4260 | 2.20 | 2.28 | 0.97 | 2.25 | 0.98 | 1.01 |
| | | | RECTANGULAR BEAMS CONTINUOUS OVER SINGLE SUPPORT (TWO SPANS) | | | | | |
| Current Investigation | LB-1 | 5130 | 0.021 | 0.021 | 1.00 | 0.021 | 1.00 | 1.00 |
| | LB-3 | 5130 | 0.056 | 0.055 | 1.02 | 0.055 | 1.02 | 1.00 |
| Washa and Fluck[24] | X1,X4 | 3230 | 0.56 | 0.63 | 0.89 | 0.65 | 0.86 | 0.97 |
| | Y1,Y4 | 3360 | 0.89 | 0.97 | 0.92 | 0.99 | 0.90 | 0.98 |
| | Z1,Z4 | 3300 | 1.04 | 1.02 | 1.02 | 1.04 | 1.00 | 0.98 |
| | X2,X5 | 3230 | 0.57 | 0.65 | 0.88 | 0.65 | 0.88 | 1.00 |
| | Y2,Y5 | 3360 | 0.93 | 1.01 | 0.92 | 1.00 | 0.93 | 1.01 |
| | Z2,Z5 | 3300 | 1.13 | 1.03 | 1.10 | 1.04 | 1.09 | 0.99 |
| | X3,X6 | 3230 | 0.62 | 0.64 | 0.97 | 0.65 | 0.95 | 0.98 |
| | Y3,Y6 | 3360 | 1.00 | 0.99 | 1.01 | 1.01 | 0.99 | 1.00 |
| | Z3,Z6 | 3300 | 1.20 | 1.03 | 1.17 | 1.04 | 1.15 | 0.99 |

[a]Both measured and computed deflections refer to combined dead-load and superimposed-load.
[b]See Figs. 6 and 7 for examples of Newmark[22] numerical solution for computing deflections using effective moments of inertia at individual sections obtained in Eqs.(23)and(24)
[c]Computed using Eqs. (25), (26), and (27).

TABLE 3. LOADS, BEAM DETAILS AND SECTION PROPERTIES FOR TEST BEAMS[a]
(This table is composed of 6 pages; the 2nd, 4th, and 6th pages being lateral extensions of the 1st, 3rd, and 5th pages, respectively.)

| Reference | Beam Designation | Superimposed Load | Dead Load | Span | Cracking Mom. | Max. Mom. | Ratio | Section Details and Properties | | | | | | | | | |
|---|---|---|---|---|---|---|---|---|---|---|---|---|---|---|---|---|---|
| | | $w_{SL}$ | $w_{DL}$ | L | $M_{cr}$ | $M_{max}$ | $\frac{M_{cr}}{M_{max}}$ | b | b' | t | d | d' | D | $^aI_g$ | $A_s$ | $p = 100 \times \frac{A_s}{bd}$ | $A'_s$ |
| | | #/ft | #/ft | ft. | in-k | in-k | -- | in | in | in | in | in | in | $in^4$ | $in^2$ | % | $in^2$ |
| A | B | C | D | E | F | G | H | I | J | K | L | M | N | O | P | Q | R |
| | | | | | | | SIMPLE SPAN RECTANGULAR BEAMS | | | | | | | | | | |
| Current Investigation | SB-1 | 41.6 | 20.8 | 9 | 9.0 | 7.6 | 1.18 | 4 | 4 | - | 4.00 | - | 5 | 41.7 | 0.11 | 0.69 | - |
| | SB-3 | 114.4 | 20.8 | 9 | 9.0 | 16.4 | .549 | 4 | 4 | - | 4.00 | - | 5 | 41.7 | 0.33 | 2.07 | - |
| Washa and Fluck[23] | A1,A4 | 281 | 97 | 20 | 86.5 | 227 | .381 | 8 | 8 | - | 10.12 | 1.88 | 12 | 1150 | 1.32 | 1.63 | 1.32 |
| | B1,B4 | 59 | 48 | 20 | 26.4 | 64.2 | .411 | 6 | 6 | - | 6.19 | 1.81 | 8 | 256 | 0.62 | 1.67 | 0.62 |
| | C1,C4 | 22 | 60 | 20.8 | 20.3 | 53.2 | .382 | 12 | 12 | - | 4.00 | 1.00 | 5 | 125 | 0.80 | 1.67 | 0.80 |
| | D1,D4 | 169 | 60 | 12.5 | 20.3 | 53.7 | .378 | 12 | 12 | - | 4.00 | 1.00 | 5 | 125 | 0.80 | 1.67 | 0.80 |
| | E1,E4 | 0 | 38 | 17.5 | 7.4 | 17.5 | .423 | 12 | 12 | - | 2.31 | 0.69 | 3 | 27.0 | 0.44 | 1.59 | 0.44 |
| | A2,A5 | 281 | 97 | 20 | 86.5 | 227 | .381 | 8 | 8 | - | 10.12 | 1.88 | 12 | 1150 | 1.32 | 1.63 | 0.62 |
| | B2,B5 | 59 | 48 | 20 | 26.4 | 64.2 | .411 | 6 | 6 | - | 6.19 | 1.81 | 8 | 256 | 0.62 | 1.67 | 0.31 |
| | C2,C5 | 22 | 60 | 20.8 | 20.3 | 53.2 | .382 | 12 | 12 | - | 4.00 | 1.00 | 5 | 125 | 0.80 | 1.67 | 0.40 |
| | D2,D5 | 169 | 60 | 12.5 | 20.3 | 53.7 | .378 | 12 | 12 | - | 4.00 | 1.00 | 5 | 125 | 0.80 | 1.67 | 0.40 |
| | E2,E5 | 0 | 38 | 17.5 | 7.4 | 17.5 | .423 | 12 | 12 | - | 2.31 | 0.69 | 3 | 27.0 | 0.44 | 1.59 | 0.22 |

TABLE 3. (Continued)

| Refer-ence | Beam Desig-nation | Section details and properties | | | | $I_{eff} = I^t_{cr} / \left(1 - b' \frac{M_1}{M_{max}}\right)$ where $M_1 = 0.1(f'_c)^{2/3} D(D-kd)$ | Ratio |
|---|---|---|---|---|---|---|---|
| | | Using $n = 29 \times 10^6/E_c$ | | | | $I_{eff}$ by Method B of Ref. 6 | $\frac{\text{Col. U}}{\text{Col. W}}$ |
| | | kd | $I^t_{cr}$ | $^b$Avg. $I_{eff}$ | $^cI_{av}$ | | |
| | | in | $in^4$ | $in^4$ | $in^4$ | $in^4$ | -- |
| A | B | S | T | U | V | W | X |
| **SIMPLE SPAN RECTANGULAR BEAMS** | | | | | | | |
| Current Investi-gation | SB-1 | - | - | -- | - | - | - |
| | SB-3 | 1.65 | 18.2 | 22.0 | - | 20.9 | 1.05 |
| Washa and Fluck[23] | A1,A4 | 3.64 | 600 | 630 | - | 655 | 0.96 |
| | B1,B4 | 2.13 | 111 | 121 | - | 122 | 0.99 |
| | C1,C4 | 1.54 | 60.0 | 63.6 | - | 65.1 | 0.98 |
| | D1,D4 | 1.54 | 60.0 | 63.6 | - | 65.1 | 0.98 |
| | E1,E4 | 0.90 | 10.9 | 12.2 | - | 12.0 | 1.02 |
| | A2,A5 | 3.82 | 583 | 614 | - | 636 | 0.97 |
| | B2,B5 | 2.50 | 108 | 118 | - | 118 | 1.00 |
| | C2,C5 | 1.60 | 59.0 | 62.7 | - | 64.0 | 0.98 |
| | D2,D5 | 1.60 | 59.0 | 62.6 | - | 63.9 | 0.98 |
| | E2,E5 | 0.93 | 10.8 | 12.1 | - | 11.9 | 1.02 |

TABLE 5. (Continued)

| A | B | C | D | E | F | G | H | I | J | K | L | M | N | O | P | Q | R |
|---|---|---|---|---|---|---|---|---|---|---|---|---|---|---|---|---|---|
| | A3,A6 | 281 | 97 | 20 | 86.5 | 227 | .381 | 8 | 8 | - | 10.12 | - | 12 | 1150 | 1.32 | 1.63 | - |
| | B3,B6 | 59 | 48 | 20 | 26.4 | 64.2 | .411 | 6 | 6 | | 6.19 | - | 8 | 256 | 0.62 | 1.67 | - |
| | C3,C6 | 22 | 60 | 20.8 | 20.3 | 53.2 | .382 | 12 | 12 | | 4.00 | - | 5 | 125 | 0.80 | 1.67 | - |
| | D3,D6 | 169 | 60 | 12.5 | 20.3 | 53.7 | .378 | 12 | 12 | | 4.00 | - | 5 | 125 | 0.80 | 1.67 | - |
| | E3,E6 | 0 | 38 | 17.5 | 7.4 | 17.5 | .423 | 12 | 12 | | 2.31 | - | 3 | 27.0 | 0.44 | 1.59 | - |
| SIMPLE SPAN T-BEAMS | | | | | | | | | | | | | | | | | |
| Yu and Winter[6] | A-1 | 349 | 91 | 20 | 100 | 264 | .379 | 12 | 6 | 2.5 | 10.2 | - | 12 | 6.82<br>1153 | 0.62 | 0.51 | - |
| | B-1 | 350 | 91 | 20 | 103 | 265 | .389 | 12 | 6 | 2.5 | 10.2 | 1.6 | 12 | 6.82<br>1153 | 0.62 | 0.51 | 0.31 |
| | C-1 | 348 | 91 | 20 | 98 | 263 | .373 | 12 | 6 | 2.5 | 10.2 | 1.6 | 12 | 6.82<br>1153 | 0.62 | 0.51 | 0.62 |
| | D-1 | 682 | 122 | 20 | 92 | 483 | .190 | 24 | 6 | 2.5 | 9.7 | - | 12 | 7.83<br>1513 | 1.20 | 0.52 | - |
| | E-1 | 752 | 90 | 14 | 108 | 248 | .436 | 12 | 6 | 2.5 | 9.8 | - | 12 | 6.82<br>1153 | 0.62 | 0.51 | - |
| | F-1 | 198 | 62 | 20 | 35.9 | 156 | .230 | 12 | 6 | 2.0 | 6.2 | - | 8 | 4.60<br>347 | 0.62 | 0.84 | - |
| RECTANGULAR BEAMS CONTINUOUS OVER SINGLE CENTER SUPPORT (TWO SPANS) | | | | | | | | | | | | | | | | | |
| Current Investigation | LB-1 | 41.6 | 20.8 | 2-<br>9 | 9.0 | 7.6<br>4.3 | 1.18<br>2.10 | 4 | 4 | - | 4 | - | 5 | 41.7 | 0.11<br>0.11 | 0.69<br>0.69 | -<br>- |
| | LB-3 | 114.4 | 20.8 | 2- | 9.0 | 16.4<br>9.2 | .549<br>.935 | 4 | 4 | - | 4 | - | 5 | 41.7 | 0.33<br>0.33 | 2.07<br>2.07 | -<br>- |

TABLE 3. (Continued)

| A | B | S | T | U | V | W | X |
|---|---|---|---|---|---|---|---|
| | A3,A6 | 4.01 | 566 | 589 | - | 615 | 0.96 |
| | B3,B6 | 2.54 | 107 | 118 | - | 117 | 1.01 |
| | C3,C6 | 1.68 | 57.5 | 61.3 | - | 62.2 | 0.99 |
| | D3,D6 | 1.68 | 57.5 | 61.2 | - | 62.2 | 0.98 |
| | E3,E6 | 0.95 | 10.7 | 12.0 | - | 11.7 | 1.03 |
| SIMPLE SPAN T-BEAMS | | | | | | | |
| Yu and Winter[6] | A-1 | 2.66 | 392 | 415 | - | 414 | 1.00 |
| | B-1 | 2.59 | 395 | 420 | - | 421 | 1.00 |
| | C-1 | 2.53 | 395 | 417 | - | 420 | 1.00 |
| | D-1 | 2.54 | 683 | 684 | - | 705 | 0.97 |
| | E-1 | 2.59 | 360 | 401 | - | 378 | 1.06 |
| | F-1 | 1.99 | 130 | 134 | - | 140 | 0.96 |
| RECTANGULAR BEAMS CONTINUOUS OVER SINGLE CENTER SUPPORT (TWO SPANS) | | | | | | | |
| Current Investigation | LB-1 | - | - | - | - | - | - |
| | LB-3 | 1.65 | 18.2 | 22.0 | 34.0 | 20.9 | 1.05 |
| | | 1.65 | 18.2 | 40.0 | | 23.3 | 1.72 |

TABLE 3. (Continued)

| A | B | C | D | E | F | G | H | I | J | K | L | M | N | O | P | Q | R |
|---|---|---|---|---|---|---|---|---|---|---|---|---|---|---|---|---|---|
| Washa | X1,X4 | 142 | 48 | 2- | 27.3 | 117.6 | .232 | 6 | 6 | - | 6.19 | 1.81 | 8 | 256 | 1.06 | 2.86 | 0.93 |
| and | | | | 20 | | 66.2 | .412 | | | | 6.19 | 1.81 | | | 0.62 | 1.67 | 0.62 |
| Fluck[24] | Y1,Y4 | 86 | 60 | 2- | 21.8 | 94.7 | .230 | 12 | 12 | - | 4.00 | 1.00 | 5 | 125 | 1.55 | 3.22 | 1.55 |
| | | | | 20.8 | | 53.3 | .409 | | | | 4.00 | 1.00 | | | 0.80 | 1.67 | 0.80 |
| | Z1,Z4 | 30 | 38 | 2- | 7.77 | 31.2 | .249 | 12 | 12 | - | 2.31 | 0.69 | 3 | 27.0 | 0.80 | 2.89 | 1.00 |
| | | | | 17.5 | | 17.6 | .441 | | | | 2.31 | 0.69 | | | 0.44 | 1.59 | 0.44 |
| | X2,X5 | 142 | 48 | 2- | 27.3 | 117.6 | .232 | 6 | 6 | - | 6.19 | 1.81 | 8 | 256 | 1.06 | 2.86 | 0.93 |
| | | | | 20 | | 66.2 | .412 | | | | 6.19 | 1.81 | | | 0.62 | 1.67 | 0.31 |
| | Y2,Y5 | 86 | 60 | 2- | 21.8 | 94.7 | .230 | 12 | 12 | - | 4.00 | 1.00 | 5 | 125 | 1.55 | 3.22 | 1.55 |
| | | | | 20.8 | | 53.3 | .409 | | | | 4.00 | 1.00 | | | 0.80 | 1.67 | 0.40 |
| | Z2,Z5 | 30 | 38 | 2- | 7.77 | 31.2 | .249 | 12 | 12 | - | 2.31 | 0.69 | 3 | 27.0 | 0.80 | 2.89 | 1.00 |
| | | | | 17.5 | | 17.6 | .441 | | | | 2.31 | 0.69 | | | 0.44 | 1.59 | 0.22 |
| | X3,X6 | 142 | 48 | 2- | 27.3 | 117.6 | .232 | 6 | 6 | - | 6.19 | 1.81 | 8 | 256 | 1.06 | 2.86 | 0.93 |
| | | | | 20 | | 66.2 | .412 | | | | 6.19 | 1.81 | | | 0.62 | 1.67 | - |
| | Y3,Y6 | 86 | 60 | 2- | 21.8 | 94.7 | .230 | 12 | 12 | - | 4.00 | 1.00 | 5 | 125 | 1.55 | 3.22 | 1.55 |
| | | | | 20.8 | | 53.3 | .409 | | | | 4.00 | - | | | 0.80 | 1.67 | - |
| | Z3,Z6 | 30 | 38 | 2- | 7.77 | 31.2 | .249 | 12 | 12 | - | 2.31 | 0.69 | 3 | 27.0 | 0.80 | 2.89 | 1.00 |
| | | | | 17.5 | | 17.6 | .441 | | | | 2.31 | - | | | 0.44 | 1.59 | - |

[a]Where two numbers appear, the top number refers to the maximum negative moment section value and the bottom number to the maximum positive moment section value; except Col. O for T-beams. In Col. O for T-beams, the top number refers to the distance from the extreme tension fiber to the centroid of the gross concrete section (neglecting all steel).

TABLE 3. (Continued)

| A | B | S | T | U | V | W | X |
|---|---|---|---|---|---|---|---|
| Washa and Fluck[24] | X1,X4 | 2.85 | 160 | 161 | 133 | 168 | 0.96 |
| | | 2.13 | 111 | 119 | | 122 | 0.98 |
| | Y1,Y4 | 1.81 | 98.5 | 99.0 | 760 | 103 | 0.96 |
| | | 1.54 | 60.0 | 64.4 | | 65.7 | 0.98 |
| | Z1,Z4 | 1.03 | 27.5 | 27.5 | 17.4 | 28.9 | 0.95 |
| | | 0.90 | 10.9 | 12.3 | | 12.0 | 1.03 |
| | X2,X5 | 2.85 | 160 | 161 | 132 | 168 | 0.96 |
| | | 2.50 | 108 | 118 | | 118 | 1.00 |
| | Y2,Y5 | 1.81 | 98.5 | 99.0 | 75.3 | 103 | 0.96 |
| | | 1.60 | 59.0 | 63.5 | | 64.6 | 0.98 |
| | Z2,Z5 | 1.03 | 27.5 | 27.5 | 17.4 | 28.9 | 0.95 |
| | | 0.93 | 10.8 | 12.3 | | 11.9 | 1.03 |
| | X3,X6 | 2.85 | 160 | 161 | 132 | 168 | 0.96 |
| | | 2.54 | 107 | 117 | | 117 | 1.00 |
| | Y3,Y6 | 1.81 | 98.5 | 99.0 | 74.4 | 103 | 0.96 |
| | | 1.68 | 57.5 | 62.1 | | 62.8 | 0.99 |
| | Z3,Z6 | 1.03 | 27.5 | 27.5 | 17.4 | 28.9 | 0.95 |
| | | 0.95 | 10.7 | 12.3 | | 11.8 | 1.04 |

[b]For simple Rectangular Beams and T-Beams: $\text{Avg.}I_{eff} = \left[\left(\frac{M_{cr}}{M_{max}}\right)^3\right] I_g + \left[1 - \left(\frac{M_{cr}}{M_{max}}\right)^3\right] I_{cr}^t$

[c]For Continuous Beams: $I_{av} = \frac{2}{3}(\text{Pos.Mom.Avg.}I_{eff}) + \frac{1}{3}(\text{Neg.Mom.Avg.}I_{eff})$

TABLE 4. CONCRETE PROPERTIES AND PARAMETERS FOR TEST BEAMS

| Reference | Beam Designation | Loading Schedule | [a]Concrete Strength at Age-When-Loaded and At 28 Days | | | Moduli of Elasticity | | | d,b Modular Ratio | $\frac{L}{D}$ | $\frac{A'_s}{A_s}$ | Tensile Steel Percentage | $\frac{w_{SL}}{w_{DL}}$ | $\frac{M_{cr}}{M_{max}}$ |
|---|---|---|---|---|---|---|---|---|---|---|---|---|---|---|
| | | | | | | [b]Measured $E_c$ | | [c]Computed $E_c$ | | | | | | |
| | | age when loaded | $f'_c$ at age when loaded | $f'_{cb}$ at age when loaded | $f'_c$ at 28 days | $E_c$ at age when loaded | $E_c$ at 28 days | $E_c$ at age when loaded | n | - | - | p | - | - |
| | | Days | psi | psi | psi | psi x $10^6$ | psi x $10^6$ | psi x $10^6$ | - | - | - | % | - | - |
| A | B | C | D | E | F | G | H | I | J | K | L | M | N | O |
| | | | | | SIMPLE SPAN RECTANGULAR BEAMS | | | | | | | | | |
| Current | SB-1 | 28 | 5130 | 539 | 5130 | 4.4 | 4.4 | 4.1 | 7 | 22 | 0 | 0.69 | 2.0 | 1.18 |
| Investigation | SB-3 | 28 | 5130 | 539 | 5130 | 4.4 | 4.4 | 4.1 | 7 | 22 | 0 | 2.07 | 5.5 | .549 |
| Washa | A1,A4 | 14 | 3630 | 452 | 4080 | 3.0 | 3.3 | 3.5 | 8 | 20 | 1.0 | 1.63 | 2.9 | .381 |
| and | B1,B4 | 14 | 3020 | 413 | 3420 | 2.7 | 3.1 | 3.2 | 9 | 30 | 1.0 | 1.67 | 1.2 | .411 |
| Fluck[23] | C1,C4 | 14 | 2940 | 406 | 3290 | 2.7 | 2.9 | 3.1 | 9 | 50 | 1.0 | 1.67 | 0.4 | .382 |
| | D1,D4 | 14 | 2920 | 405 | 3530 | 2.6 | 2.8 | 3.1 | 9 | 30 | 1.0 | 1.67 | 2.8 | .378 |
| | E1,E4 | 14 | 2990 | 410 | 3660 | 2.7 | 3.0 | 3.2 | 9 | 70 | 1.0 | 1.59 | 0 | .423 |
| | A2,A5 | 14 | 3630 | 452 | 4080 | 3.0 | 3.3 | 3.5 | 8 | 20 | 0.5 | 1.63 | 2.9 | .381 |
| | B2,B5 | 14 | 3020 | 413 | 3420 | 2.7 | 3.1 | 3.2 | 9 | 30 | 0.5 | 1.67 | 1.2 | .411 |
| | C2,C5 | 14 | 2940 | 406 | 3290 | 2.7 | 2.9 | 3.1 | 9 | 50 | 0.5 | 1.67 | 0.4 | .382 |
| | D2,D5 | 14 | 2920 | 405 | 3530 | 2.6 | 2.8 | 3.1 | 9 | 30 | 0.5 | 1.67 | 2.8 | .378 |
| | E2,E5 | 14 | 2990 | 410 | 3660 | 7.7 | 3.0 | 3.2 | 9 | 70 | 0.5 | 1.59 | 0 | .423 |

TABLE 4. (Continued)

| A | B | C | D | E | F | G | H | I | J | K | L | M | N | O |
|---|---|---|---|---|---|---|---|---|---|---|---|---|---|---|
| | A3,A6 | 14 | 3630 | 452 | 4080 | 3.0 | 3.3 | 3.5 | 8 | 20 | 0 | 1.63 | 2.9 | .381 |
| | B3,B6 | 14 | 3020 | 413 | 3420 | 2.7 | 3.1 | 3.2 | 9 | 30 | 0 | 1.67 | 1.2 | .411 |
| | C3,C6 | 14 | 2940 | 406 | 3290 | 2.7 | 2.9 | 3.1 | 9 | 50 | 0 | 1.67 | 0.4 | .382 |
| | D3,D6 | 14 | 2520 | 405 | 3530 | 2.7 | 2.8 | 3.1 | 9 | 30 | 0 | 1.67 | 2.8 | .378 |
| | E3,E6 | 14 | 2990 | 410 | 3660 | 2.6 | 3.0 | 3.2 | 9 | 70 | 0 | 1.59 | 0 | .423 |
| SIMPLE SPAN T-BEAMS | | | | | | | | | | | | | | |
| Yu | A-1 | 30 | 3680 | 455 | 3680 | 3.1,2.6 | 3.1,2.6 | 3.5 | 9 | 20 | 0 | 0.51 | 3.8 | .379 |
| and | B-1 | 29 | 3880 | 467 | 3880 | 3.1,2.5 | 3.1,2.5 | 3.6 | 9 | 20 | 0.5 | 0.51 | 3.8 | .389 |
| Winter[6] | C-1 | 28 | 3530 | 445 | 3530 | 3.1,2.5 | 3.1,2.5 | 3.4 | 9 | 20 | 1.0 | 0.51 | 3.8 | .373 |
| | D-1 | 31 | 3680 | 455 | 3680 | 3.1,2.6 | 3.1,2.6 | 3.5 | 9 | 20 | 0 | 0.52 | 5.6 | .190 |
| | E-1 | 29 | 4260 | 450 | 4260 | 3.1,2.6 | 3.1,2.6 | 3.8 | 9 | 14 | 0 | 0.51 | 8.4 | .436 |
| | F-1 | 34 | 4260 | 490 | 4260 | 3.1,2.6 | 3.1,2.6 | 3.8 | 9 | 30 | 0 | 0.84 | 3.2 | .230 |
| RECTANGULAR BEAMS CONTINUOUS OVER SINGLE CENTER SUPPORT | | | | | | | | | | | | | | |
| Current | LB-1 | 28 | 5130 | 539 | 5130 | 4.4 | 4.4 | 4.1 | 7 | 22 | 0 | 0.69 | 2.0 | 1.18 |
| Investi- | | | | | | | | | | | 0 | 0.69 | | 2.10 |
| gation | LB-3 | 28 | 5130 | 539 | 5130 | 4.4 | 4.4 | 4.1 | 7 | 22 | 0 | 2.07 | 5.5 | .549 |
| | | | | | | | | | | | 0 | 2.07 | | .975 |
| Washa | X1,X4 | 14 | 3230 | 426 | 3680 | 2.8 | 3.4 | 3.3 | 9 | 30 | 0.9 | 2.86 | 3.0 | .232 |
| and | | | | | | | | | | | 1.0 | 1.67 | | .412 |
| Fluck[24] | Y1,Y4 | 14 | 3360 | 435 | 3990 | 2.9 | 3.4 | 3.4 | 9 | 50 | 1.0 | 3.22 | 1.4 | .230 |
| | | | | | | | | | | | 1.0 | 1.67 | | .409 |
| | Z1,Z4 | 14 | 3300 | 431 | 3760 | 2.9 | 3.3 | 3.3 | 9 | 70 | 1.3 | 2.89 | 0.8 | .249 |
| | | | | | | | | | | | 1.0 | 1.59 | | .441 |

TABLE 4. (Continued)

| A | B | C | D | E | F | G | H | I | J | K | L | M | N | O |
|---|---|---|---|---|---|---|---|---|---|---|---|---|---|---|
| | X2,X5 | 14 | 3230 | 426 | 3680 | 2.8 | 3.4 | 3.3 | 9 | 30 | 0.9 | 2.86 | 3.0 | .232 |
| | | | | | | | | | | | 0.5 | 1.67 | | .412 |
| | Y2,Y5 | 14 | 3360 | 435 | 3990 | 2.9 | 3.4 | 3.4 | 9 | 50 | 1.0 | 3.22 | 1.4 | .230 |
| | | | | | | | | | | | 0.5 | 1.67 | | .409 |
| | Z2,Z5 | 14 | 3300 | 431 | 3760 | 2.9 | 3.3 | 3.3 | 9 | 70 | 1.3 | 2.89 | 0.8 | .249 |
| | | | | | | | | | | | 0.5 | 1.59 | | .441 |
| | X3,X6 | 14 | 3230 | 426 | 3680 | 2.8 | 3.4 | 3.3 | 9 | 30 | 0.9 | 2.86 | 3.0 | .232 |
| | | | | | | | | | | | 0 | 1.67 | | .412 |
| | Y3,Y6 | 14 | 3360 | 435 | 3990 | 2.9 | 3.4 | 3.4 | 9 | 50 | 1.0 | 3.22 | 1.4 | .230 |
| | | | | | | | | | | | 0 | 1.67 | | .409 |
| | Z3,Z6 | 14 | 3300 | 431 | 3760 | 2.9 | 3.3 | 3.3 | 9 | 70 | 1.3 | 2.89 | 0.8 | .249 |
| | | | | | | | | | | | 0 | 1.59 | | .441 |

[a] All concrete compressive strengths determined by 6" by 12" cylinder tests. The modulus of rupture, $f'_{cb}$ was computed using $f'_{cb} = 7.5 \sqrt{f'_c}$

[b] Values in Cols. G and H refer to: Secant value at 0.45 $f'_c$ for References 23 and 24; the initial tangent modulus for the current investigation; and the initial tangent modulus and secant value at 0.5 $f'_c$, respectively, for Reference 6. The measured initial tangent value for $E_c$ at the age when loaded was used in all calculations, except where this was not obtained, in which case the computed value for $E_c$ at the age when loaded was used.

[c] Computed values of $E_c$ determined using $E_c = 57{,}700 \sqrt{f'_c}$ , where $f'_c$ is the concrete compressive strength at the age when loaded.

[d] Modular ratio determined (and rounded off) using $n = 29 \times 10^6/E_c$.

# V. DISCUSSION OF TEST RESULTS

The experimental phase of this investigation was undertaken in order to evaluate the effects of certain variables heretofore not clearly distinguished. Relatively high quality concrete beams of moderate span-depth ratios and loaded so that moderate cracking occurred provided a useful distinction from most of the other deflection tests that have been reported; which were of average concrete quality, average-to-large span-depth ratios (up to 70 which is abnormally large), and severely cracked (see Tables 3 and 4). Also, the test beams herein were carefully designed with different steel percentages so that the computed maximum concrete compressive stresses were the same for the corresponding simple and continuous beams (the 1-bar beams -- also the 3-bar beams); also that the computed maximum concrete compressive stresses were the same at all points along the 1-bar and 3-bar simple beams -- also the same at all points along the 1-bar and 3-bar continuous beams. Compression steel was not included as a variable in the current experimental program.

## 5.1 Shrinkage Warping

Primary interest with regard to analytical methods for computing shrinkage warping centers around the basic assumptions and hence the pertinent variables involved. For example, the quasi elastic "tensile force" method given by Eq. (16) includes a flexural rigidity expression not found in Miller's method given by Eq. (18).

$$\phi_{sh} = \frac{T_s e}{E_{ct}\, I_{ct}} \quad \text{where } T_s = (A_s + A_s') \, \epsilon_{sh} \, E_s \tag{16}$$

$$\phi_{sh} = \frac{\epsilon_{sh}}{d} \, (1 - \epsilon_s / \epsilon_{sh}) \tag{18}$$

The latter equation results in a warping expression as a function of the free shrinkage, effective depth and a constant (parenthesis) which was specified in a general way to be 0.9 for heavily reinforced members and 0.7 for moderately reinforced members. The method is applicable to singly-reinforced beams only, whereas Eq. (16) is applicable to both singly- and doubly-reinforced beams. Basic to Miller's approach is the assumption that a concrete member restrained at some point outside the kern limit on one side, will not shrink more (but rather will undergo an equal shrinkage) than the free shrinkage on the opposite extreme fiber, as the tensile force method of Eq. (16) predicts.

The curves of the current investigation shown in Fig. 8 indicate that the extreme fiber does shrink more than the free shrinkage of the companion specimen, but not much more. Hence the effects of the eccentric steel resistance, outside the kern limit of the section, do seem to produce "greater than free" shrinkage of the opposite extreme fiber. But Miller's approach would certainly appear to be a close approximation. Of course, in deeper beams (greater eccentricity) the assumption would tend to be further in error, but in these cases the increased depth greatly reduces the shrinkage-warping curvatures anyway.

The current and other shrinkage data have been tabulated in Tables 5 and 6 and the results compared with the following procedures for computing shrinkage warping:

Eq. (16) is modified to use the simpler expressions $(E_c/2)(I_g)$ in place of $E_{ct}\ I_{ct}$ and $e_g$ which refers to the gross section. This Eq. (27) is applicable to both singly- and doubly-reinforced beams. Closer agreement with test results was found as a result of this convenient modification.

$$\phi_{sh} = \frac{T_s\ e_g}{\frac{E_c}{2}\ I_g} \tag{27}$$

Miller's Eq. (18) is applicable only to singly-reinforced beams.

The following new empirical expressions, which provide the closest agreement with test results, are introduced. Eqs. (28) and (29) are applicable to both singly- and doubly-reinforced beams.

$$\phi_{sh} = (0.7)\ \frac{\epsilon_{sh}}{D}\ (p-p')^{1/3} \left(\frac{p-p'}{p}\right)^{1/2}, \text{ for } (p-p') \leqq 3.0\% \tag{28}$$

and

$$\phi_{sh} = \frac{\epsilon_{sh}}{D}, \text{ for } (p-p') > 3.0\% \tag{29}$$

For singly-reinforced beams, p' = 0, and Eq. (28) reduces to

$$\phi_{sh} = (0.7)\ \frac{\epsilon_{sh}}{D}\ p^{1/3} \tag{30}$$

With regard to comparisons with 16 test results, the following agreements were found and are shown in Cols. K, N, and P in Table 6:

<u>Using Eq. (27)</u> Results agreed with test data in 25% of the cases within 10%.

Using Eq. (18) Results agreed with test data in 23% of the cases within 10%.
Using Eqs. (28),(29),(30) Results agreed with test data in 69% of the cases within 10%.
Keeping in mind the nature of the problem, the latter agreement is thought to be reasonably good.

Eq. (28) is an adaption of Miller's approach. For example, his method results in the following expressions for singly-reinforced beams only:

$$\phi_{sh} = 0.7 \frac{\epsilon_{sh}}{d} \quad \text{for moderately reinforced beams.}$$

$$\phi_{sh} = 0.9 \frac{\epsilon_{sh}}{d} \quad \text{for heavily reinforced beams.}$$

Eq. (30) for singly-reinforced beams results in the following:

| | | | |
|---|---|---|---|
| $\phi_{sh}$ = 0.56 | $\epsilon_{sh}/D$ | when $(p - p')$ = | 0.5 |
| = .70 | " | | 1.0 |
| = .80 | " | | 1.5 |
| = .88 | " | | 2.0 |
| = .96 | " | | 2.5 |
| = 1.01 | " | | 3.0 |

The use of the more convenient overall depth D instead of the effective depth d was found to provide closer agreement with the data. The difference is negligible for all but shallow beams and for these, the use of D seemed to provide the best fit. It is, of course, assumed that abnormal covers (abnormal differences in D and d) are excluded from consideration.

Eqs. (28) and (29) refer to both singly- and doubly-reinforced beams. The expression in the last parenthesis of Eq. (28),

$$\left(\frac{p - p'}{p}\right)^{1/2} \tag{31}$$

was found to be required in order to produce a somewhat smaller curvature for doubly-reinforced members than for singly-reinforced members when $(p - p')$ for the doubly-reinforced members is equal to p for the singly-reinforced members; other conditions being the same. It is seen that the modifier of Eq. (31) becomes unity when $p' = 0$. Eqs. (28),(29), and (30) provide very simple expressions for computing shrinkage warping in terms of only two section properties (D and p or $(p - p')$) and the free shrinkage $\epsilon_{sh}$. However, the data in Tables 5 and 6 tend to indicate that the methods discussed should be used with caution when dealing with high-strength concrete.

It should be mentioned that consideration has not been given to effects of cracking on shrinkage warping in either the experimental studies of the current investigation and others reported in the literature or in the analytical methods discussed. At least according to the tensile force method, cracking would tend to increase the eccentricity of the tensile steel in singly-reinforced beams and would therefore seem to increase shrinkage warping. However, according to the other approach discussed, effects of cracking should play a minor role in producing shrinkage warping since the extreme fiber is still assumed to shrink an amount equal to the free shrinkage, and the resistance factor provided by the empirical constant (0.7) and the steel percentage term or terms would not seem to be much different in the case of warping of cracked sections.

With regard to shrinkage deflections of continuous beams, if the effect of moment redistribution resulting from shrinkage curvatures are neglected, the effects of shrinkage on deflections can be determined using any moment-area technique or numerical procedure and the curvature expressions discussed herein (by substituting the curvature $\phi$ for M/EI). Eqs. (18),(27),(28),(29), and (30) all define shrinkage curvatures at individual sections, although these expressions are usually constant for a considerable length of a reinforced concrete beam.

## 5.2 Deformational Behavior of Test Beams

In addition to the shrinkage strain and curvature data for the shrinkage specimens shown in Figs. A.2 and A.3, the total (instantaneous plus time-dependent) and instantaneous plus creep strain data are shown in Figs. A.4 through A.7. Since the curves have markedly "leveled off", and with the additional information shown in Fig. 9 for projecting 2-month values to 20-year or "ultimate" values, certain quantitative as well as qualitative conclusions can be drawn with regard to ultimate deformational behavior.

In Figs. A.6 and A.7, the tension-gage strains are seen to decrease with time in cases where shrinkage strains exceed the creep strains. The basic curvature and deflection data for the test beams are shown in Figs. A.8, A.9, and A.10, and further represented in Fig. 11 and Table 7. The testing period reported for the beams of this investigation was 2 months.

Average values for the creep coefficients (defined as ratio of creep strain to initial strain) shown in Fig. 10 were virtually the same for the tension and compression gages, although the greater variation was observed for the tension gages. This was probably due to the random cracking at some of the gage locations on the tension side of the beams. The average values for the time-dependent (shrinkage plus creep) deflection coefficients (defined as ratio of time-dependent deflection to initial deflection) are shown in Fig. 11.

At 2 months the average tensile and compressive creep coefficient was about 0.9 while the average time-dependent deflection coefficient was about 1.5. Projecting these values to 20-year values using Fig. 9 (multiplying by 2) results in corresponding coefficients of 1.8 and 3.0 respectively. Results in Table 7 indicate that shrinkage curvatures varied from 11% to 19% of the total time-dependent curvature, so that the corresponding average creep deflection coefficient (defined as ratio of creep deflection to initial deflection) would be about 2.6. By comparing the ultimate creep strain coefficient of 1.8 with the ultimate creep deflection coefficient of 2.6, it is suggested that other effects seem to have a definite influence on so called creep deflections other than direct concrete creep strains. Undoubtedly one of the principal explanations is that of a shifting neutral axis and time-dependent adjustments in the stress as well as strain distributions along the beam. This is also discussed with regard to the experimental curvatures obtained.

For relatively high strength concrete, loads applied at age 28-days (considered an average loading age -- not particularly early or late), and 59% average relative humidity, the value for the ultimate creep coefficient given in Table 1 is about 2.5.

Thus suggested in the previous paragraphs is the nature of the theoretical as well as empirical vagueness of the approaches available for applying creep or shrinkage plus creep coefficients to instantaneous deflections when computing creep or shrinkage plus creep deflections.

The effects of cracking on instantaneous deflections were studied in Section IV and are further evident with regard to time-dependent deflections in Fig. A.10. For example, the maximum moment for the simple beam SB-3 was about twice the moment corresponding to first cracking, while the simple beam SB-1 was uncracked. However, the time-dependent deflection coefficients at 2 months were 0.146/0.153 = 0.95 for SB-3 and 0.0435/0.0410 = 1.06 for SB-1, indicating that extent of cracking does not seem to materially affect one's choice of time-dependent deflection coefficients.

Tabulated in Table 7 are the instantaneous curvatures, and curvatures at the end of the testing period for all of the gage locations. These curvatures were obtained by dividing the algebraic difference in the top and bottom gage readings by the distance between them at each gage location.

From Table 7, Cols. D and E, it can be seen that even though the design stresses for the 1-bar beams were the same, the ratio of experimental instantaneous curvatures to moment for the 3-bar beams were of the order of twice that of the 1-bar beams, which were subjected to the correspondingly smaller loads. This demonstrates the tendency for relatively large steel-percentage beams to undergo considerably greater curvatures and deflections when designed for the same allowable stresses by elastic theory. Similar behavior is seen for the instantaneous plus creep curvatures in Table 7, Cols. L and M but to a slightly lesser degree.

Interesting results are shown in Table 7, Cols. H and I where in every case the ratios of time-dependent to initial curvatures are larger in the smaller moment regions. The same is true for the creep ratios (with one exception in eight cases -- and it thought to be insignificant) of Table 7, Cols. N and O. This would suggest that in regions of higher moment (within working stress ranges -- that is, below any high overload range) larger early creep strains tend to cause greater reductions in concrete stresses with accompanying greater reductions in creep curvatures with time. Involved is the phenomenon of the shifting neutral axis with time as a result of the shrinkage and creep behavior of a nonhomogeneous (particularly so when cracked), composite steel-concrete structural member.

The brief discussion of this section serves only to demonstrate a number of fundamental phenomena regarding instantaneous and time-dependent characteristics of reinforced concrete beams as observed in a limited number of test results. Methods for computing deflections that take into account most of these effects have been discussed in this report and in the case of cracking effects and shrinkage warping, new procedures set forth. It appears that the gap between fundamental answers related to deformational behavior of such beams and empirical approaches for controlling structural deflections remains a formidable but not impossible one to materially close in the not too distant future.

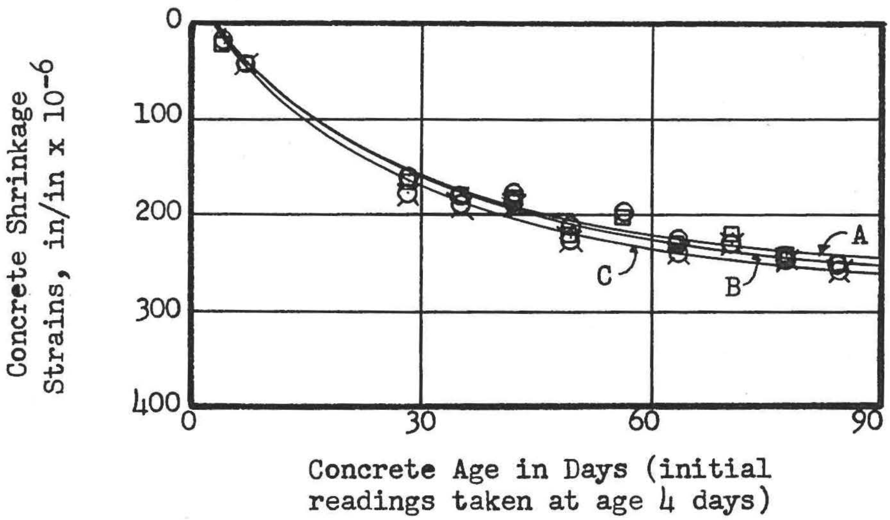


⊙ A--Shrk. Spec. With No Steel (p=0), All Gages Used
⊡ B--Shrk. Spec. With One Bar (p=0.69%), All Gages Used
⌧ C--Shrk. Spec. With Three Bars (p=2.07%), All Gages Used

Fig. 8--Comparison of shrinkage strains at the top fiber for the specimens with different steel percentages (strains proportioned to extreme fiber using a linear distribution with the top and bottom gages)

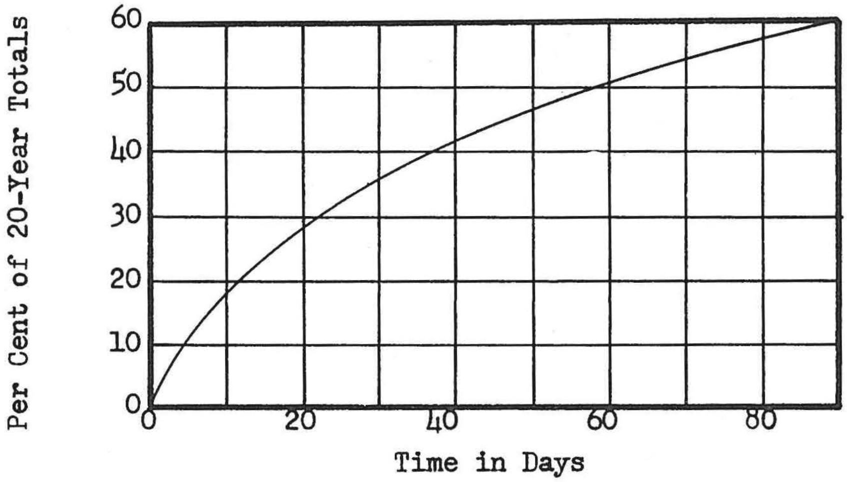


Based on "Long-Time Creep and Shrinkage Tests of Plain and Reinforced Concrete," by Troxell, Raphael and Davis, Proceedings ASTM, V. 58, 1958

Fig. 9--Average rate of increase for shrinkage and creep strains

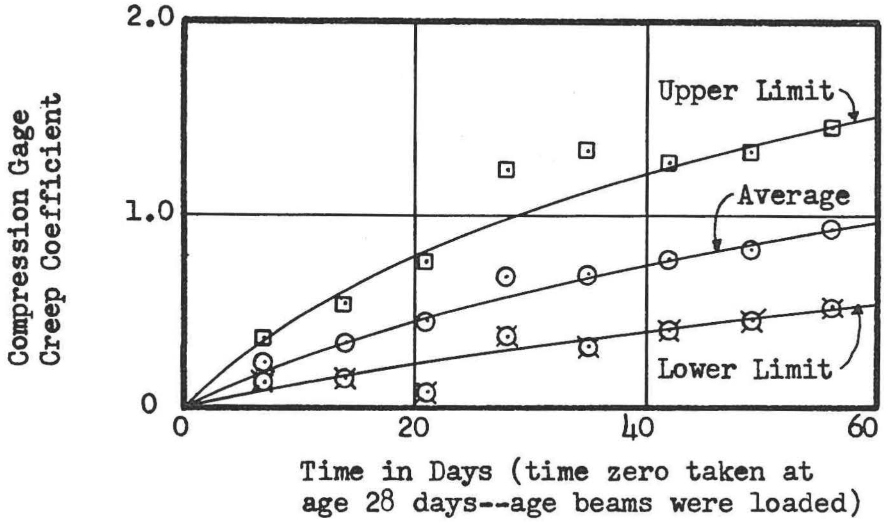


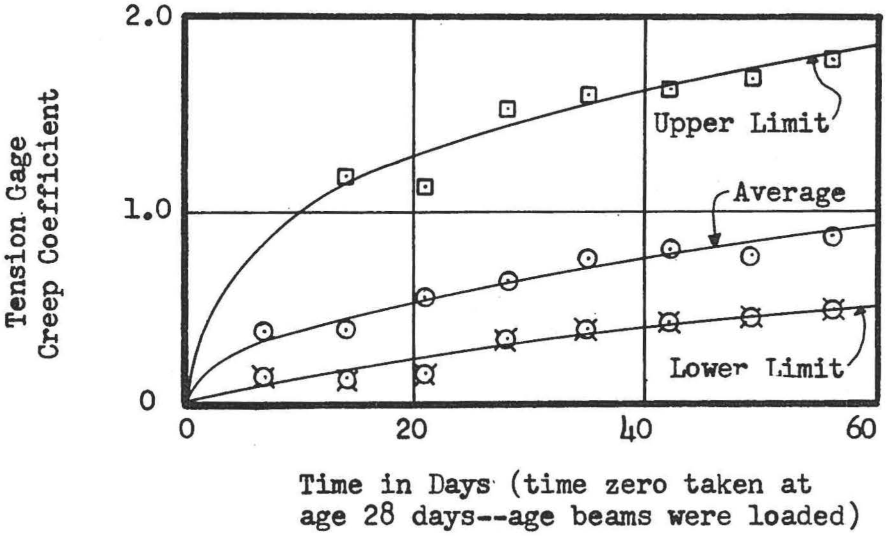


Creep Coefficients Defined as Ratio of
Creep Strain to Initial Strain

Fig. 10--Compression and tension gage creep coefficient
versus time curves for four test beams

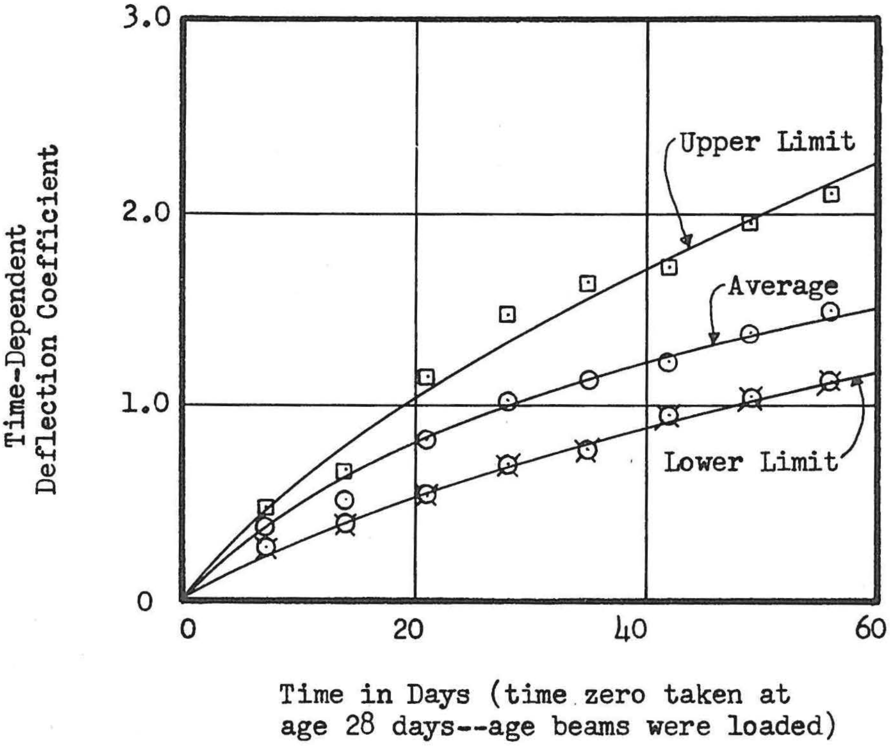


Time-Dependent Deflection Coefficient Defined as Ratio of Time-Dependent Deflection to Initial Deflection

Fig. 11--Time-dependent deflection coefficient versus time curves for four test beams

TABLE 5. BEAM DETAILS AND CONCRETE PROPERTIES FOR SHRINKAGE SPECIMENS

| Reference | Beam Designation | Section Details and Properties | | | | | | | | | Span | Age Initial Readings Taken | Duration of Test |
|---|---|---|---|---|---|---|---|---|---|---|---|---|---|
| | | $b$ | $d$ | $D$ | $e_g$ | $I_g$ | $A_s$ | $A'_s$ | $a_p$ | $a_{p'}$ | $L$ | -- | -- |
| | | in | in | in | in | $in^4$ | $in^2$ | $in^2$ | % | % | ft | days | months |
| A | B | C | D | E | F | G | H | I | J | K | L | M | N |
| Current Investigation | B-1 | 4 | 4 | 5 | 1.5 | 41.7 | 0.11 | 0 | 0.69 | 0 | 9 | 4 | 3 |
| | B-3 | 4 | 4 | 5 | 1.5 | 41.7 | 0.33 | 0 | 2.07 | 0 | 9 | 4 | 3 |
| Miller[18] | Series 1,2 | | | | | | | | | | | | |
| | 3" | 3.25 | 2.25 | 3 | 0.75 | 7.3 | 0.22 | 0 | 3.01 | 0 | 3.5 | 1 | 3 |
| | 4" | 3.25 | 3.25 | 4 | 1.25 | 17.4 | 0.22 | 0 | 2.08 | 0 | 3.5 | 1 | 3 |
| | 5" | 3.25 | 4.25 | 5 | 1.75 | 33.9 | 0.22 | 0 | 1.60 | 0 | 3.5 | 1 | 3 |
| | 6" | 3.25 | 5.25 | 6 | 2.25 | 58.5 | 0.22 | 0 | 1.29 | 0 | 3.5 | 1 | 3 |
| | Series 3,4 | | | | | | | | | | | | |
| | 3" | 3.25 | 2.25 | 3 | 0.75 | 7.3 | 0.11 | 0 | 1.50 | 0 | 3.5 | 1 | 3 |
| | 4" | 3.25 | 3.25 | 4 | 1.25 | 17.4 | 0.11 | 0 | 1.04 | 0 | 3.5 | 1 | 3 |
| | 5" | 3.25 | 4.25 | 5 | 1.75 | 33.9 | 0.11 | 0 | 0.80 | 0 | 3.5 | 1 | 3 |
| | 6" | 3.25 | 5.25 | 6 | 2.25 | 58.5 | 0.11 | 0 | 0.65 | 0 | 3.5 | 1 | 3 |
| Washa and Fluck[23] | C2,C5 | 12 | 4.00 | 5 | 0.50 | 125 | 0.80 | 0.40 | 1.67 | 0.84 | 20.8 | 14 | 30 |
| | D2,D5 | 12 | 4.00 | 5 | 0.50 | 125 | 0.80 | 0.40 | 1.67 | 0.84 | 12.5 | 14 | 30 |
| | E2,E5 | 12 | 2.31 | 3 | 0.27 | 27.0 | 0.44 | 0.22 | 1.59 | 0.80 | 17.5 | 14 | 30 |
| | C3,C6 | 12 | 4.00 | 5 | 1.5 | 125 | 0.80 | 0 | 1.67 | 0 | 20.8 | 14 | 30 |
| | D3,D6 | 12 | 4.00 | 5 | 1.5 | 125 | 0.80 | 0 | 1.67 | 0 | 12.5 | 14 | 30 |
| | E3,E6 | 12 | 2.31 | 3 | 0.81 | 27.0 | 0.44 | 0 | 1.59 | 0 | 17.5 | 14 | 30 |

[a] $p = \left(\frac{A_s}{bd}\right) 100; \quad p' = \left(\frac{A'_s}{bd}\right) 100$

TABLE (Continued)

| Reference | Beam Designation | Relative Humidity: Extremes | Relative Humidity: Avg. | Concrete Properties: Strength At 28 Days | Concrete Properties: Modulus Of Elasticity At 28 days | Concrete Properties: Measured Free Shrinkage At End Of Test |
|---|---|---|---|---|---|---|
| | | -- | -- | f'c | $^bE_c$ | sh |
| | | % | % | psi | psi x $10^6$ | in/in x $10^{-6}$ |
| A | B | O | P | Q | R | S |
| Current Investigation | B-1 | 32-72 | 59 | 5130 | 4.1 | 245 |
| | B-3 | 32-72 | 59 | 5130 | 4.1 | 245 |
| Miller[18] | Series 1,2 | | | | | |
| | 3" | 50 | 50 | 3500 | 3.4 | 650 |
| | 4" | 50 | 50 | 3500 | 3.4 | 650 |
| | 5" | 50 | 50 | 3500 | 3.4 | 650 |
| | 6" | 50 | 50 | 3500 | 3.4 | 650 |
| | Series 3,4 | | | | | |
| | 3" | 50 | 50 | 3500 | 3.4 | 550 |
| | 4" | 50 | 50 | 3500 | 3.4 | 550 |
| | 5" | 50 | 50 | 3500 | 3.4 | 550 |
| | 6" | 50 | 50 | 3500 | 3.4 | 550 |
| Washa and Fluck[23] | C2,C5 | 20-80 | 50 | 3290 | 3.3 | 750 |
| | D2,D5 | 20-80 | 50 | 3530 | 3.4 | 750 |
| | E2,E5 | 20-80 | 50 | 3660 | 3.5 | 750 |
| | C3,C6 | 20-80 | 50 | 3290 | 3.3 | 750 |
| | D3,D6 | 20-80 | 50 | 3530 | 3.4 | 750 |
| | E3,E6 | 20-80 | 50 | 3660 | 3.5 | 750 |

$^b$Computed using $E_c = 57{,}700 \sqrt{f'_c}$

TABLE 6. COMPUTED SHRINKAGE WARPING COMPARED WITH TEST DATA

| Reference | Beam Designation | Concrete Strength At 28 Days f'c | Span L | Overall Depth D | p | p' |
|---|---|---|---|---|---|---|
| | | psi | ft. | in | % | % |
| A | B | C | D | E | F | G |
| Current Investigation | B-1 | 5130 | 9 | 5 | 0.69 | 0 |
| | B-3 | 5130 | 9 | 5 | 2.07 | 0 |
| Miller[18] | Series 1,2 | | | | | |
| | 3" | 3500 | 3.5 | 3 | 3.01 | 0 |
| | 4" | 3500 | 3.5 | 4 | 2.08 | 0 |
| | 5" | 3500 | 3.5 | 5 | 1.60 | 0 |
| | 6" | 3500 | 3.5 | 6 | 1.29 | 0 |
| | Series 3,4 | | | | | |
| | 3" | 3500 | 3.5 | 3 | 1.50 | 0 |
| | 4" | 3500 | 3.5 | 4 | 1.04 | 0 |
| | 5" | 3500 | 3.5 | 5 | 0.80 | 0 |
| | 6" | 3500 | 3.5 | 6 | 0.65 | 0 |
| Washa and Fluck[23] | C2,C5 | 3290 | 20.8 | 5 | 1.67 | 0.84 |
| | D2,D5 | 3530 | 12.5 | 5 | 1.67 | 0.84 |
| | E2,E5 | 3660 | 17.5 | 3 | 1.59 | 0.80 |
| | C3,C6 | 3290 | 20.8 | 5 | 1.67 | 0 |
| | D3,D6 | 3530 | 12.5 | 5 | 1.67 | 0 |
| | E3,E6 | 3660 | 17.5 | 3 | 1.59 | 0 |

TABLE 6. (Continued)

| Reference | Beam Designation | Experimental Values: Average Curvature Along Beam | Experimental Values: [a]Midspan Deflection | Computed Deflections And Comparisons: b,a Using Eq.(27) | Col.I / Col.J | c $\epsilon_s / \epsilon_{sh}$ Selected For Use In Eq.(18) | d,a Using Eq.(18) | Col.I / Col.M | e,a Using Eq.(28), (29) | Col.I / Col.O |
|---|---|---|---|---|---|---|---|---|---|---|
| | | $\frac{1}{in} \times 10^{-6}$ | in | in | -- | -- | in | -- | in | -- |
| A | B | H | I | J | K | L | M | N | O | P |
| Current Investigation | B-1 | 9 | 0.013 | 0.020 | 0.43 | 0.4 | 0.053 | 0.25 | 0.043 | 0.30 |
| | B-3 | 20 | 0.029 | 0.060 | 0.33 | 0.2 | 0.071 | 0.41 | 0.064 | 0.45 |
| | Series 1,2 | | | | | | | | | |
| Miller[18] | 3" | 225 | 0.050 | 0.055 | 0.91 | 0.1 | 0.064 | 0.78 | 0.049 | 1.02 |
| | 4" | 150 | 0.033 | 0.038 | 0.87 | 0.2 | 0.039 | 0.85 | 0.032 | 1.03 |
| | 5" | 108 | 0.024 | 0.028 | 0.86 | 0.3 | 0.026 | 0.92 | 0.024 | 1.00 |
| | 6" | 80 | 0.018 | 0.021 | 0.86 | 0.3 | 0.019 | 0.95 | 0.018 | 1.00 |
| | Series 3,4 | | | | | | | | | |
| | 3" | 130 | 0.029 | 0.023 | 1.26 | 0.3 | 0.042 | 0.69 | 0.032 | 0.91 |
| | 4" | 88 | 0.019 | 0.016 | 1.19 | 0.3 | 0.026 | 0.73 | 0.022 | 0.86 |
| | 5" | 66 | 0.015 | 0.012 | 1.25 | 0.3 | 0.023 | 0.65 | 0.016 | 0.94 |
| | 6" | 57 | 0.013 | 0.009 | 1.44 | 0.4 | 0.015 | 0.87 | 0.012 | 1.08 |
| Washa and Fluck[23] | C2,C5 | - | 0.50 | 0.49 | 1.02 | - | - | - | 0.54 | 0.93 |
| | D2,D5 | - | 0.20 | 0.17 | 1.18 | - | - | - | 0.20 | 1.00 |
| | E2,E5 | - | 0.45 | 0.45 | 1.00 | - | - | - | 0.63 | 0.71 |
| | C3,C6 | - | 1.20 | 0.98 | 1.22 | 0.3 | 1.00 | 1.20 | 0.97 | 1.24 |
| | D3,D6 | - | 0.35 | 0.34 | 1.03 | 0.3 | 0.36 | 0.97 | 0.35 | 1.00 |
| | E3,E6 | - | 1.20 | 0.90 | 1.33 | 0.3 | 0.72 | 1.67 | 1.13 | 1.06 |

TABLE 6. (Continued)

[a]Deflections determined using $\Delta = \phi \frac{L^2}{8}$ when curvatures and not deflections were reported; also used to compute deflections from curvatures in Cols. J, M, and 0.

[b]Eq. (27), $\phi_{sh} = \frac{T_s e_g}{\frac{Ec}{2} I_g}$, where $T_s = (A_s + A_s') \in_{sh} E_s$

[c]Using Miller's suggested values of $\in s/\in sh$ = .3 for moderately reinforced members and $\in s/\in sh$ = .1 for heavily reinforced members.

[d]Eq.(18), $\phi_{sh} = \frac{\in_{sh}}{d} \left(1 - \in s/\in sh\right)$, Applies only to singly-reinforced beams.

[e]Eq. (28) $\phi_{sh} = (0.7) \frac{\in_{sh}}{D} (p-p')^{1/3} \left(\frac{p-p'}{p}\right)^{1/2}$, when $(p - p') \leqq 3.0\%$

Eq. (29), $\phi_{sh} = \frac{\in_{sh}}{D}$, when $(p - p') > 3.0\%$

ABL F MOM S A XPE NTA URV ES LL LC IONS R T EST MS THE CURRENT INVESTIGATION.

| [a] Beam Designation | [b] Max. Mom. (At Midspan of Simple Beams And At Center Support of Cont. Beams) Under Dead-Load Plus Super-imposed-Load | [b] Mom. At ¼-Point of Simple Beams and At Point of Max. Elastic Defl. of Cont. Beams Under Dead-Load Plus Super-imposed-Load | [c,d] Instantaneous Beam Curvatures Under Dead-Load Plus Super-imposed-Load. | |
|---|---|---|---|---|
| | | | Same Points As Col. B | Same Points As Col. C |
| | in-kips | in-kips | $\frac{1}{in} \times 10^{-6}$ | $\frac{1}{in} \times 10^{-6}$ |
| A | B | C | D | E |
| Simple Beam, SB-1 | 7.6 | 5.7 | 31<br>4.1 | 20<br>3.5 |
| Continuous Beam, LB-1 | 7.6 | 4.3 | 30<br>4.0 | 14<br>3.3 |
| Simple Beam, SB-3 | 16.4 | 12.3 | 122<br>7.4 | 80<br>6.5 |
| Continuous Beam, LB-3 | 16.4 | 9.2 | 136<br>8.3 | 54<br>5.9 |

[a] Note that the cross-sections of the 1-bar beams (SB-1 and LB-1) were identical; also that the cross-sections of the 3-bar beams (SB-3 and LB-3) were identical.

[b] Redundant moments were determined by elastic theory for prismatic members in cols. B and C.

[c] All beams were loaded at age 28-days. According to Fig. 9, 60-day test values can be projected to 20-year values by multiplying by a factor of about 2.0.

[d] Bottom numbers are ratios of curvatures to moments; Col. D/ Col. B, Col. E/ Col. C, Col. L/ Col. B, Col. M/ Col. C.

TABLE 7. (Continued)

| [a]Beam Designation | Beam Curvatures Under Dead-Load Plus Superimposed-Load. Values At End of 2-Months Loading Period. | | | | | | | | | |
|---|---|---|---|---|---|---|---|---|---|---|
| | Total (Instantaneous Plus Time-Dependent) | | [e] Time Dependent (Shrinkage Plus Creep) | | Shrinkage | | [d] Instantaneous Plus Creep | | [e] Creep | |
| | Same Points As Col. B | Same Points As Col. C | Same Points As Col. B | Same Points As Col. C | Same Points As Col. B | Same Points As Col. C | Same Points As Col. B | Same Points As Col. C | Same Points As Col. B | Same Points As Col. C |
| | $\frac{1}{in} \times 10^{-6}$ | $\frac{1}{in} \times 10^{-6}$ | $\frac{1}{in} \times 10^{-6}$ | $\frac{1}{in} \times 10^{-6}$ | $\frac{1}{in} \times 10^{-6}$ | $\frac{1}{in} \times 10^{-6}$ | $\frac{1}{in} \times 10^{-6}$ | $\frac{1}{in} \times 10^{-6}$ | $\frac{1}{in} \times 10^{-6}$ | $\frac{1}{in} \times 10^{-6}$ |
| A | F | G | H | I | J | K | L | M | N | O |
| SB-1 | 60 | 50 | 29<br>0.9 | 30<br>1.5 | 5 | 5 | 55<br>7.2 | 45<br>7.9 | 24<br>0.8 | 25<br>1.2 |
| LB-1 | 85 | 40 | 1.8 | 1.9 | 5 | 5 | 80<br>10.6 | 35<br>8.2 | 50<br>1.7 | 21<br>1.5 |
| SB-3 | 210 | 165 | 0.7 | 1.1 | 8 | 8 | 202<br>12.3 | 157<br>12.8 | 80<br>0.7 | 77<br>1.0 |
| LB-3 | 220 | 105 | 0.6 | 0.9 | 8 | 8 | 212<br>12.9 | 97<br>10.6 | 76<br>0.6 | 43<br>0.8 |

[e] Bottom numbers are ratios of curvatures at end of 2 months to initial curvatures; Col. H/ Col. D, Col. I/ Col. E, Col. N/ Col. D, Col. O/ Col. E.

## VI. CONCLUDING REMARKS

An attempt has been made to study the complex deformational behavior of reinforced concrete flexural members as influenced by the interrelated effects of cracking, shrinkage warping, creep, tensile and compressive steel percentage, continuity, moment redistribution in statically indeterminate beams, etc. Initially, a detailed review and discussion of existing methods, guides and rules of thumb for predicting deflections was presented for the purpose of examining the nature of the deflection problem.

A new and practical method was presented for computing shrinkage warping which agrees more closely with test data than previous methods advanced. See Eqs. (28), (29), or (30) for the appropriate curvature expressions to be intergrated across the span. For example, the mid span deflection $\Delta = \phi L^2/8$ for a simple span. However, only shrinkage warping of uncracked specimens has been investigated experimentally to the writer's knowledge, and effects of cracking on shrinkage curvature in unsymmetrical sections represents an area requiring further study. A number of interesting observations related to effects of steel percentage, cracking and the phenomenon of the shifting neutral axis with time on deflections were made from the experimental curvatures and deflections.

Consideration was given to the effects of cracking on deflections and recommended design procedures presented for predicting these effects. A method was demonstrated for including the effect of moment redistribution due to cracking in computing deflections of statically indeterminate beams. Deflections computed by these procedures compared reasonably well with the experimental data obtained in this investigation and other data on deflections of simple and continuous reinforced concrete beams. See Eqs. (23) through (26). Comparisons are tabulated to show the nature of the agreement that can be expected between analytical and experimental deflections.

It appears that future studies should concentrate on the effects of random cracking on deflections since both instantaneous-load cracks and progressive cracking under sustained loads in many cases play a dominant role in determining deflection behavior. In the case of statically indeterminate beams, moment redistribution effects resulting from shrinkage, creep and cracking also drastically influence deflections in many cases and represent an area that has not been extensively explored.

The problem of deflection prediction and control of reinforced concrete flexural members involves a number of complex and interrelated influences herein discussed. In addition to the largely empirical approaches that constitute the main tools for present-day prediction of deflections, more attention should undoubtedly be given in the future to the statistical aspects of the problem as related to statistically optimum designs, confidence intervals for computed deflections, etc.

## VII. REFERENCES CITED

1. Pauw, Adrian, "Static Modulus of Elasticity of Concrete as Affected by Density," ACI Journal, Proceedings V. 57, No. 6, Dec. 1960, pp. 679-687.

2. Proposed Revision of "Building Code Requirements for Reinforced Concrete," American Concrete Institute, Apr. 1963.

3. ACI-ASCE Joint Committee 323, "Tentative Recommendations for Prestressed Concrete," ACI Journal, Proceedings V. 54, No. 7, Jan. 1958, pp. 545-578.

4. Schorer, Herman, "Prestressed Concrete, Design Principles and Reinforcing Units," ACI Journal, Proceedings V. 39, No. 4, pp. 493-528.

5. Levi, Franco, "Work of the European Concrete Committee," ACI Journal, Proceedings V. 57, No. 9, Mar. 1961, pp. 1041-1070.

6. Yu, Wei-Wen and Winter, George, "Instantaneous and Long-Time Deflections of Reinforced Concrete Beams Under Working Loads," ACI Journal, Proceedings V. 57, No. 1, July 1960, pp. 29-50.

7. Murashev, V. E., "Theory of Appearance and Opening of Cracks, Computation of Rigidity of Reinforced Concrete Members," Stroitelnaya Promishlenost, No. 11, Soviet Union, 1940.

8. Myrlea, T. D., Author-Chairman, "Deflection of Reinforced Concrete Members," Progress Report of ACI Committee 307, ACI Journal, Proceedings V. 27, 1931, p. 351.

9. Whitney, Charles S., "Plastic Theory of Reinforced Concrete Design," ASCE Transactions, 107, 1942, p. 251.

10. Report of ASCE-ACI Joint Committee on "Ultimate Strength Design," ASCE Proceedings-Separate 809, Oct. 1955.

11. Corning, Leo H., Chairman, Report of ACI-ASCE Committee 327, "Ultimate Strength Design," ACI Journal, Proceedings V.52, No. 7, Jan. 1956, p. 505.

12. Portland Cement Association, "Deflection of Reinforced Concrete Members," ST-70, 1952.

13. The American Association of State Highway Officials, "Standard Specifications for Highway Bridges," Eighth Edition, 1961.

14. Dunham, C. W., "Theory and Practice of Reinforced Concrete," McGraw-Hill Book Company, Inc., 1953.

15. Large, G. E., "Basic Reinforced Concrete Design," Second Edition, The Ronald Press Company, 1957.

16. Ferguson, P. M., Discussion of "Warping of Reinforced Concrete Due to Shrinkage," by A. L. Miller, ACI Journal, Proceedings V. 54, No. 6, Dec. 1958, pp. 1393-1402.

17. Private correspondence with M. V. Pregnoff, San Francisco, California, to be published as an ACI Committee 435 Report.

18. Miller, Alfred L., "Warping of Reinforced Concrete Due to Shrinkage," ACI Journal, Proceedings V. 54, No. 11, May 1958, pp. 939-950.

19. Ross, A. D., "Creep of Concrete Under Variable Stress," ACI Journal, Proceedings V. 54, No. 9, Mar. 1958, pp. 739-758.

20. McHenry, Douglas, "A New Aspect of Creep in Concrete and Its Application to Design," Proceedings ASTM, V. 43, 1943, pp. 1969-1984.

21. Concrete Reinforcing Steel Institute, "CRSI Design Handbook," Revised 1959.

22. Newmark, N. M., "Numerical Procedure for Computing Deflections, Moments, and Buckling Loads," Transactions, ASCE, V. 108, pp. 1161-1234.

23. Washa, G. W., and Fluck, P. G., "The Effect of Compressive Reinforcement on the Plastic Flow of Reinforced Concrete Beams," ACI Journal, Proceedings V. 49, No. 8, Oct. 1952, pp. 89-108.

24. Washa, G. W., and Fluck, P. G., "Plastic Flow (Creep) of Reinforced Concrete Continuous Beams," ACI Journal, Proceedings V. 52, No. 5, Jan. 1956, pp. 549-561.

# VIII. APPENDIX

## 8.1 Specimen Details and Experimental Data Obtained in the Investigation

TABLE A.1. DESIGN DETAILS FOR THE TEST BEAMS OF THE CURRENT INVESTIGATION

| Description | One # 3 Bar, p = 0.69%, $w_{SL}/w_{DL}$ = 2.0 | | Three # 3 Bars, p = 2.07%, $w_{SL}/w_{DL}$ = 5.5 | |
|---|---|---|---|---|
| | Beams 4" x 5", b = 4", d = 4", L = 9', $f'_c$ = 5000 psi, $A_s$ = 0.11 in$^2$, n= 6, kd = 1.00", $I^t_{cr}$ = 7.27 in$^4$, $I_g$ = 41.7 in$^4$, $w_{DL}$ = 20.8 #/ft, $w_{SL}$ = 41.6 #/ft | | Beams 4" x 5", b = 4", d = 4", L = 9', $f'_c$ = 5000 psi, $A_s$ = 0.33 in$^2$, n = 6, kd = 1.56", $I^t_{cr}$ = 24.7 in$^4$, $I_g$ = 41.7 in$^4$, $w_{DL}$ = 20.8 #/ft, $w_{SL}$ = 114.4 #/ft | |
| | Simple Beam | Continuous Beam | Simple Beam | Continuous Beam |
| aMax. Positive Mom. | 0.1250 $wL^2$ at ℄ | 0.0703 $wL^2$ at .375L | 0.1250 $wL^2$ at ℄ | 0.0703 $wL^2$ at .375L |
| bMax. Pos. Mom., in-lb | 2530 + 5060 = 7590 | 1420 + 2840 = 4260 | 2530 + 13,920=16,450 | 1420 + 7820 = 9240 |
| aMax. Negative Mom. | --- | 0.1250 wL2 at Suppt. | --- | 0.1250 $wL^2$ at Suppt. |
| bMax. Neg. Mom., in-lb | --- | 2530 + 5060 = 7590 | --- | 2530 + 13,920=16,450 |
| cMax. Pos. Mom. $f_c$, psi | 348 + 696 = 1044* | 196 + 391 = 587* | 160 + 879 = 1039* | 90 + 495 = 585* |
| cMax. Neg. Mom. $f_c$, psi | --- | 348 + 696 = 1044* | --- | 160 + 879 = 1039* |
| cMax. Pos. Mom. $f_s$, psi | 6250 + 12500 = 18,750 | 3510 + 7020 = 10,530 | 1500 + 8250 = 9,750 | 843 + 4527 = 5,370 |
| cMax. Neg. Mom. $f_s$, psi | --- | 6250 + 12500 = 18,750 | --- | 1500 + 8250 = 9,750 |
| dMax. v, psi | 14 | 18 | 30 | 38 |
| dMax. u, psi | 68 | 85 | 148 | 185 |
| eMax. Pos. Mom. $f_t$, psi | 149 + 297 = 446 | 84 + 167 = 251 | 142 + 778 = 920 | 80 + 437 = 527 |
| eMax. Neg. Mom. $f_t$, psi | --- | 149 + 297 = 446 | --- | 142 + 778 = 920 |

* Note that the computed maximum concrete compressive stresses are the same for the -- cont.

corresponding simple and continuous beams (the 1-bar beams--also the 3-bar beams); also that the computed maximum concrete compressive stresses are the same at all points along the 1-bar and 3-bar simple beams--also the same at all points along the 1-bar and 3-bar continuous beams.

[a]In the case of the continuous beams, all moments are computed by elastic theory for prismatic members.

[b]Where 3 numbers appear, they refer to DL + SL = Total Load effects, respectively. One number refers to total load effects.

[c]Maximum stresses $f_c$ and $f_s$ were computed using the cracked transformed section properties and a modular ratio of 6, according to the AASHO Specifications.

[d]Computed using $v = V/bd$ and $u = V/\Sigma_o jd$.

[e]Maximum concrete tensile stresses $f_t$ were computed using the uncracked transformed section properties.

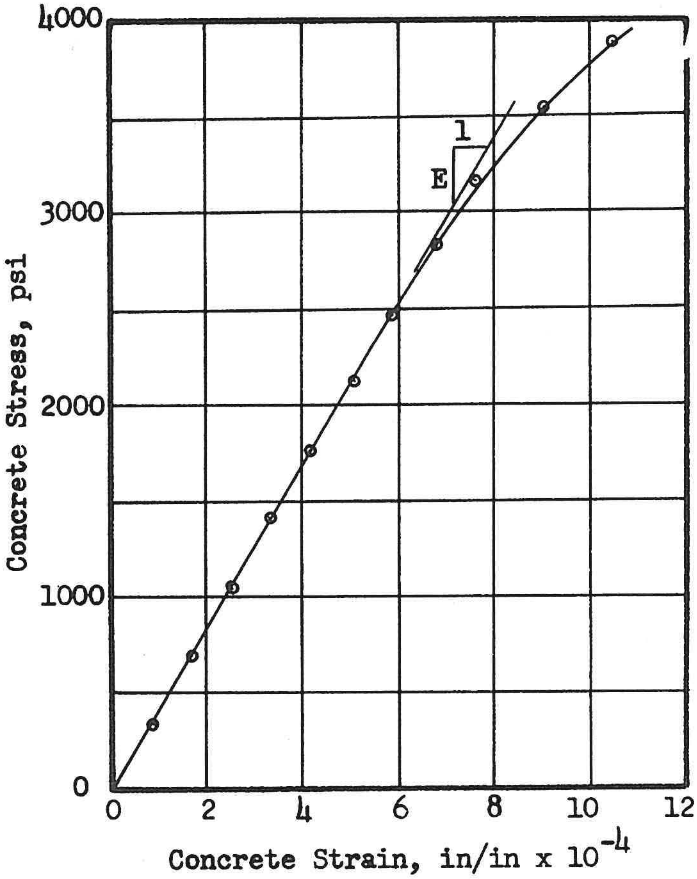


$f'_c$ = 5130 psi; E = $4.4 \times 10^6$ psi

Fig. A.1--Average 28-day concrete stress-strain curve (6" x 12" cylinder tests)

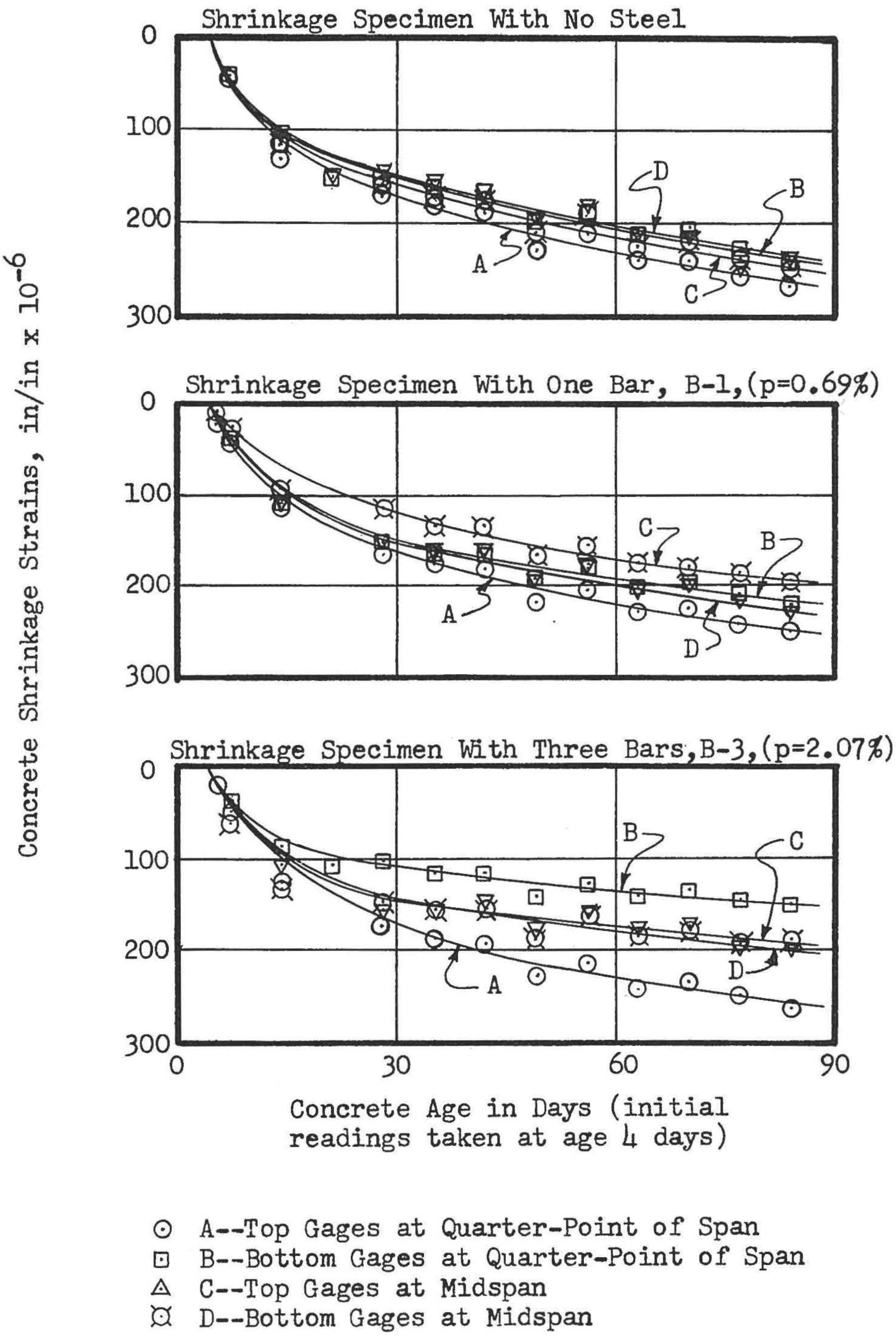


Fig. A.2--Concrete shrinkage versus time curves for specimens containing different steel percentages (duplicate shrinkage specimens were used)

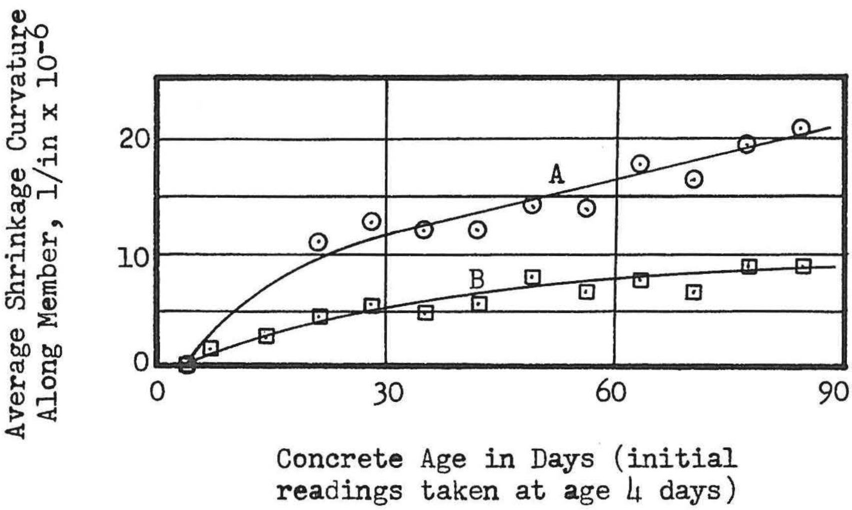


⊙ A--Shrinkage Specimen With Three Bars, B-3, (p=2.07%)
⊡ B--Shrinkage Specimen With One Bar, B-1, (p=0.67%)

Fig. A.3--Average shrinkage curvature along members versus time curves

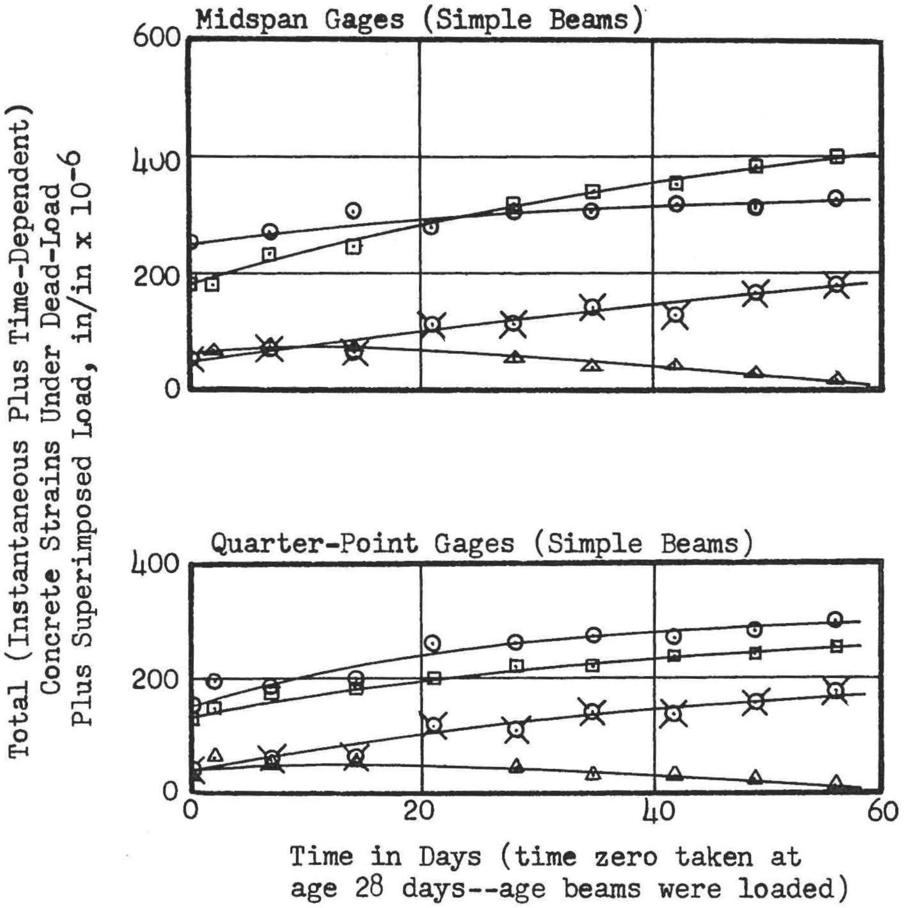


⊙ --Bottom Gage (Tension) For Three-Bar Simple Beam, SB-3, (p = 2.07%, $w_{SL}/w_{DL}$ =5.5)

⊡ --Top Gage (Compression) For Three-Bar Simple Beam, SB-3, (p = 2.07%, $w_{SL}/w_{DL}$ =5.5)

△ --Bottom Gage (Tension) For One-Bar Simple Beam, SB-1, (p = 0.67%, $w_{SL}/w_{DL}$ =2.0)

⌧ --Top Gage (Compression) For One-Bar Simple Beam, SB-1, (p = 0.67%, $w_{SL}/w_{DL}$ =2.0)

Fig. A.4--Total (instantaneous plus time-dependent) concrete strain versus time curves for two simple beams with different steel percentages and loading, but the same computed elastic concrete stresses

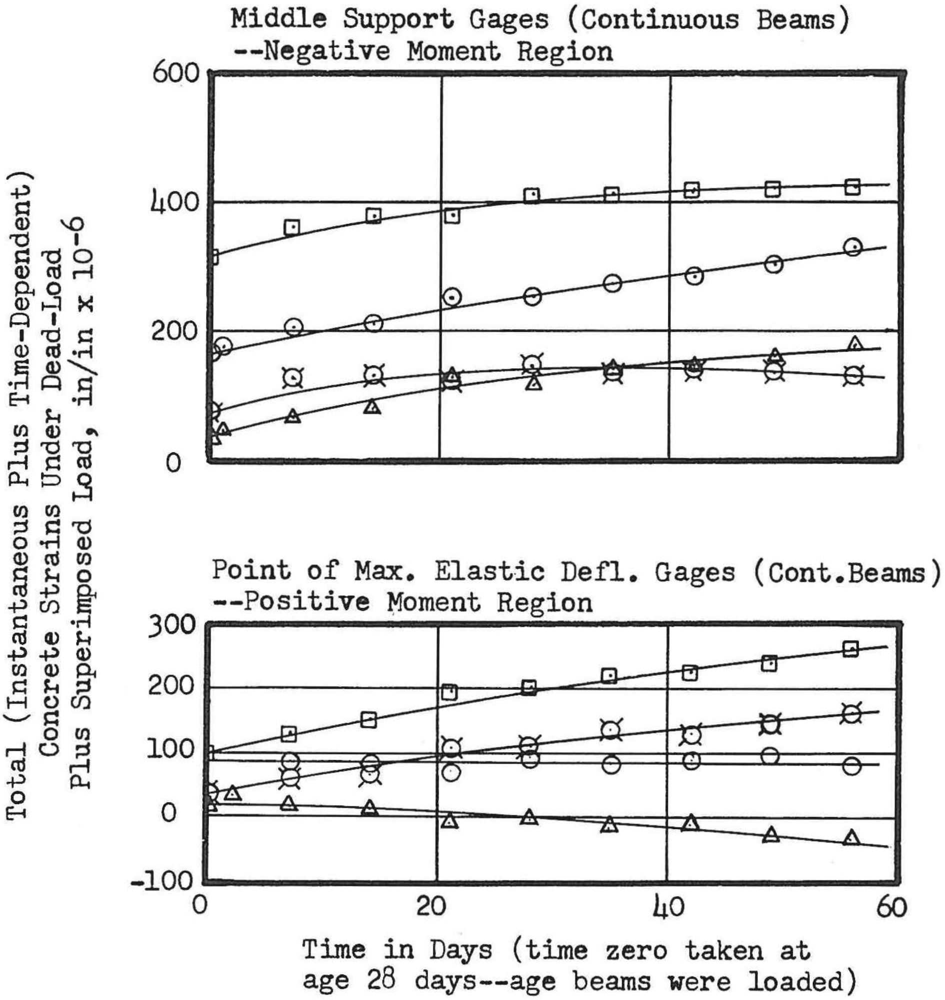


⊙ --Bottom Gage (Tension-Pos.Mom., Compression-Neg.Mom.) For Three-Bar Continuous Beam, LB-3, ($p$=2.07%, $w_{SL}/w_{DL}$=5.5)

⊡ --Top Gage (Compression-Pos.Mom., Tension-Neg.Mom.) For Three-Bar Continuous Beam, LB-3, ($p$=2.07%, $w_{SL}/w_{DL}$=5.5)

△ --Bottom Gage (Tension-Pos.Mom., Compression-Neg.Mom.) For One-Bar Continuous Beam, LB-1, ($p$=0.67%, $w_{SL}/w_{DL}$=2.0)

⧖ --Top Gage (Compression-Pos.Mom., Tension-Neg.Mom.) For One-Bar Continuous Beam, LB-1, LB-1, ($p$=0.67%, $w_{SL}/w_{DL}$=2.0)

Fig. A.5--Total (instantaneous plus time-dependent) concrete strain versus time curves for two continuous beams with different steel percentages and loading, but the same computed elastic concrete stresses

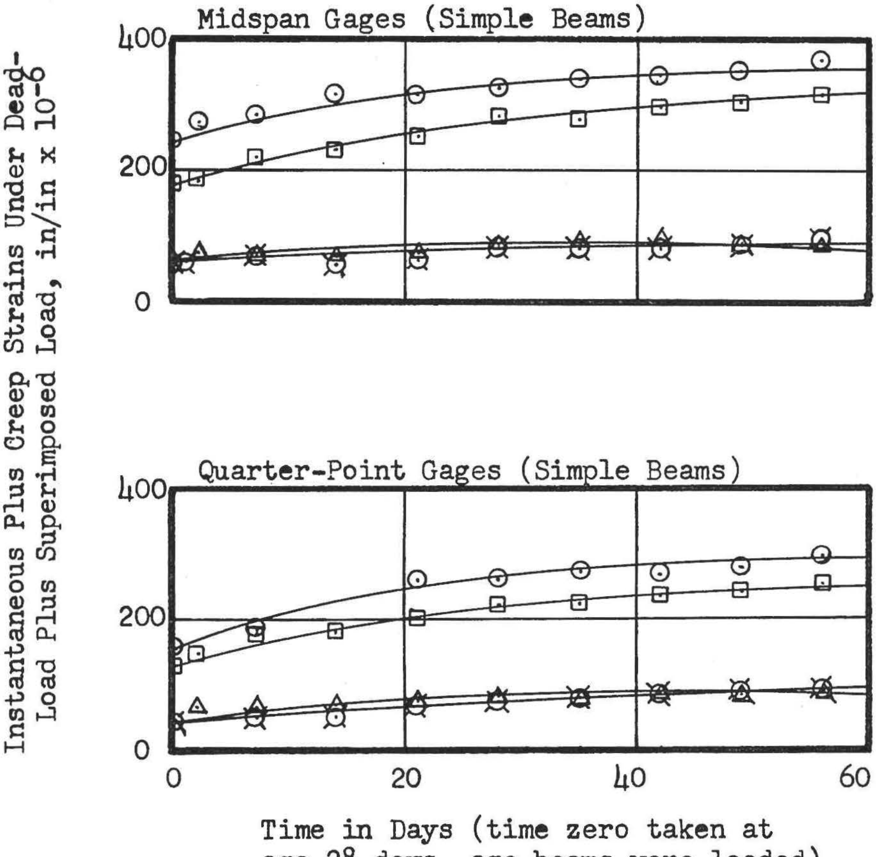


⊙ --Bottom Gage (Tension) For Three-Bar Simple Beam, SB-3, ($p$ = 2.07%, $w_{SL}/w_{DL}$ = 5.5)

⊡ --Top Gage (Compression) For Three-Bar Simple Beam, SB-3, ($p$ = 2.07%, $w_{SL}/w_{DL}$ = 5.5)

△ --Bottom Gage (Tension) For One-Bar Simple Beam, SB-1, ($p$ = 0.67%, $w_{SL}/w_{DL}$ = 2.0)

⊠ --Top Gage (Compression) For One-Bar Simple Beam, SB-1, ($p$ = 0.67%, $w_{SL}/w_{DL}$ = 2.0)

Fig. A.6--Instantaneous plus creep strain versus time curves for two simple beams with different steel percentages and loading,but the same computed elastic concrete stresses

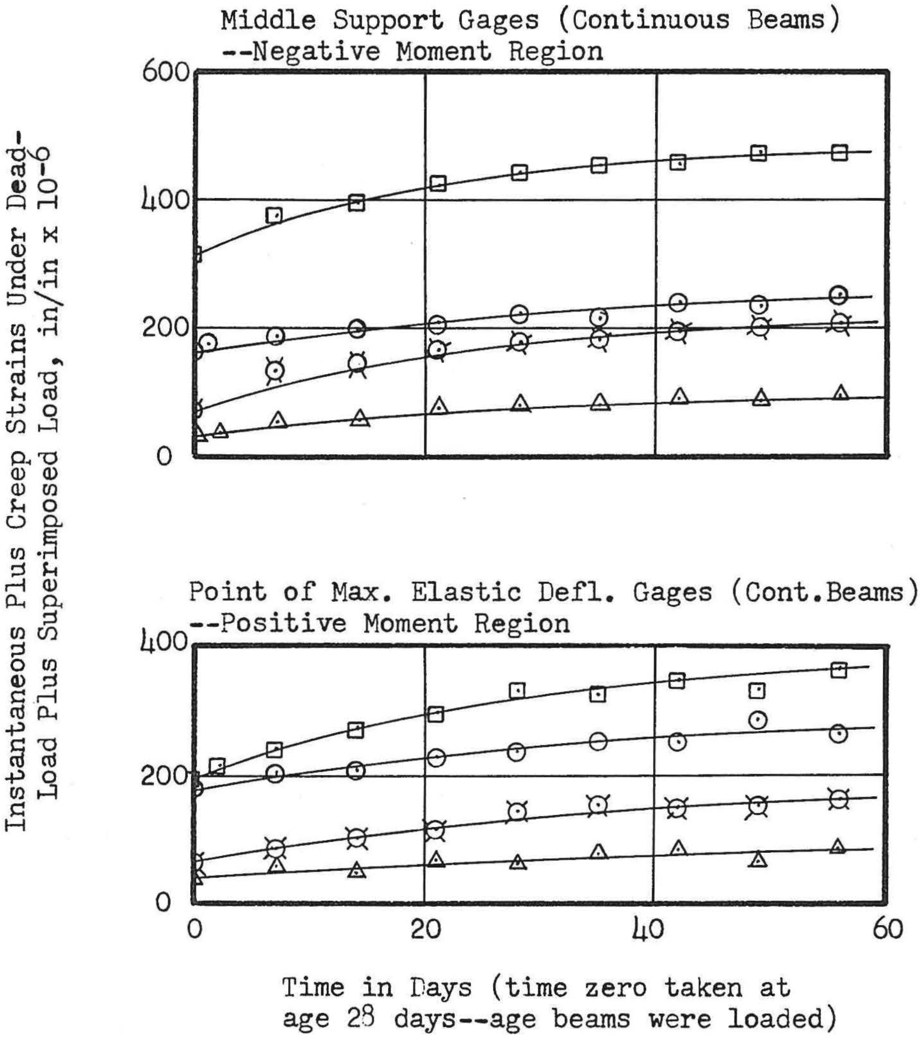


⊙ --Bottom Gage (Tension-Pos.Mom., Compression-Neg.Mom.) For Three-Bar Continuous Beam,LB-3,(p=2.07%,$w_{SL}/w_{DL}$=5.5)

⊡ --Top Gage (Compression-Pos.Mom., Tension-Neg.Mom.) For Three-Bar Continuous Beam, LB-3,(p=2.07%,$w_{SL}/w_{DL}$=5.5)

△ --Bottom Gage (Tension-Pos.Mom., Compression-Neg.Mom.) For One-Bar Continuous Beam,LB-1,(p=0.67,$w_{SL}/w_{DL}$=2.0)

¤ --Top Gage (Compression-Pos.Mom., Tension-Neg.Mom.) For One Bar-Continuous Beam,LB-1,(p=0.67%,$w_{SL}/w_{DL}$=2.0)

Fig. A.7--Instantaneous plus creep strain versus time curves for two continuous beams with different steel percentages and loading, but the same computed elastic concrete stresses

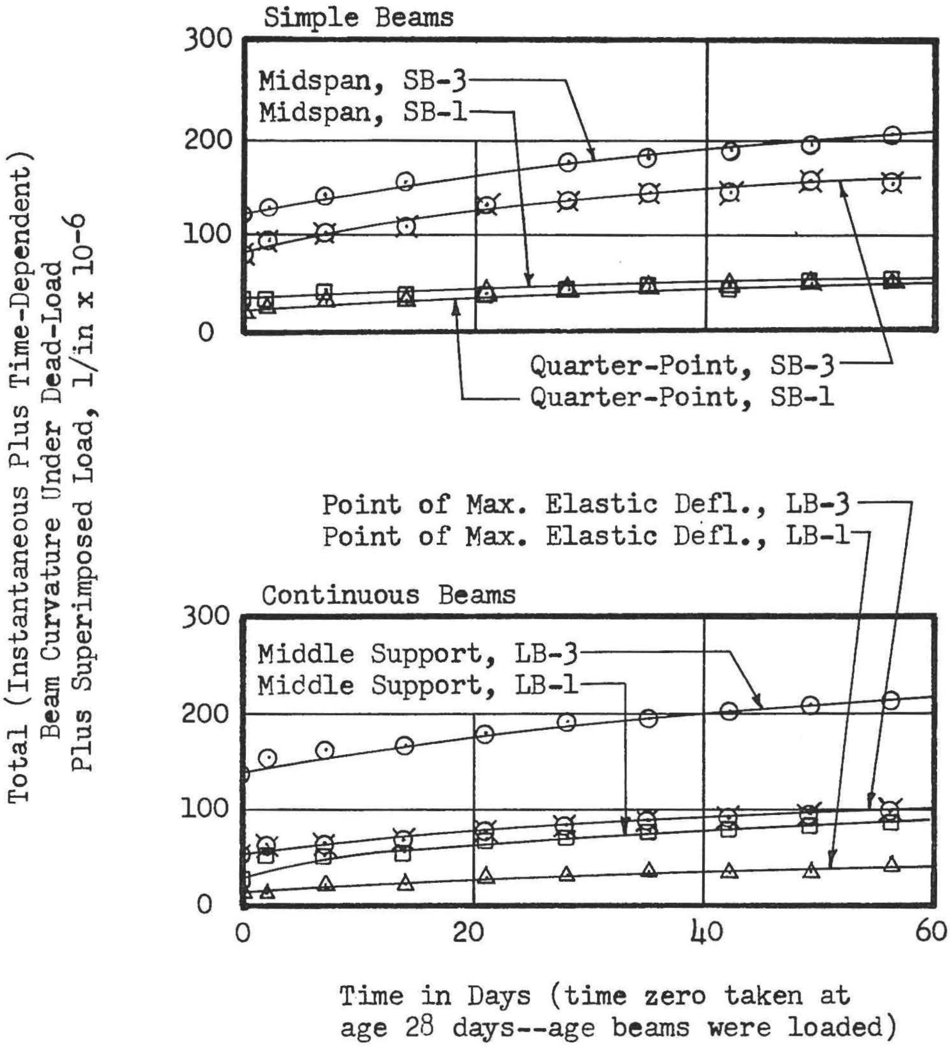


Fig. A.8--Total (instantaneous plus time-dependent) curvature versus time curves for four test beams

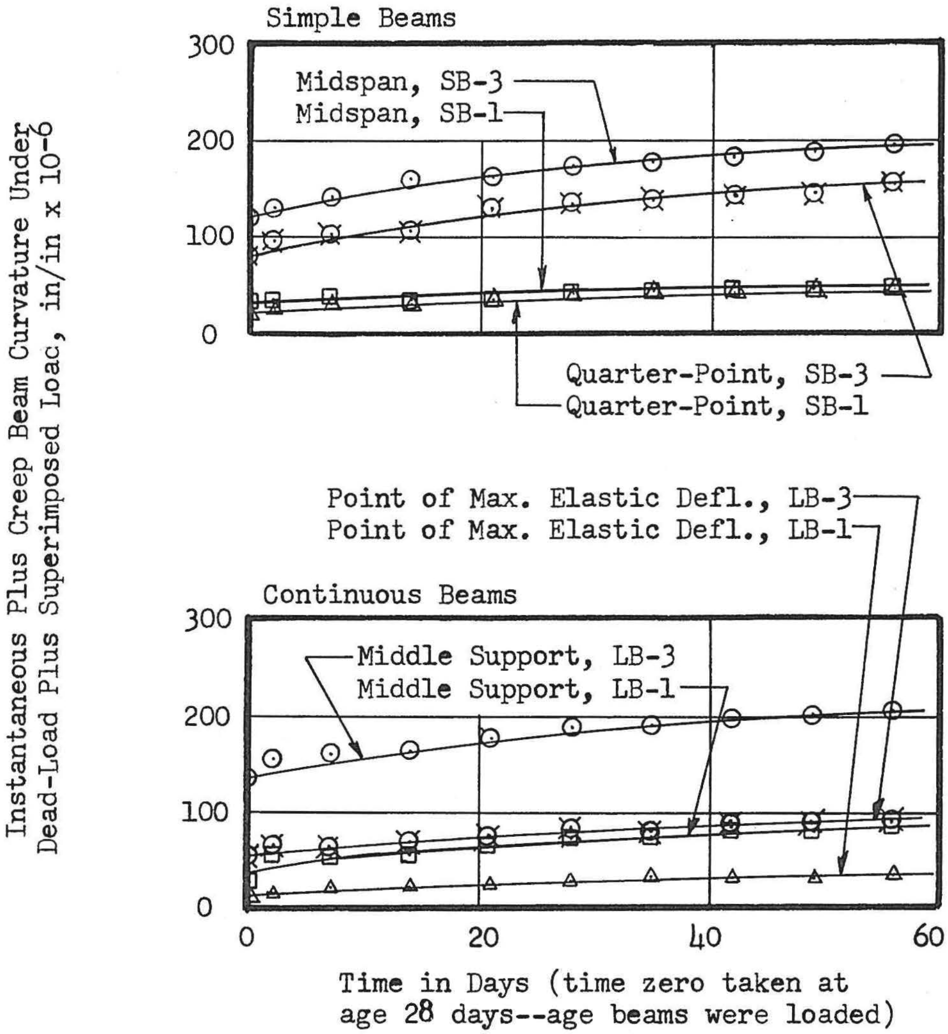


Fig. A.9--Instantaneous plus creep curvature versus time curves for four test beams

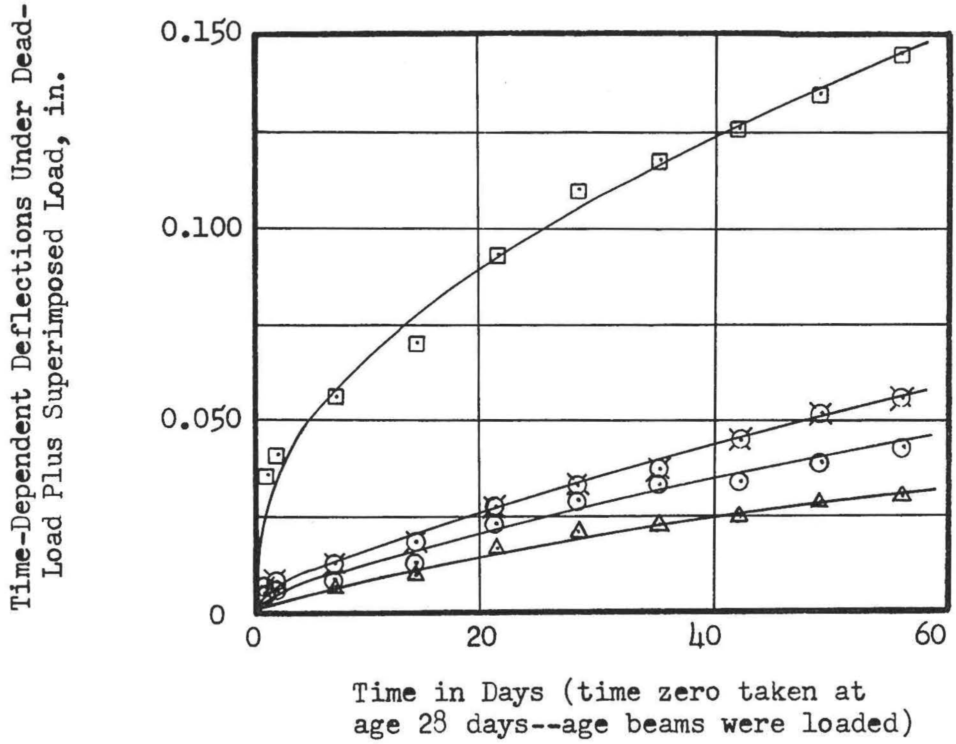


⊡ Simple Beam, SB-3, $\Delta_{initial}$ = 0.153 in.

⊙ Simple Beam, SB-1, $\Delta_{initial}$ = 0.041 in.

⨂ Continuous Beam, LB-3, $\Delta_{initial}$ = 0.056 in.

△ Continuous Beam, LB-1, $\Delta_{initial}$ = 0.021 in.

Fig. A.10--Time-dependent deflection versus
time curves for four test beams

# INSTANTANEOUS AND TIME-DEPENDENT DEFLECTIONS OF SIMPLE AND CONTINUOUS REINFORCED CONCRETE BEAMS

PART II

by

Gene Alan Metz
Associate Professor of Civil Engineering
Auburn University

DEPARTMENT OF CIVIL ENGINEERING
AND
AUBURN RESEARCH FOUNDATION
AUBURN UNIVERSITY
1964

# TABLE OF CONTENTS

# LIST OF FIGURES

# I. INTRODUCTION

Part II of this study consists of a rerun of tests in Part I and an analysis of the resulting data.

The tests of Part I were rerun because some of the beams were honeycombed and one of the beams (L-B1) was cracked while being moved into position for loading.

Concrete for the beams of Part II was vibrated during pouring in order to minimize the honeycomb.

It was judged desirable to determine the effect, if any, of the condition of the beams of Part I upon the results of the study.

# II. DESCRIPTION OF EXPERIMENTAL INVESTIGATION

A total of four beams was tested, two simple beams and two continuous beams (each with two equal spans continuous over a center support). One simple beam (SB - 1) and one continuous beam (LB - 1) were reinforced with one #3 bar. The other simple beam (SB - 3) and continuous beam (LB - 3) were reinforced with three #3 bars. All spans were 9' long, the continuous beams having an overall length of 18'. In addition to the four test beams, six shrinkage specimens were tested. The shrinkage specimens were the same size as the simple beams. Two were reinforced with three #3 bars, two with one #3 bar, and two were without reinforcement. The shrinkage specimens were placed on one side on a smooth, oiled, plywood surface in an attempt to eliminate any frictional effects which might influence the shrinkage measurements. Details of the test beams are shown in Fig. 3 of Part I of this study.

The properties of the materials were as follows:

Concrete slump . . . . . . . . . . . . $2\frac{1}{2}$"
28 day concrete cylinder strength. . 4450 psi
Concrete modulus of elasticity . . . $3.5 \times 10^6$ psi
Tensile yield point of the steel . . 49,000 psi

The concrete strains were measured by using a Whittemore mechanical strain gage with a 10" gage length. Gage points were imbedded near the top and bottom of each beam at six different locations giving a total of 12 gages and 24 gage points for each beam. Six gages and 12 gage points were used on each shrinkage specimen. Temperature effects on strains were eliminated through the use of a temperature bar made of invar metal having the same coefficient of thermal expansion as the concrete.

## III. TESTING PROCEDURES

All beams were loaded at age 28 days with iron bricks. The bricks were spaced continuously in the 3 - bar beams and uniformly in the 1 - bar beams. The loading was the same as in Part I of this study and can be seen in Fig. 4 of Part I.

The deflection and strain readings reported were the average of those on each side of the beam in the same position in order to eliminate any torsional effects. Also, only the average of corresponding strain readings on the shrinkage specimens and test beams were reported.

## IV. COMPARISON OF TEST RESULTS

Figures in Part II correspond to figures in Part I as follows:

| Part II | | Part I |
|---|---|---|
| Fig. 1 | corresponds to | Fig. 8 |
| Fig. 2 | " " | Fig. 10 |
| Fig. 3 | " " | Fig. 11 |
| Fig. 4 | " " | Fig. A-1 |
| Fig. 5 | " " | Fig. A-2 |
| Fig. 6 | " " | Fig. A-3 |
| Fig. 7 | " " | Fig. A-4 |
| Fig. 8 | " " | Fig. A-5 |
| Fig. 9 | " " | Fig. A-6 |
| Fig. 10 | " " | Fig. A-7 |
| Fig. 11 | " " | Fig. A-8 |
| Fig. 12 | " " | Fig. A-9 |
| Fig. 13 | " " | Fig. A-10 |

A comparison of Fig. 4 of Part II with Fig. A-1 of Part I shows that both $f'_c$ and E were somewhat higher in tests conducted in Part I as opposed to those of Part II. The modulus of elasticity was 26% higher in Part I as compared to the modulus of elasticity of the concrete in Part II.

Figures 1 and 5 of Part II and Figures 8 and A-2 of Part I show that the shrinkage was about 20% greater in Part I than in Part II. This was to be expected because a rich concrete will tend to shrink more than a lean one. In general, all other curves for strains and deflections ran higher in Part II than in Part I by amounts ranging from 15% to about 40%. Since the modulus of elasticity of the concrete in Part I was 26% higher than in Part II, these larger strains and deflections appear quite reasonable. The only exceptions to this occur in the tension gage creep coefficients of Fig. 2 and the concrete strains in the positive moment region of Fig. 8. These were about the same to slightly lower in Part II as compared to Part I. In the writer's opinion, this was probably caused by tension cracking of the concrete and a redistribution of moments in the continuous beams.

## V. CONCLUSIONS

The test results in Part II agree quite well with those of Part I. Strains and deflections are somewhat higher in the second set of tests than in the first, but this is caused by the lower modulus of elasticity of the concrete in Part II. Because of the close agreement of the test results, it is the writer's opinion that neither the honeycomb of the test beams in Part I or the hairline crack of beam L - B1 had any effect on the data.

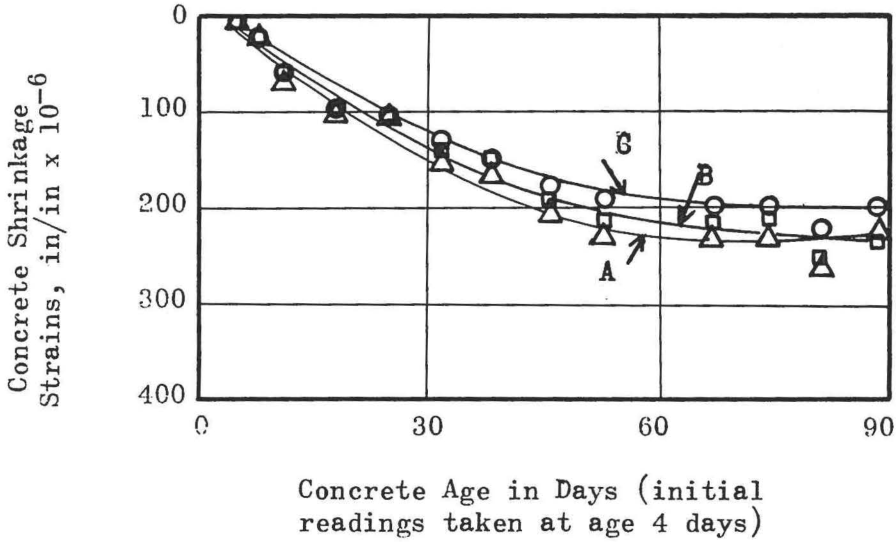


A--Shrk. Spec. With No Steel (p=0), All Gages Used
B--Shrk. Spec. With One Bar (p=0.69%), All Gages Used
C--Shrk. Spec. With Three Bars (p=2.07%), All Gages Used

Fig. 1--Comparison of shrinkage strains at the top fiber for the specimens with different steel percentages (strains proportioned to extreme fiber using a linear distribution with the top and bottom gages)

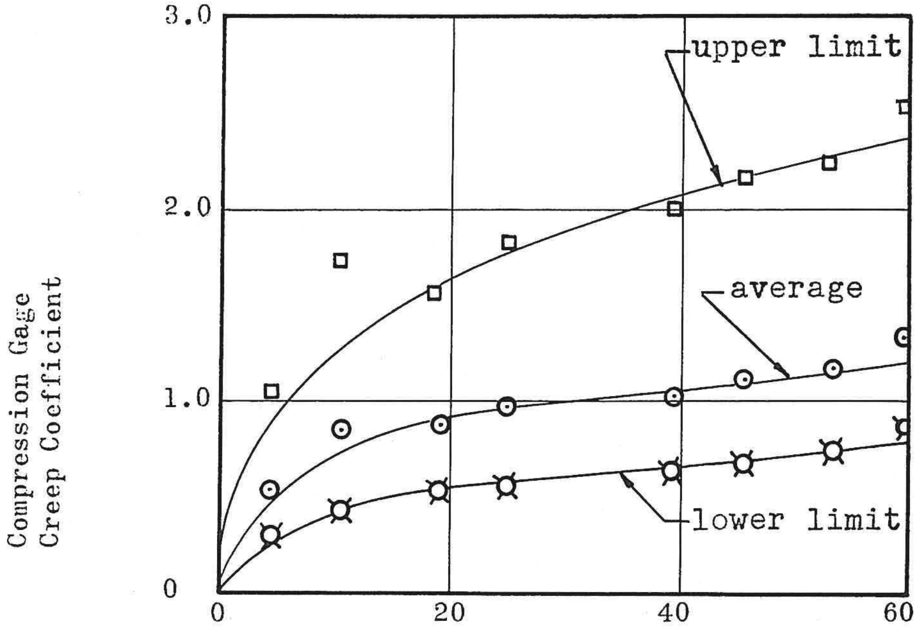


Time in Days (time zero taken at age 28 days--age beams were loaded)

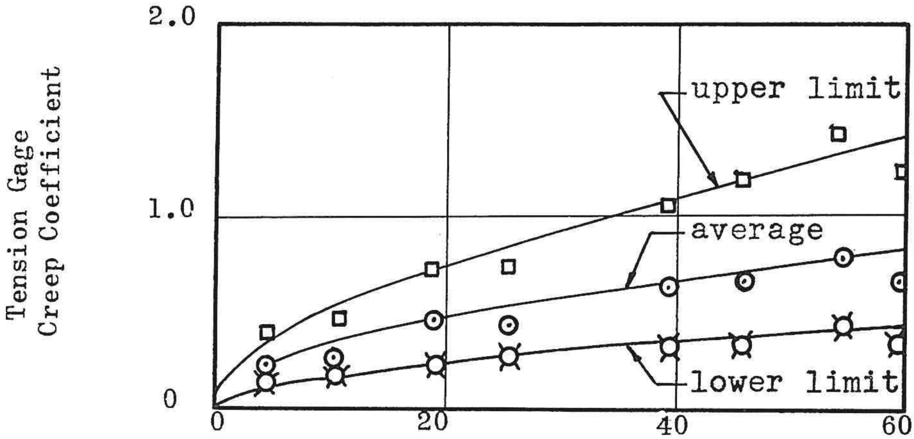


Time in Days (time zero taken at age 28 days--age beams were loaded)

Creep Coefficients Defined as Ratio of Creep Strain to Initial Strain

Fig. 2--Compression and tension gage creep coefficient versus time curves for four test beams

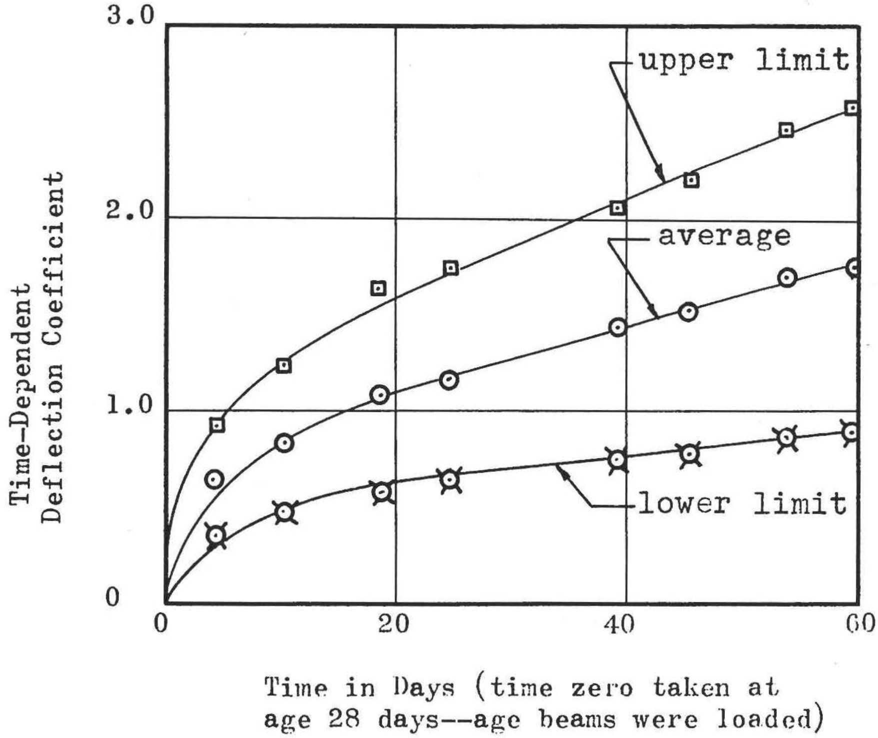


Time-Dependent Deflection Coefficient Defined as Ratio of Time-Dependent Deflection to Initial Deflection

Fig. 3--Time-dependent deflection coefficient versus time curves for four test beams

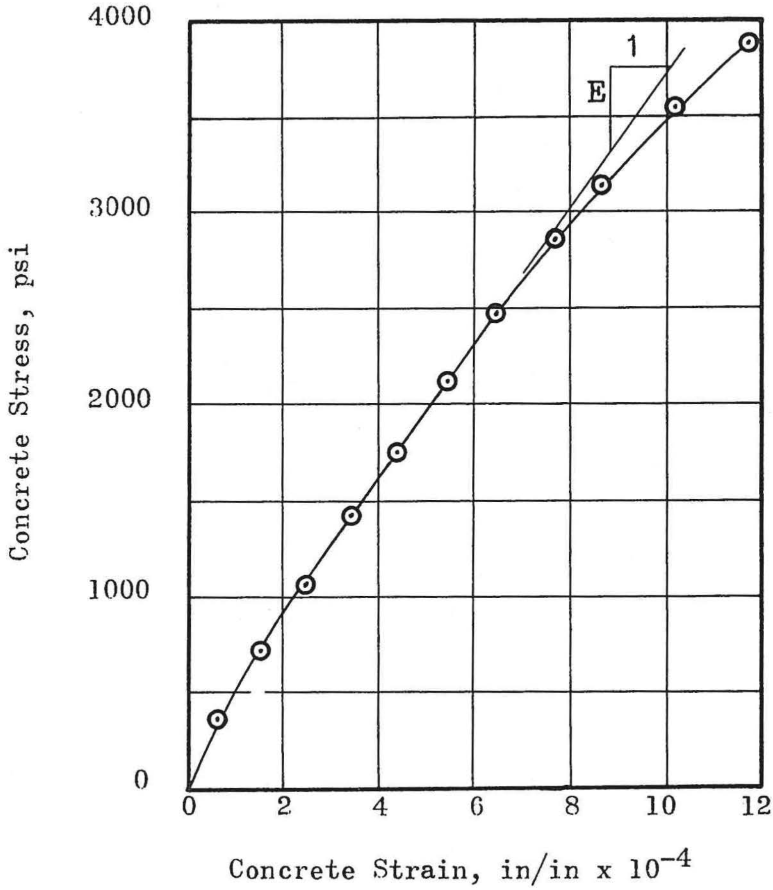


$f'_c$ = 4450 psi    E = 3.5 x $10^6$ psi

Fig. 4--Average 28-day concrete stress-strain curve (6" x 12" cylinder tests)

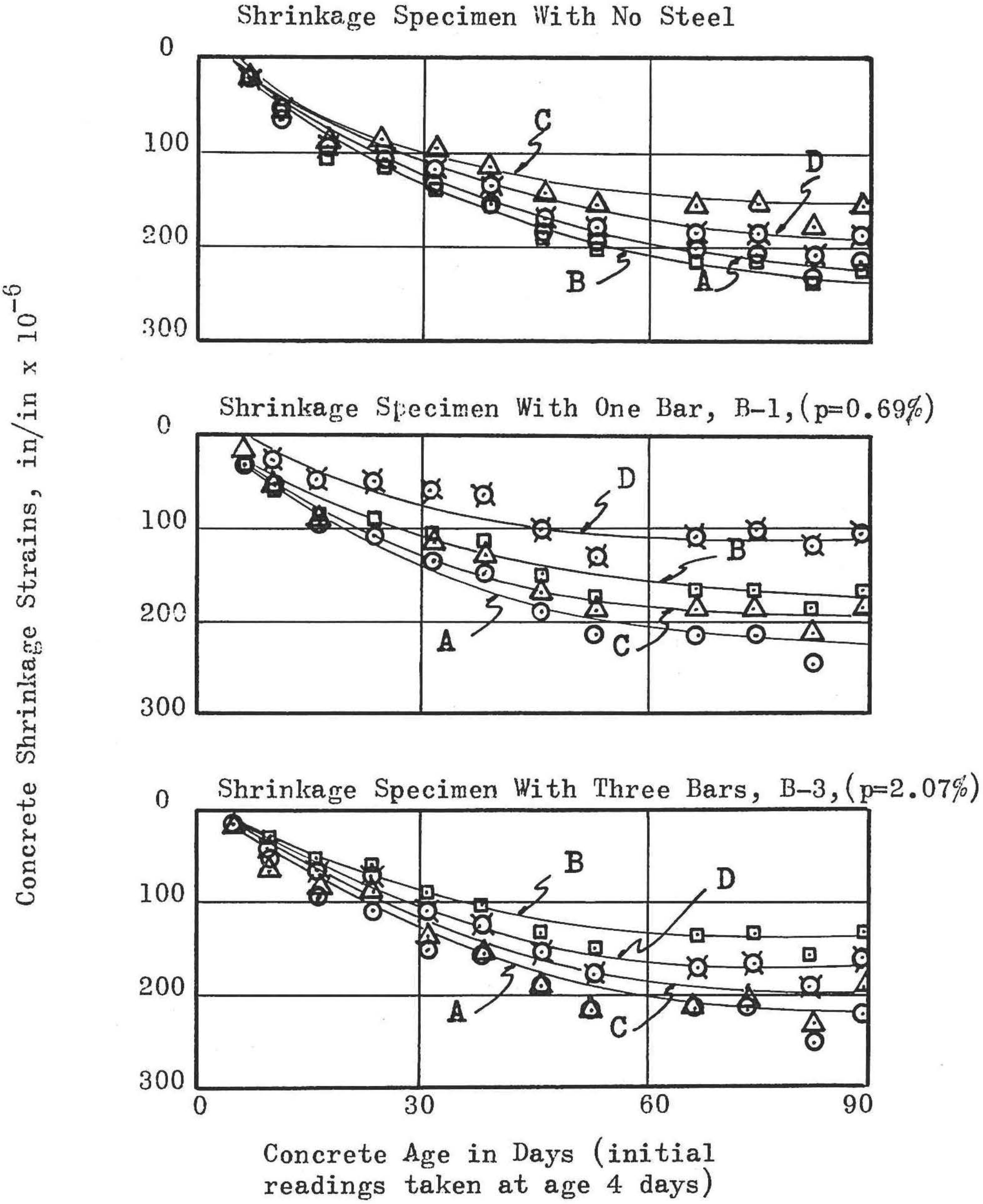


A--Top Gages at Quarter-Point of Span
B--Bottom Gages at Quarter-Point of Span
C--Top Gages at Midspan
D--Bottom Gages at Midspan

Fig. 5--Concrete shrinkage versus time curves for specimens containing different steel percentages (duplicate shrinkage specimens were used)

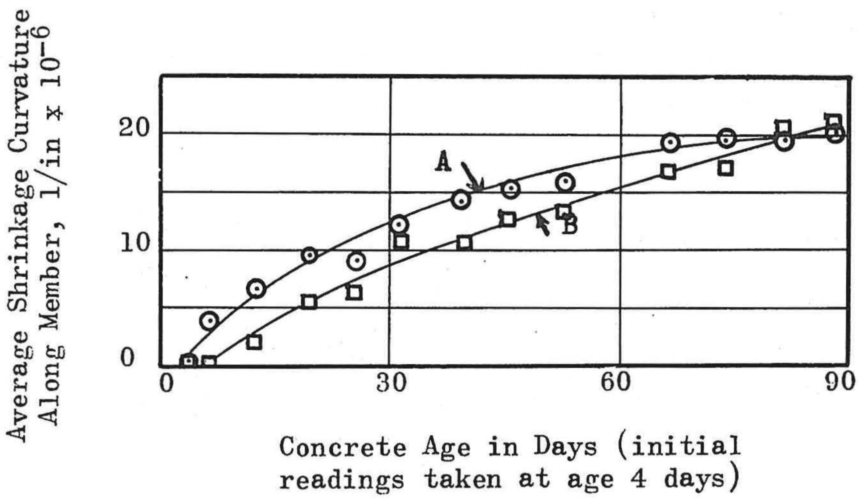


A--Shrinkage Specimen With Three Bars, B-3, (p=2.07%)
B--Shrinkage Specimen With One Bar, B-1, (p=0.67%)

Fig. 6--Average shrinkage curvature along members versus time curves

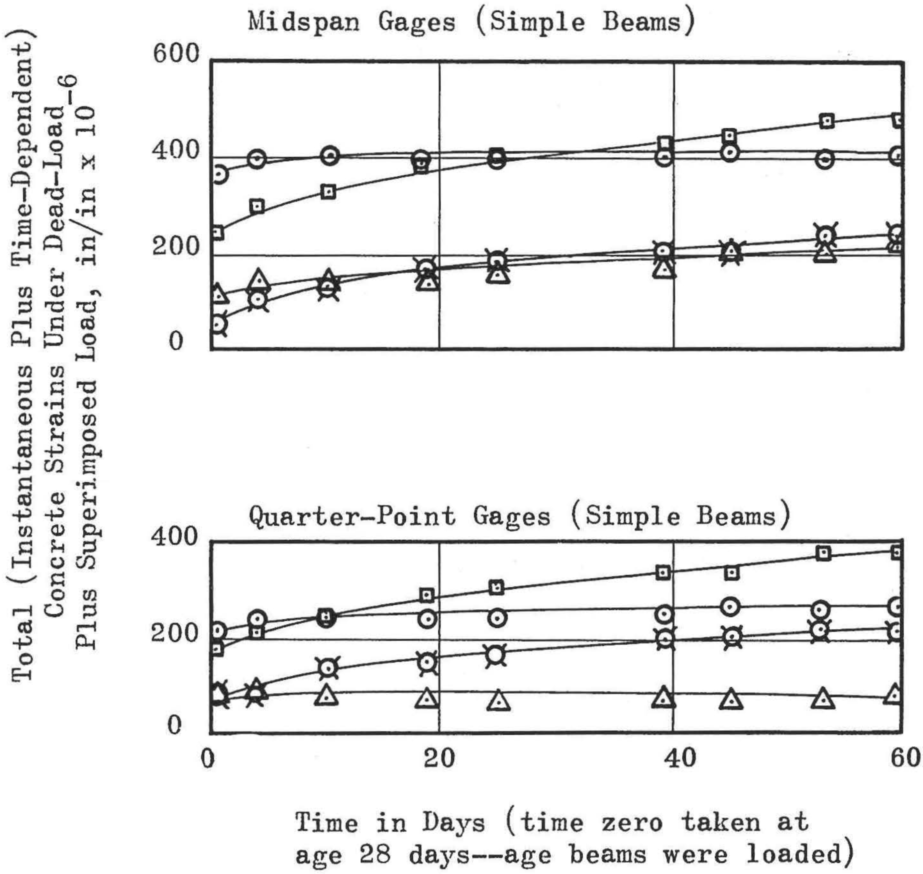


⊙ -- Bottom Gage (Tension) For Three-Bar Simple Beam, SB-3, ($p = 2.07\%$, $w_{SL}/w_{DL} = 5.5$)

⊡ -- Top Gage (Compression) For Three Bar Simple Beam, SB-3, ($p = 2.07\%$, $w_{SL}/w_{DL} = 5.5$)

△ -- Bottom Gage (Tension) For One-Bar Simple Beam, SB-1, ($p = 0.67\%$, $w_{SL}/w_{DL} = 2.0$)

-- Top Gage (Compression) For One-Bar Simple Beam, SB-1, ($p = 0.67\%$, $w_{SL}/w_{DL} = 2.0$)

Fig. 7--Total (instantaneous plus time-dependent) concrete strain versus time curves for two simple beams with different steel percentages and loading, but the same computed elastic concrete stresses

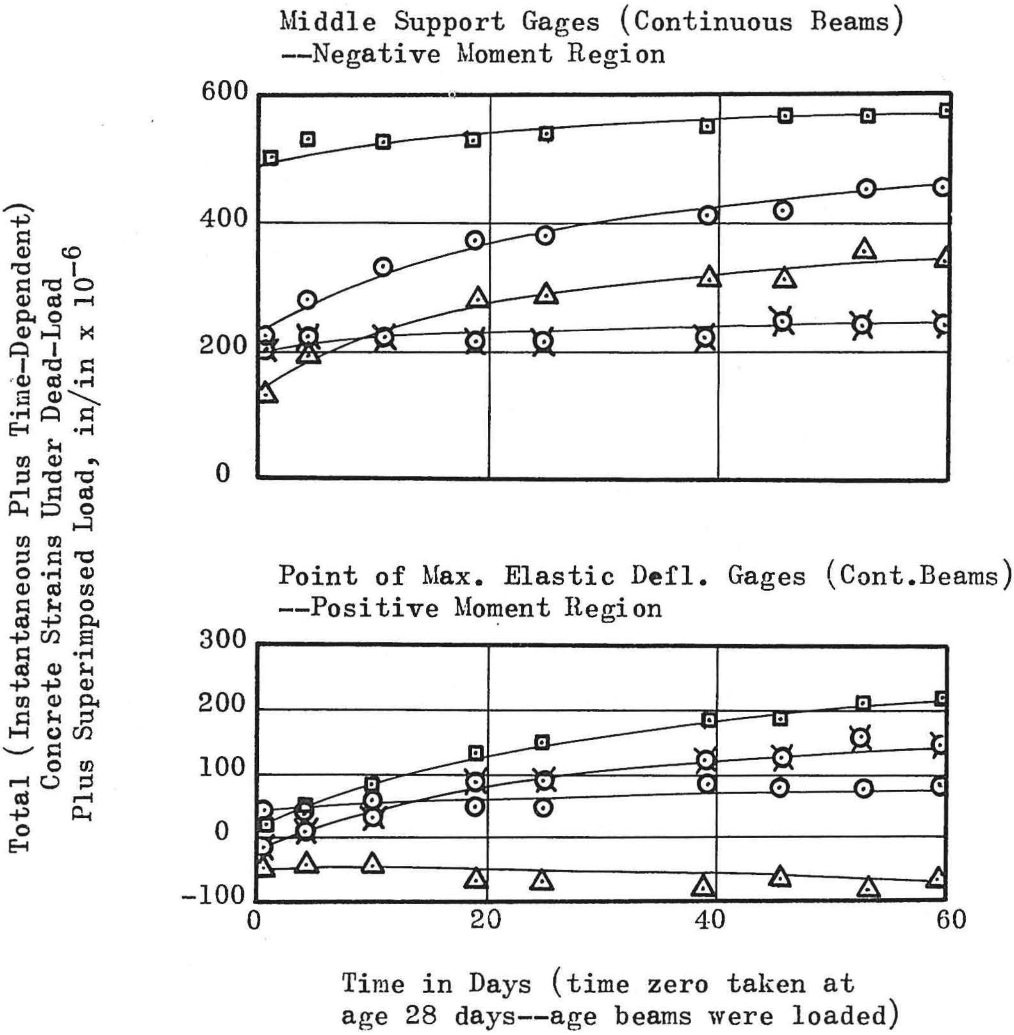


⊙ -- Bottom Gage (Tension-Pos.Mom., Compression-Neg.Mom.) For Three-Bar Continuous Beam, LB-3, ($p=2.07\%$, $w_{SL}/w_{DL}=5.5$)

⊡ -- Top Gage (Compression-Pos.Mom., Tension-Neg.Mom.) For Three-Bar Continuous Beam, LB-3, ($p=2.07\%$, $w_{SL}/w_{DL}=5.5$)

△ -- Bottom Gage (Tension-Pos.Mom., Compression-Neg.Mom.) For One-Bar Continuous Beam, LB-1, ($p=0.67\%$, $w_{SL}/w_{DL}=2.0$)

⊗ -- Top Gage (Compression-Pos.Mom., Tension-Neg.Mom.) For One-Bar Continuous Beam, LB-1, LB-1, ($p=0.67\%$, $w_{SL}/w_{DL}=2.0$)

Fig. 8--Total (instantaneous plus time-dependent) concrete strain versus time curves for two continuous beams with different steel percentages and loading, but the same computed elastic concrete stresses

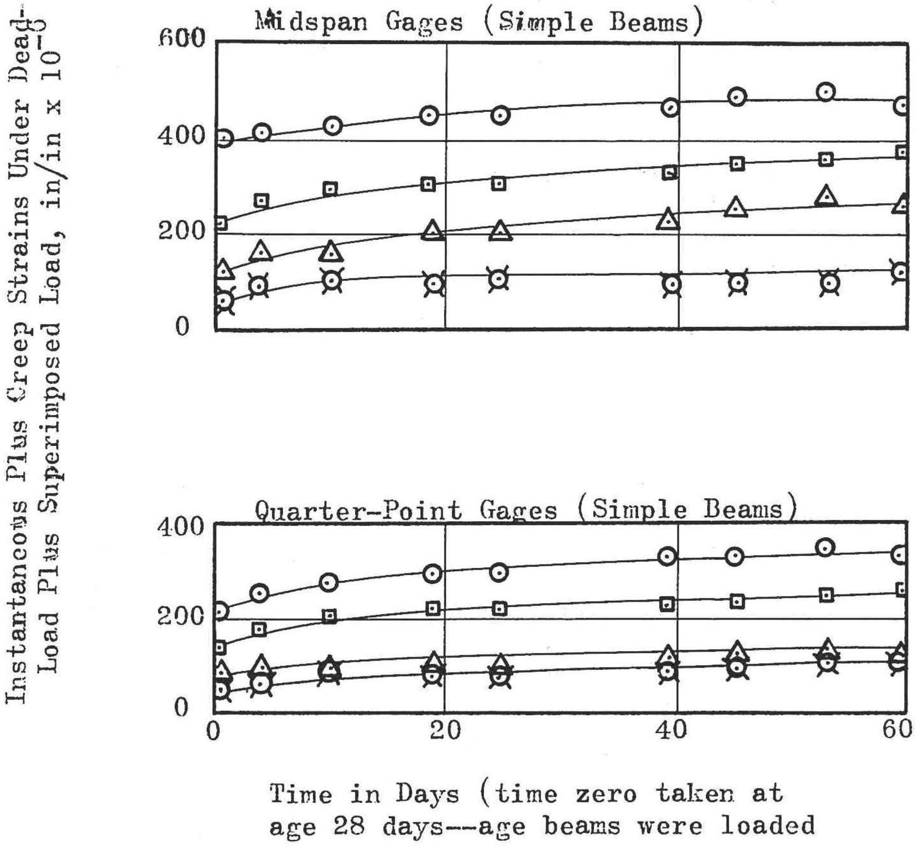


⊙ -- Bottom Gage (Tension) For Three-Bar Simple Beam, SB-3, (p = 2.07%, $w_{SL}/w_{DL}$ = 5.5)

⊡ -- Top Gage (Compression) For Three-Bar Simple Beam, SB-3, (p = 2.07%, $w_{SL}/w_{DL}$ = 5.5)

△ -- Bottom Gage (Tension For One-Bar Simple Beam, SB-1, (p = 0.67%, $w_{SL}/w_{DL}$ = 2.0)

⊗ -- Top Gage (Compression) For One-Bar Simple Beam, SB-1, (p = 0.67%, $w_{SL}/w_{DL}$ = 2.0)

Fig. 9--Instantaneous plus creep strain versus time curves for two simple beams with different steel percentages and loading, but the same computed elastic concrete stresses

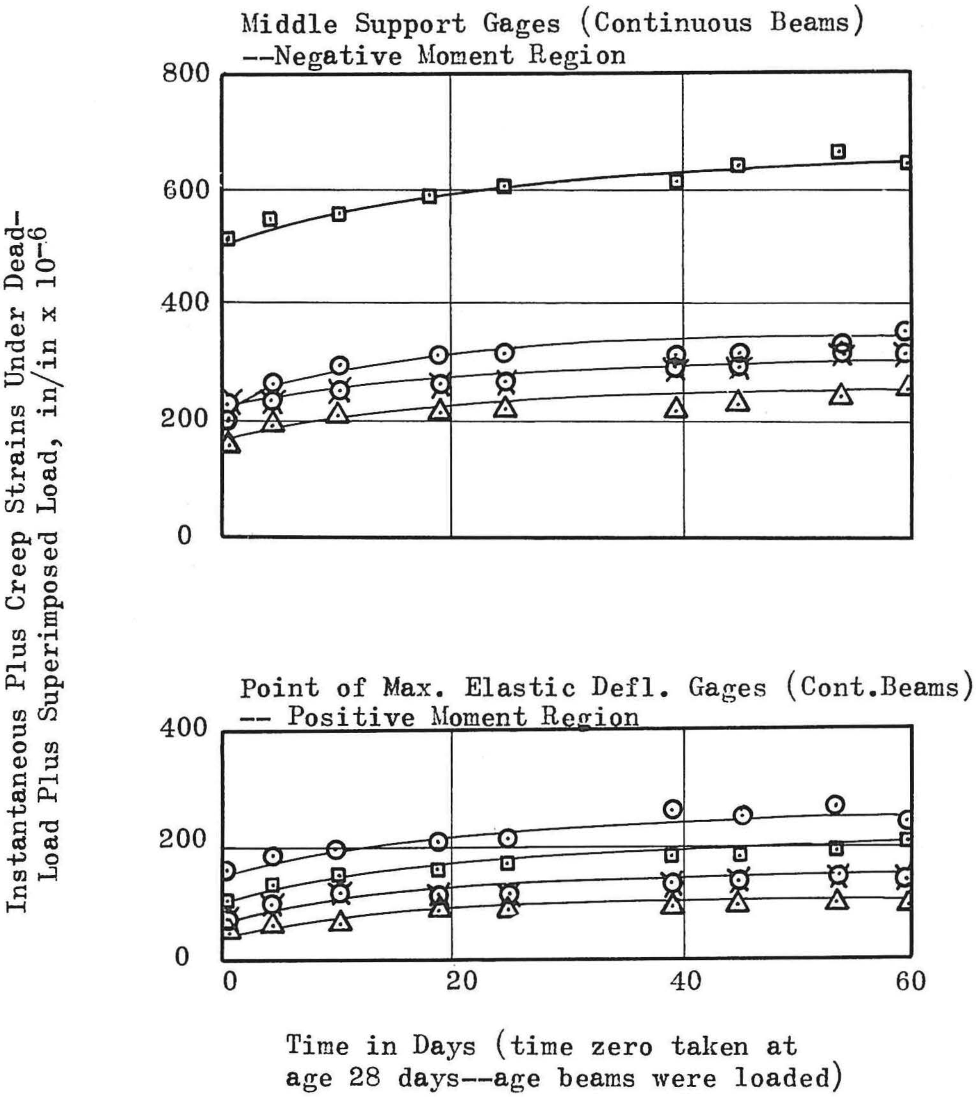


⊙ -- Bottom Gage (Tension-Pos.Mom., Compression-Neg.Mom.) For Three-Bar Continuous Beam, LB-3, ($p$=2.07%, $w_{SL}/w_{DL}$=5.5)

⊡ -- Top Gage (Compression-Pos.Mom., Tension-Neg.Mom.) For Three-Bar Continuous Beam, LB-3, ($p$=2.07%, $w_{SL}/w_{DL}$=5.5)

△ -- Bottom Gage (Tension-Pos.Mom., Compression-Neg.Mom.) For One-Bar Continuous Beam, LB-1, ($p$=0.67, $w_{SL}/w_{DL}$=2.0)

⊗ -- Top Gage (Compression-Pos.Mom., Tension-Neg.Mom.) For One Bar-Continuous Beam, LB-1, ($p$=0.67%, $w_{SL}/w_{DL}$=2.0)

Fig. 10--Instantaneous plus creep strain versus time curves for two continuous beams with different steel percentages and loading, but the same computed elastic concrete stresses

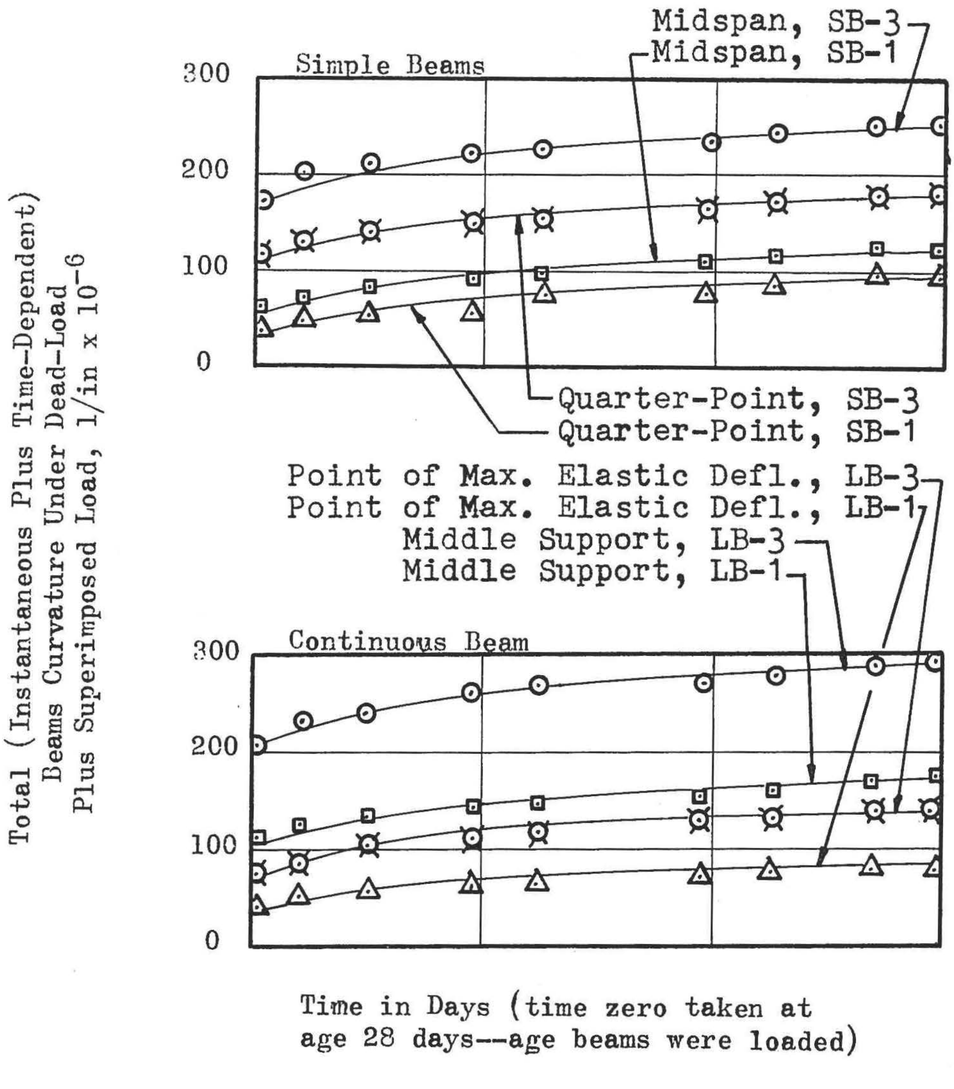


Fig. 11--Total (instantaneous plus time-dependent) curvature versus time curves for four test beams

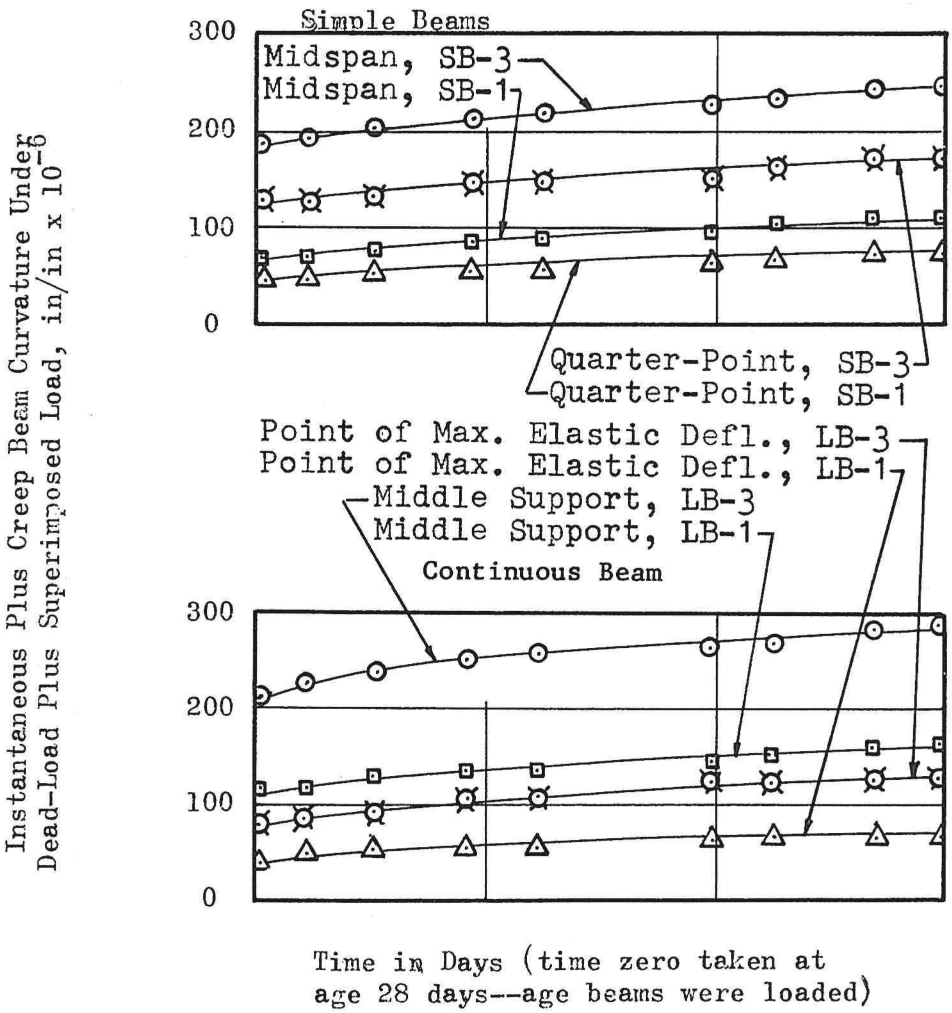


Fig. 12--Instantaneous plus creep curvature versus time curves for four test beams

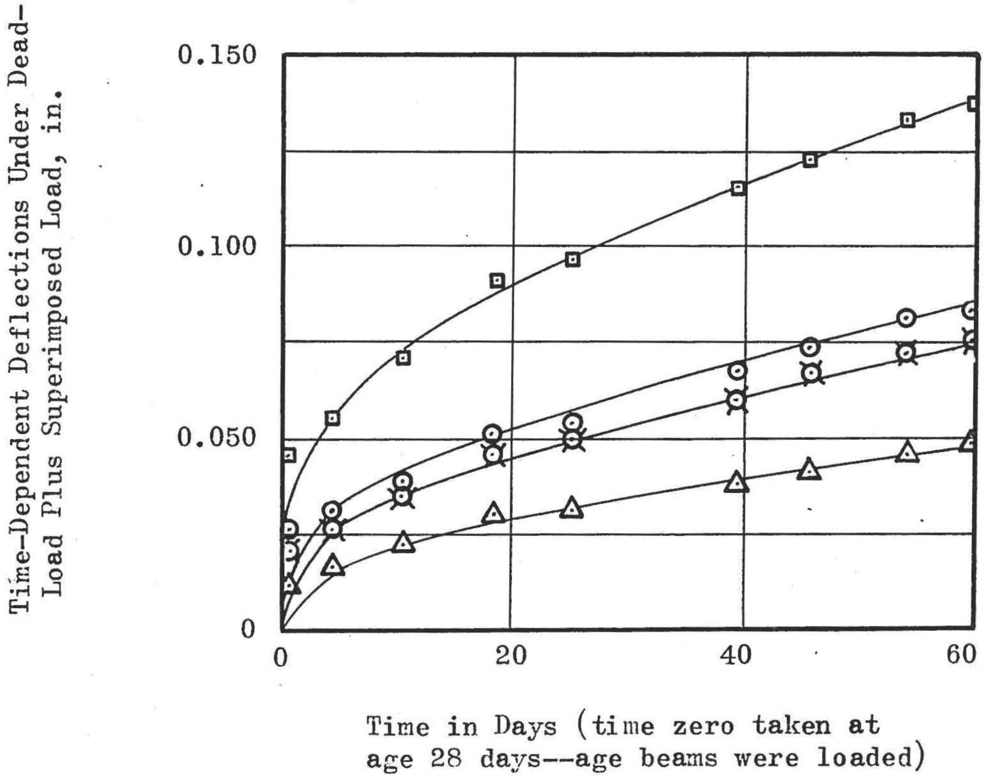


Simple Beam, SB-3, initial = 0.157 in.

Simple Beam, SB-1, initial = 0.036 in.

Continuous Beam, LB-3, initial = 0.061 in.

Continuous Beam, LB-1, initial = 0.019 in.

Fig. 13 --Time-dependent deflection versus time curves for four test beams